OCCUPATIONAL EXPOSURE ASSESSMENT FOR NANOPARTICLES

A DISSERTATION
SUBMITTED TO THE FACULTY OF THE GRADUATE SCHOOL
OF THE UNIVERSITY OF MINNESOTA

BY

Ji Young Park

IN PARTIAL FULFILLMENT OF THE REQUIREMENTS
FOR THE DEGREE OF
DOCTOR OF PHILOSOPHY

Gurumurthy Ramachandran, Ph.D., Advisor

July 2009

INFORMATION TO USERS

The quality of this reproduction is dependent upon the quality of the copy submitted. Broken or indistinct print, colored or poor quality illustrations and photographs, print bleed-through, substandard margins, and improper alignment can adversely affect reproduction.
In the unlikely event that the author did not send a complete manuscript and there are missing pages, these will be noted. Also, if unauthorized copyright material had to be removed, a note will indicate the deletion.

ProQuest LLC
789 East Eisenhower Parkway
P.O. Box 1346
Ann Arbor, MI 48106-1346

Acknowledgements

I would like to thank Dr. Ramachandran, my advisor, for his academic guidance as well as for his encouragement and faith. I could not have made it through my studies at the University of Minnesota without his help.

My deepest gratitude goes out to Dr. Raynor for his valuable comments and helpful feedback and Dr. Eberly for her precise and effective advice. For their significant contributions to my research, I also would like to acknowledge my other dissertation committee members: John Mulhausen and Bruce Alexander.

For the instrumentation and technical support, I want to thank Gregory Olson Jr. and Avula Sreenath in TSI Inc. For the financial support, I would like to acknowledge 3M Company and the Midwest Center for Occupational Health and Safety (MCOHS). Also I want to thank the staffs at the Campus Club, the QX Die Casting facility, and the Center for Diesel Research in Department of Mechanical engineering at University of Minnesota for providing me invaluable data.

Special thanks are extended to Girard Griggs for his proofreading and to Sook Ja Cho for her encouragement. I also want to thank Joo Yeon Hwang, Tara Oberg, Jodi Quam, Mira Grice, Monika Vadali, Carrie Rigdon, and Andrea Bartekova.

Finally, I am grateful to my gorgeous husband, Seung Won Kim, and my adorable

son, Aidan, for their love and I would like to express my gratitude to my family and friends in Korea for their incessant love and support.

Abstract

This dissertation consists of four sections which address various aspects of assessing exposure to nanoparticles and monitoring methods.

The first section examines the appropriateness of different exposure metrics using multiple-metric measurements that were carried out in multiple locations of workplaces generating incidental nanoparticles to construct aerosol maps. The concentration peaks of SA and fine particle number agreed more with locations of nanoparticle sources and showed larger concentration ratios between work areas than mass concentration. This indicates that SA and fine particle number concentrations are more appropriate for nanoparticle than mass.

The second section examines the ability of various exposure metrics to distinguish between exposure categories. Multiple-metric measurements were obtained in high and low exposure zones in workplaces generating incidental nanoparticles. SA and fine particle concentrations showed higher 'contrast' in mean concentrations and larger concentration ratios between zones than mass concentrations. The results suggest that SA and fine particle number concentrations are more efficient than mass for classifying worker exposures into categories. The results suggest that the choice of appropriate exposure metrics is critical for classifying workers into similarly exposed groups.

In the third section, SA concentrations were estimated in two ways based on

number and/or mass concentrations using aerosol instruments and compared with SA directly measured using a diffusion charger. Estimated SA was derived from particle size distribution by number and was calculated using a simple inversion method. Both estimated SA overestimated measured SA but were correlated with measured SA. The results suggest that the estimated SA may a good predictor of measured SA.

In the fourth section, three SA estimating methods were applied and evaluated based on number and/or mass concentrations measured by readily available instruments. Estimated SA was derived from particle size distribution by number and was calculated using two different inversion procedures. The estimated SA was compared with the reference SA obtained from the scanning mobility particle sizer and optical particle counter. All estimated SA had qualitatively similar trends to the reference. The results suggest that all estimation methods may be used as an interim solution for the purpose of classifying exposure zones within a workplace.

Table of Contents

List of Tables

Chapter II.

Chapter III.

Chapter IV.

Chapter V.

List of Figures

Chapter II.

Chapter III.

Chapter IV.

Chapter V.

Chapter I

Introduction & Background

Nanotechnology and nanoparticles

Nanotechnology is the manufacturing and application of materials and devices at the nanoscale (1-100 nm) by using unique characteristics of nanoparticles that are different than those of fine or coarse particles (Royal Society, 2004). Over the last two decades nanotechnology has grown rapidly. It is now considered a 21st century industrial revolution. New products have emerged from the laboratories and into the worldwide commercial market estimated to be as large as $1 trillion by 2015 (Roco, 2005). While nanotechnology has made remarkable advances, there is great uncertainty regarding the health hazards arising from this new technology.

Nanoparticles are defined as particles greater than 1 nm and smaller than 100 nm in two or three dimensions (ISO, 2008). Nano-sized particles can be formed in the environment through natural processes such as gas-to-particle conversion and aerosol emissions from plants (Maynard and Kuempel, 2005). Generally airborne nanoparticles are divided into two groups: incidentally formed and engineered nanoparticles. Incidental nanoparticles, sometimes called ultrafine particles, are particles unintentionally produced during an intentional operation. Combustion, welding, metal processing, and emissions from diesel engines are examples of major sources of incidental nanoparticles. Engineered nanoparticles are particles designed and produced intentionally to have a certain structure and size, usually less than 100 nm.

Incidental nanoparticles show more complex chemical composition, irregular shapes, and polydispersed size distribution as compared to engineered particles (Kreyling *et al.* 2006, Oberdörster et al, 2005). Although nanoparticles from different sources show

different characteristics, similar toxicological fundamentals apply because they share many particle-related factors that determine biological activities, such as small particle size and large reactive surface area (Oberdörster *et al.*, 2005, Nel *et al.*, 2006).

Particles smaller than 50 nm may obey quantum physics laws instead of classical physics and in response may exhibit physico-chemically unique optical, magnetic, and electrical characteristics which can be applied favorably in technology compared to larger particles or bulk material (Kreyling *et al.*, 2006). Another reason that makes nanoparticles much different from corresponding bulk material is their large surface area per unit mass provided by high particle counts per mass. As the diameter of particles decreases to the nanoscale, the proportion of atoms or molecules on the surface rapidly increases (Kreyling *et al.*, 2006, Oberdörster *et al.*, 2005, Welland and Porter, 2005). This may increase surface reactivity in the technical application and biologic activity in the case of human exposure. Chemical bonds on surfaces of particles are more unstable (more reactive) than those in the center. These unstable bindings may try to obtain stability through the reactions with their surroundings. Thus a higher proportion of atoms on the surface can allow a greater likelihood of interactions with biologically reactive groups that may cause further toxicity (Bell, 2007, Kreyling *et al.*, 2006).

Toxicity of nanoparticles

The toxicological mechanisms of nano-sized particles are being explored but their unique characteristics - small size, increased surface area per unit of mass, and surface reactivity- have been believed to play an important role in adverse health effects

(Gwinn and Vallyathan, 2006, Nel *et al.*, 2006).

The first characteristic of nanosized particles related to their toxicity is size. The extremely small size compared to cell structures could lead to increased probability of transfer to epithelial lining cells and could cause more pulmonary toxicity (Donaldson *et al.*, 2001, Nel *et al.*, 2006). Some toxicological research showed that the low toxic particles in the fine size range could become more toxic as nano-sized particles (Oberdörster *et al.*, 1992, Oberdörster *et al.*, 1994, Renwick *et al.*, 2001, Ferin 1992). Titanium dioxide (TiO_2) had been known as a low soluble and low toxic material. However, Oberdörster *et al.* (1992) found that TiO_2 ultrafine particles (~ 20 nm) deposited in the alveolar region of rat lungs caused greater inflammatory responses and accessed the interstitium more easily than TiO_2 fine particles (~ 200 nm).

Nanoparticles are cleared by alveolar macrophages less effectively than larger particles (Kreyling *et al.*, 2006). Macrophage phagocytosis in the alveolar regions plays an important role in particle clearance from the lung. Nanoparticles with large surface areas can be an overload even at low mass concentrations and cause impairment of the clearance mechanism (Ferin *et al.*, 1992). Renwick *et al.* (2001) found that macrophages exposed to ultrafine particles were damaged more than those exposed to fine particles on an equal mass basis. This could prevent macrophage phagocytosis of other particles and, consequently, increase the burden in the lung and cause inflammation.

Several studies demonstrated that ultrafine particles brought about more oxidative stress than fine particles (Li *et al.*, 1996, Wilson *et al.*, 2002, Stone *et al.*, 1998). These results were attributed to a large surface area and number of particles per unit mass of nanoparticles. While the mechanism is not clear, it is thought that reduced phagocytosis

could increase interaction between ultrafine particles and the epithelium and increase oxidative stress due to the large surface area of nanoparticles. This oxidative stress and free radical formation from the surface of the ultrafine particle induces pro-inflammatory cytokine and chemokine production (Donaldson *et al.*, 2001). Inflammation via oxidative stress in the lung can lead to airway diseases such as chronic obstructive pulmonary disease (COPD) and asthma (Donaldson and Stone, 2003, MacNee and Donaldson, 2003).

After inhalation, nanoparticles may be able to translocate from the alveolar region in the lung to the extra-pulmonary organs (liver, heart, spleen, etc.) via systemic blood circulation. There is some toxicological evidence of nano-size particles translocating in humans (Nemmar *et al.*, 2002) and in animals (Kreyling *et al.*, 2002, Takenaka *et al.*, 2001, Oberdörster *et. al*., 2002). More recently, Oberdörster *et al.* (2004) found that the central nervous system (CNS) could be targeted by airborne solid ultrafine particles through deposition on the olfactory mucosa in the nasopharyngeal region and subsequent translocation via the olfactory nerve. Therefore, nanoparticles may cause adverse effects on the whole body as well as the respiratory organs.

Measurement of health related exposure metrics

The choice of a more appropriate exposure metric will be critical to determine an exposure-response relationship. For occupational exposure assessment, workers are assigned to similar exposure groups (SEGs). Each SEG represents a group of workers believed to have the same general exposure profile (Mulhausen and Damiano, 1998). Designating SEGs appropriately based on the correct exposure information is important

for future occupational epidemiologic studies that will investigate the relationship between aerosol contaminants and health effects. If exposure concentration is determined by a less relevant exposure metric when assigning workers to categories, then workers could be misclassified into incorrect categories resulting in a less exposure-response association (Flegal *et al.*, 1991).

Ever since a good correlation between pneumoconiosis and particle mass concentration was determined (Chamberlain *et al.*, 1970), mass concentration has been used as the most appropriately associated exposure metric with ill health for particle exposures except for fiber exposures. Occupational exposure limits for particles exposure were established based on the mass concentration. However, the appropriateness of the mass concentration metric for nanoparticles has been called into question because nanoparticles feature high particle counts and large surface area per mass. Exposure assessments using mass concentration of ultrafine particles will underestimate their toxicity because nanoparticles do not contribute much to the total mass concentration despite their high numbers. Kreyling *et al.* (2003) reported that the proportion of nano-sized particles is less than 10% of PM2.5 concentrations in terms of mass but more than 90% of the fine particle number concentration. Thus, a case could be made that mass based occupational exposure limits for nanoparticles should be re-evaluated and other factors such as number or surface should be considered seriously.

Serita *et al.* (1999) exposed rats to different concentrations of ultrafine nickel particles and found that only a single exposure of ultrafine nickel particles caused severe lung damage at the Japanese occupational exposure limit (1 mg/m^3) established based on

fine nickel particle data. Thus, for the purpose of controlling or managing nanoparticle exposures, mass based exposure limits may not useful or effective.

A change of the exposure paradigm for nano-sized particles from a mass basis has been suggested (Maynard and Aitken, 2007, Kreyling *et al.*, 2006). Particle number and surface area concentrations have been proposed as alternative metrics. The number metric (particle count per unit air volume) has been used previously for asbestos and fiber exposure assessment. Aerosol instruments using the principle of vapor saturation and condensation are used for measuring number concentrations but usually they cannot distinguish particles emitted from the process of concern and background particles (Maynard and Kuempel, 2005). However, the number concentration metric is most sensitive to particle emission sources and can be used to identify particle generation sources (Brouwer *et al.*, 2004, Peters *et al.*, 2006).

McCawley *et al.* (2001) showed that particle number concentration was the more appropriate metric for chronic beryllium disease and found no correlation between mass and number concentration. Peters *et al.* (1997) found that a decrease of peak expiratory flow (PEF) among 27 nonsmoking asthmatics had stronger association with number concentration than mass concentration.

Recently, surface area concentration has been highlighted for characterizing exposure to nanoparticles (Maynard 2003). Several toxicological studies have shown that the inflammatory responses in the lung by low solubility ultrafine particles and fine particles showed a better dose-response relationship with surface area deposited regardless of particle size (Oberdörster *et al.*, 2000, Trans *et al.*, 2000, Brown *et al.*, 2001, Monteiller *et al.*, 2007). Driscoll (1996) demonstrated that overload tumors were best

correlated with surface area, and not number or mass concentration. The damage of particle clearance was related to lung surface area dose, not to lung mass dose for non-toxic particles like TiO_2 and Ba_2SO_4 (Tran *et al.*, 2000).

There are a few epidemiological studies that explore the relationship between surface area metrics and health outcomes. Schwartz and Marcus (1990) have analyzed daily air pollution measurements expressed as mass concentrations and mortality and found a nonlinear relationship between them. Using the same data set but converting the mass concentrations into surface area concentrations, Maynard and Maynard (2002) have shown a linear relationship between the ambient aerosol surface area and mortality data. This indicates that the surface area metric may be a more suitable metric for aerosol exposure. Significant reduction of lung function and increases in pulmonary symptoms among Austrian children 7 to 10 years of age have been found with increases in surface area concentration (Moshammer and Neuberger, 2003).

Even though many toxicological studies have reported better dose-response relationships with surface area versus mass concentrations, the toxicological mechanisms of nanoparticles regarding surface area dose have not yet been understood completely. At present, no scientific consensus exists for the appropriate exposure metric for nano-sized particles (Paik *et al.* 2008, Maynard and Aitken 2007). Therefore, a multi-metric sampling approach appears to be reasonable at this point.

Maynard and Aitken (2007) evaluated the relevance of four different metrics (mass, number, surface area, and length) to nine classes of engineered nanoparticles. They also factored in each nanoparticles' characteristics that could influence a health effect of concern. The surface area metric was found to be the most relevant for various types of

engineered nanoparticles and attribute combinations, and the mass metric was useful for some combinations. They proposed the development of a universal aerosol monitor that can measure particle mass, number, and surface area simultaneously. This is a meaningful approach to the nanoparticle measurement question. An array of available aerosol instruments for multiple-metric measurements is possible and can be a practical solution. This will provide scientists and industrial hygienists with much needed tools that are necessary to yield better characterization of nanoparticles exposure.

The multiple-metric sampling has been used for characterizing incidental nanoparticles exposure (Ramachandran *et al.*, 2005, Heitbrink *et al.* 2009). Ramachandran *et al.* (2005) conducted exposure assessments using multiple metrics including active surface area, particle counts, mass, and elemental carbon mass concentrations. They characterized three job groups – bus drivers, bus mechanics, and parking garage attendants – and found that the exposure groups presented different exposure rankings depending on the metrics chosen. Heitbrink *et al.* (2009) measured active surface area, respirable mass, and particle number concentrations simultaneously in an automotive engine plant to investigate the relationship among several exposure metrics. They investigated the relationships between different exposure metrics; active surface area concentrations showed a strong correlation with number concentration and a weak relationship with mass concentration. These studies suggest that the stand-alone mass concentration metric cannot be a surrogate for number or surface area concentration metrics.

Measurement and estimation of surface area concentrations

Although several studies have suggested that surface area is a better metric than others, this needs to be confirmed for its appropriateness in occupational and environmental settings through epidemiological studies. As mentioned above, toxicological studies demonstrating the significance of the surface area metric for nanoparticle exposure have measured geometric surface area using the Brunauner Emmett Teller (BET) gas adsorption method or transmission electron microscope (TEM) analysis. This indicates the significance of geometrical surface area with regard to biological responses. Therefore, more accurate measurement of geometric surface area is needed to determine the true values. BET and TEM are potentially good standard methods for surface area measurements. However, they are not real time measurements and present other practical problems. These measurements require a large mass for each sample and difficult analysis process and are labor.

Only a few devices are currently available to measure surface area concentration. Many of them are research grade instruments and not designed for routine measurements in the workplaces. The first device developed for surface area measurement was the epiphaniometer that determines the mass transport rate of a gas-phase radionuclide to aerosol. The mass transport rate is proportional to the Fuchs surface area (McMurry, 2000). This device is not appropriate for occupational environments due to its radioactive source (Maynard 2003).

Recently, TSI Inc. has developed a nanoparticle surface area monitor for use in occupational environments that measures surface area of particles that have the ability to

be deposited in the tracheobronchial (TB) or the alveolar regions of the human lung (Shin *et al.* 2007). The particles in the sampled aerosol are charged with unipolar positive ions by diffusion in a mixing chamber. The electric charge on the particles are measured in an electrometer and are proportional to the surface area of lung-deposited surface area based on the ICRP (International Commission on Radiological Protection) lung deposition model for a reference worker (ICRP 1994).

The LQ1-DC diffusion charger (Matter Engineering, Switzerland) contains an aerosol diffusion charger and an electrometer to measure the attachment rate of unipolar ions to particles, and directly measures Fuch's or active surface area. On the other hand, the portable diffusion charger can be used in occupational settings. While it underestimates the surface area of particles with diameters larger than 100 nm, the measurements are comparable to the geometric surface area for particles less than 100 nm (Ku and Maynard 2005). One additional challenge is that there is no standard method or standard particle with which to calibrate these instruments.

Since commercially available devices are limited, alternative methods to estimate surface area need to be explored based on aerosol measurements. If a relationship between different metrics was known and size distributions or particle generation characteristics were consistent, surface area concentrations could be estimated using the relationships such as a surface area to mass ratio or surface area to number ratio (NIOSH, 2009). Also surface area can be estimated using particle size distribution characteristics. If an estimation method based on a small number of simple measurements can be developed, it would be useful in determining the best exposure metric for assessing exposure to nanoparticles.

Woo *et al.* (2001) estimated surface area concentrations using three measurements: number, mass, and charge. The size distribution parameters were determined by minimizing the difference between measured and theoretical values based on an assumed aerosol size distribution and instrument calibrations. The calculated surface area concentrations obtained by integrating the retrieved aerosol size distributions showed systematically higher but good agreement with those from the measured particle size distribution. However, the instruments used in that study (an electrical aerosol detector and a research grade particle counter) are neither widely available nor easily usable in the occupational and environmental fields for exposure assessments.

Maynard (2003) developed a surface area estimation method based on mass and number concentration measurements by assuming a lognormal aerosol size distribution with a specific geometric standard deviation. Although the surface area values estimated using this method are up to four times greater than the values calculated using measured number size distributions, the correlation between them was high (R^2=0.98). This result provides a positive prospect for estimating surface area concentration from number and mass measurements using readily available occupational health instruments.

If particle size distribution is known, total aerosol surface area concentration can be calculated using size distribution parameters under some assumptions such as the spherical shape of particles. In the case of no direct measurements for the particle size distribution, it could be retrieved from a set of discrete measurements through inversion techniques. Such techniques reconstruct unknown parameters of a system from indirect measurements. Inversion methods have been used for cascade impactors, a parallel diffusion battery, and light scattering measurement in aerosol science (Fiebig *et al.* 2005,

Ramachandran *et al.* 1996). Ramachandran and Vincent (1997) used a chi-square minimization of the differences between actual and calculated measurements. They assumed a log-normal particle size distribution to reconstruct continuous particle size distribution from the discrete sets of personal cascade impactor measurements. From the reconstructed size distribution, the inhalable, thoracic, and respirable fractions were determined well. If the aerosol is assumed to be unimodal with a lognormal size distribution, it can be described by three unknown parameters: the median diameter, the GSD, and the total concentration. Three independent measurements are needed to obtain the three unknown values.

Research objectives

The long-range goal of this research is to determine the most relevant exposure metrics for nanoparticle exposure assessment. The objectives of this study are twofold. First, to characterize worker's exposures to nanoparticles in three incidental nanoparticle generating workplaces using multiple exposure metrics. Second, to develop surface area estimation methods based on the currently available monitoring methods.

This research is unique in that it (1) uses various parameters calculated from different exposure metrics such as exposure rankings, concentrations ratios, and statistical mean differences between different exposure categories to find appropriate exposure metrics for nanoparticles; (2) introduces statistical parameters calculated from the exposure variability to evaluate the efficiency of exposure metrics to classify exposure groups; (3) examines practical surface area estimating methods

using particle size distribution statistics as interim solutions prior to a broader use of surface area monitoring instruments.

The rationale for this study is that a more appropriate exposure metric for nanoparticles will allow for more accurate evaluation of nanoparticle exposure, contribute to better exposure-response relationship, and eventually protect workers' safety and health in nanotechnology fields. To achieve the objectives, the specific aims for this study are:

1. Examine aerosol spatial concentration distributions measured simultaneously by different exposure metrics and the appropriateness of different exposure metrics
2. Characterize nanoparticle exposure in two different exposure zones in three different workplaces using multiple metric measurements and evaluate the ability of various exposure metrics to distinguish between exposure categories using contrast and precision, exposure ranking, and concentration ratios between different exposure categories.
3. Evaluate surface area estimation methods based only on mass and/or number concentration measurements (which are routinely used in the industrial and environmental hygiene fields) and determine if the estimated surface area concentration can predict the reference surface area concentration.

References

Aitken R.J., Creely K.S., Tran C.L., 2004. Nanoparticles: An occupational hygiene review. HSE Research Report 274. Available from URL http://www.hse.gov.uk/research/rrpdf/rr274.pdf. Accessed July 2009

Bell T. E., 2007. Understanding risk assessment of nanotechnology. Available from URL http://www.nano.gov/Understanding_Risk_Assessment.pdf. Accessed June 2009.

Brouwer D.H., Gijsbers J.H.J., Lurvink M.W.M., 2004. Personal exposure to ultrafine particles in the workplace: exploring sampling techniques and strategies. Annals of Occupational Hygiene 48, 439-453.

Brown, D.M., Stone V., Findlay P., MacNee W., Donaldson K., 2000. Increased inflammation and intracellular calcium caused by ultrafine carbon black is independent of transition metals or other soluble components. Occupational and Environmental Medicine **57,** 685-691.

Chamberlain E.A.C., Makower A.D., Walton W.H., 1970. New gravimetric dust standards and sampling procedures for British coal mines. Inhaled particles III. Unwin Brothers Ltd., London, UK pp.111-124.

Donaldson K., Stone V., 2003. Current hypotheses on the mechanisms of toxicity of ultrafine particles. Annl 1st Super Sanita 39, 405-10.

Donaldson K., Stone V., Clouter A., Renwick L., MacNee W., 2001. Ultrafine Particles. Occup Environ Med 58, 211-216.

Driscoll K.E., 1996. Role of inflammation in the development of rat lung tumors in response to chronic particle exposure. Inhalation Toxicology 8(suppl), 139–153.

Ferin J., Oberdörster G., Penney. D.P., 1992. Pulmonary retention of ultrafine and fine particles in rats. American Journal of Respiratory Cell Molecular Biology 6, 535-542.

Fiebig M., Stein C., Schröder F., Feldpausch P., Petzold A., 2005. Inversion of data containing information on the aerosol particle size distribution using multiple instruments.

Journal of Aerosol Science 36, 1353-1372.

Flegal, K.M., Keyl P.M., Nieto F.J., 1991. Differential misclassification arising from nondifferential errors in exposure measurement. American Journal of Epidemiology 134, 1233-1241.

Gwinn, M.R., Vallyathan V., 2006. Nanoparticles: Health Effects-Pros and Cons. Environmental Health Perspectives 114, 1818-1825.

Heitbrink W.A., Evans D.E., Ku B.K., Maynard A.D., Slavin T.J., Peters T.M., 2009. Relationships among particle number, surface area, and respirable mass concentrations in automotive engine manufacturing. Journal of Occupational Environmental Hygiene 6, 19-31.

International Commission on Radiological Protection (ICRP), 1994. International Commission on Radiological Protection Publication 66 Human Respiratory Tract Model for Radiological Protection, New Youk, Elsevier Science Ltd.

International Organization for Standardization (ISO), 2008. ISO/TS 27687:2008 Terminology and definitions for nanoparticles.

Kreyling W.G., Tuch T., Peters A., Pitz M., Heinrich J., Stolzel M., Cyrys J., Heyder J., Wichmann H.E., 2003. Diverging long-term trends in ambient urban particle mass and number concentrations associated with emission changes caused by the German unification. Atmospheric Environment 37, 3841-3848.

Kreyling W.G., Semmer-Behnke M., Möller W., 2006. Health implications of nanoparticles. Journal of nanoparticle research 8, 543-562.

Ku B.K., Maynard A.D., 2005. Comparing aerosol surface-area measurements of monodisperse ultrafine silver agglomerates by mobility analysis, transmission electron microscopy and diffusion charging. Journal of Aerosol Science 36, 1108-1124.

Li X.Y., Gilmour P.S., Donaldson K., MacNee W., 1996. Free radical activity and pro-inflammatory effects of particulate air pollution (PM_{10}) *in vivo and in vitro*. Thorax 51, 1216-1222.

MacNee W., Donaldson K., 2003. Mechanism of lung injury caused by PM_{10} and

ultrafine particles with special referance to COPD. European Respiratory Journal **21,** 47S-51S.

Maynard A.D., 2003. Estimating Aerosol Surface Area fro Number and Mass Concentration Measurements. Annals of Occupational Hygiene 42, 123-144.

Maynard A.D., Kuempel R.D., 2005. Airborne nanostructured particles and occupational health. Journal of nanoparticle Research 7, 587-614.

Maynard A.D., Aitken R.J., 2007. Assessing exposure to airborne nanomaterials: Current abilities and future requirements. Nanotoxicology 1, 26-41.

Maynard A.D., Stone V., 2005. Airborne nanostructured particles and occupational health. Journal of nanoparticle research 7, 587-614.

Maynard, A.D., Maynard R.L., 2002. A derived association between ambient aerosol surface area and excess mortality using historic time series data. Atmospheric Environment 36, 5561-5567.

McCawley M.A., Kent M.S., Berakis M.T., 2001. Ultrafine beryllium number concentration as a possible metric for chronic beryllium disease risk. Applied Occupational Environmental Hygiene 16, 631-638.

McMurry P.H., 2000. A review of atmospheric aerosol measurements. Atmospheric Environment 34, 1959-1999.

Monteiller, C., Tran L., MacNee W., Faux S., Jones A., Miller B., Donaldson K., 2007. The pro-inflammatory effects of low-toxicity low-solubility particles, nanoparticles and fine particles, on epithelial cells in vitro: the role of surface area. Occupational Environmental Medicine 63, 609-615.

Moshammer H., Neuberger M, 2003. The active surface of suspended particles as a predictor of lung function and pulmonary symptoms in Austrian school children. Atmospheric Environment **37,** 1737-1744.

Mulhausen J.R., Damiano J., 1998. A strategy for assessing and managing occupational exposures, AIHA Press, Fairfax USA.

National Institute for Occupational Safety and Health (NIOSH), 2009. Approaches to Safe Nanotechnology; An Information Exchange with NIOSH. Available from URL www.cdc.gov/niosh/topics/nanotech/nano_exchange.html. Accessed July 2009.

Nel A., Xia T., Madler L.V., Li N., 2006. Toxic Potential of Materials at the Nanolevel. Science 311, 622-627.

Nemmar, A., Hoet P.H.M., Vanquickenborne B., Dinsdale D., Thomeer M., Hoylaerts M.F., Vanbilloen H., Mortelmans L., Nemery B., 2002. Passage of inhaled particles into the blood circulation in humans. Circulation **105,** 411-414.

Oberdörster G, Oberdörster O. E., Oberdörster J., 2005. Nanotoxicology: An Emerging Discipline Evolving from Studies of Ultrafine Particles. Environmental Health Perspectives 113, 823-839.

Oberdörster G., 2000. Toxicology of ultrafine particles: in vivo studies. Philosophical transactions of the Royal Society of London A 358, 2719-2740.

Oberdörster, G., Ferin J., Lehnert B.E., 1994. Correlation Between Particle-Size, in-Vivo Particle Persistence, and Lung Injury. Environmental Health Perspectives 102(S5), 173-179.

Oberdörster, G., Ferin J., Gelein R., Soderholm S.C., Finkelstein J., 1992. Role of the alveolar macrophage in lung injury: Studies with ultrafine particles. Environmental Health Perspectives 97, 193-199.

Oberdörster, G., Sharp Z., Atudorei V., Elder A., Gelein R., Lunts A., Kreyling W., Cox C., 2002. Extrapulmonary translocation of ultrafine carbon particles following whole-body inhalation exposure of rats. Journal of Toxicology and Environmental Health Part A **65,** 1531-1543.

Paik S.Y., Zalk D.M., Swuste P., 2008. Application of a pilot control banding tool for risk level assessment and control of nanoparticle exposures. Annals of Occupational Hygiene 52, 419-428.

Peters A., Wichmann H.E., Tuch T., Heinrich J., Heyder J., 1997. Respiratory effects are associated with the number of ultrafine particles. American Journal of Respiratory

Critical Care Medicine 155, 1376-1383.

Peters, M.T., Heitbrink W.A., Evans D.E., Slavin T.J., Maynard A.D., 2006. The mapping of fine and ultrafine particle concentrations in an engine machining and assembly facility. Annals of Occupational Hygiene 50, 249-257.

Ramachandran G., Paulsen D., Watts W., Kittelson D., 2005. Mass, surface area and number metrics in diesel occupational exposure assessment. Journal of Environmental Monitoring 7, 728-735.

Ramachandran G., Johnson E.W., Vincent J.H., 1996. Inversion techniques for personal cascade impactor data. Journal of Aerosol Science 27, 1083-1097.

Ramachandran G., Vincent J.H., 1997. Evaluation of Two Inversion Techniques for Retrieving Health-Related Aerosol Fractions from Personal Cascade Impactor Measurements. American Industrial Hygiene Association Journal 58, 15–22.

Renwick, L.C., Donaldson K. Clouter A., 2001. Impairment of alveolar macrophage phagocytosis by ultrafine particles. Toxicology and Applied Pharmacology 172, 119-127.

Roco M.C., 2005. Environmentally responsible development of nanotechnology. Environmental Science and Technology 39, 106A-112A.

Royal Society, 2004. Nanosicence and nanotechnology; opportunities and uncertainties. Available from URL http://www.nanotec.org.uk/report/Nano%20report%202004%20fin.pdf. Accessed July 2009.

Schwartz J., Marcus A., 1990. Mortality and air pollution in London: A time series analysis. American Journal of Epidemiology 131, 185-194.

Serita F., Kyono H., Seki Y., 1999. Pulmonary clearance and lesions in rats after a single inhalation of ultrafine metallic nickel at dose levels comparable to the threshold limit value. Industrial Health 37, 353-363.

Shin W.G., Pui D.Y.H., Fissan H., Neumann S., Trampe A., 2007. Calibration and numerical simulation of Nanoparticle Surface Area Monitor (TSI Model 3550 NSAM).

Journal of Nanoparticle Research 9, 61-69.

Stone, V., Shaw J., Brown D.M., MacNee W., Faux S.P., Donaldson K., 1998. The role of oxidative stress in the prolonged inhibitory effect of ultrafine carbon black on epithelial cell function. *Toxicology in Vitro* **12,** 649-59.

Takenaka, S., Karg E., Roth C., Schulz H., Ziesenis A., Heinzmann U., Schramel P. Heyder J., 2001. Pulmonary and systemic distribution of inhaled ultrafine silver particles in rats. Environmental Health Perspectives **109,** 547-551.

Tran C.L., Buchanan D, Cullen R.T., Searl A., Jones A.D., Donaldson K., 2000. Inhalation of poorly soluble particles. II. Influence of particle surface area on inflammation and clearance. Inhalation Toxicology 12, 1113-1126.

Welland M., and A. Porter (2005). Why Nanoparticles Are Different? Available from URL http://www.royalsoc.ac.uk/downloaddoc.asp?id=2372. Accessed July 2009.

Wilson M.R., Lightbody J.H., Donaldson K., Sales J., Stone V., 2002. Interactions Between Ultrafine Particles and Transition Metals *in vivo* and *in vitro*. Toxicology Applied Pharmacology 184,172-179.

Woo K., Chen D., Pui DYH., Wilson WE. (2001) Use of Continuous Measurements of Integral Aerosol Parameters to Estimate Particle Surface Area. *Aerosol Science and Technology*; 34:57-65.

Chapter II

Determination of workplace nanoparticle exposure rankings by spatial mapping of particle mass, number, and surface area concentrations

Measurements using several exposure metrics were carried out in a restaurant and a die casting plant to compare the spatial distributions of particle number, mass, and surface area (SA) concentrations and establish exposure rankings of similar exposure groups (SEGs) for those metrics. The appropriateness of different exposure metrics for incidental nanoparticle and fine particle exposures was evaluated using the exposure rankings, statistical differences among groups, and concentration ratios between different exposure groups. In the die casting plant, group exposure rankings and spatial distributions differed by the exposure metrics chosen. SA and fine particle number concentrations were greatest near incidental nanoparticle sources and were significantly different among three exposure areas. However, mass and coarse particle number concentrations were found to be similar throughout the facility and rankings of the work areas based on these metrics were different from those of SA and fine number concentrations. In the restaurant, concentrations in the kitchen for all metrics were significantly higher than in the serving area, although SA and fine particle number concentrations showed larger differences between the two areas than either the mass or the coarse particle number concentrations. Thus, the choice of appropriate exposure metric has significant implications for exposure groupings in epidemiological and occupational exposure studies.

Introduction

The choice of appropriate exposure metrics that are biologically relevant and reflect the physical characteristics of nanoparticles will be important for accurate assessments of

exposure to nanoparticles and determining a dose-response relationship. The mass concentration metric, which has traditionally been used for aerosol exposure assessment, may not be appropriate for nanoparticle exposure because nanoparticles frequently account for only a small fraction of the total mass concentration (Ramachandran et al. 2005, Heitbrink *et al*. 2007, Maynard and Aitken 2007).

Numerous epidemiologic, *in vivo*, and *in vitro* studies have found an association between cardiovascular/pulmonary diseases and ambient fine particle exposure, and it has been suggested that the ultrafine component of fine particles may be the etiologically relevant metric (Brook *et al.*, 2004, Brown *et al.*, 2001, Dick *et al.*, 2003, Dockery *et al.*, 1993, Pope *et al.*, 1999, Pope *et al.*, 2004, Sun *et al.*, 2005). Particle number concentrations are dominated by the ultrafine and fine particles (Hinds 1999). Their unique characteristics - small size, increased surface area (SA) per unit of mass, and surface reactivity- are thought to play an important role in adverse health effects (Gwinn and Vallyathan, 2006, Nel *et al.*, 2006).

Increased attention is being given to number and SA exposure concentration metrics as more relevant measures for nanoparticle exposure assessment than mass concentration metrics. Ramachandran *et al*. (2005) conducted exposure assessments in three job groups – bus drivers, bus mechanics, and parking garage attendants – using active surface area, particle number, and elemental carbon mass concentrations. They found that the exposure groups presented different exposure rankings depending on the metrics chosen. Heitbrink *et al*. (2009) measured active surface area, respirable mass, and particle number concentrations simultaneously in an automotive engine plant to investigate the relationship among several exposure metrics. They showed that active surface area

concentrations showed a strong correlation with number concentration and a weak relationship with mass concentration. These studies suggest that the mass concentration metric cannot be a surrogate for number or SA concentration metrics.

Spatial concentration mapping is a technique that can be used to represent voluminous field data in a more comprehensible form that allows easier visualization of spatial or temporal variability of the aerosol concentration distributions in a given workplace. This approach can be used as a pre-survey tool to identify contaminant sources or determine the sampling locations for exposure assessment. Dasch *et al*. (2005) constructed aerosol maps in automotive plants using mass concentration. The maps were used as a quantitative tool to develop cost-effective engineering controls. In a workplace utilizing metalworking fluids (MWFs), O'Brien (2003) used mapping to represent the spatial distribution of MWF exposure using mass concentration before and after installation of mist collectors. He also combined the aerosol map with the locations of cases and controls. Based on the map and job locations, three different exposure categories – low, medium, and high – were classified. Hypersensitivity pneumonitis (HP) incidence rates calculated by exposure categories suggested a relationship between exposure to MWF mists and HP occurrence. Peters *et al*. (2006) conducted multi-metric measurements that included mass, number, and SA concentrations for aerosol mapping. They constructed number and mass maps that were used to investigate temporal variability and to find sources that were not generated by the main process.

Concentration mapping can be utilized to classify similar exposure groups (SEGs) within a workplace. SEGs are defined as "groups of workers believed to have the same general exposure profile due to the similarity and frequency of the tasks they perform, the

materials and processes with which they interact, and the similarity in the way they perform the tasks" (Mulhausen and Damiano, 1998). Designating SEGs appropriately based on the correct information is important for exposure assessment and management and for future occupational epidemiologic studies that will investigate the relationship between aerosol contaminants and health effects.

In this study, aerosol measurements for mapping were made to determine the spatially-distributed aerosol concentration in two occupational settings. One was in a restaurant and the other was in an aluminum die casting plant. Incidental nanoparticles were generated in both settings. They are called by some as ultrafine particles and defined as particles smaller than 100 nm, unintentionally produced during an intentional operation (Gwinn and Vallyathan, 2006). Several direct reading aerosol monitors were used to measure the exposure metrics of interest. The purposes of this study were to compare the spatial distributions of particle number, mass, and SA concentrations and to evaluate the appropriateness of the different exposure metrics for nanoparticle exposure assessment using the exposure rankings, statistical differences among groups, and concentration ratios between different worker groups.

Methods

Description of facilities

The concentration mapping measurements took place in a restaurant and an

aluminum die-casting plant in Minnesota. The restaurant was a faculty club establishment rather than a general retail restaurant. As shown in Figure 1-(a), it was divided into two areas: a kitchen and a serving area. The serving area included a serving station for attendants, bar, general seating area, private rooms, and a hallway. It did not have any combustion sources. The kitchen area was composed of a baking oven area, a cooking grill area, and a dish washing area. The oven area had gas burners, flat top grills, and gas convection ovens that are all sources that can generate combustion particles. Most foods were prepared in the oven area. The grill area was for serving food to customers during lunch time. Most entrees were prepared in the oven area, while other foods were warmed or made-to-order in the grill area. The deep fryers, flat top grills, and gas grill were located in a corner of the grill area. The restaurant air was circulated by a heating, ventilating, and air-conditioning (HVAC) system. Cooking appliances were equipped with canopy hoods that draw air from the vicinity of the appliances.

The die casting plant produced aluminum alloy products. As shown in Figure 1-(b), it was divided into three sections: die casting, trim/repair, and machining. The sections were physically separated with walls that each had two openings. The die casting area contained two large furnaces to melt aluminum, seven die casting machines that received the molten aluminum, and two trim presses. Aluminum was melted in the furnaces and delivered to each die casting machine by forklift trucks. In the trim/maintenance area, the castings were trimmed to size in the trim presses and then stacked and stored. The dies were repaired in the tool repair section. Trimmed castings were sent to the machining area, where milling, broaching, and turning machines were utilized to finish the castings.

Sampling equipment

In both occupational environments, aerosol measurements were obtained to determine the spatially distributed concentrations in each workplace using five different real-time instruments: two aerosol photometers (DustTrak Model 8520 TSI Inc., Shoreview, MN) with PM1.0 and respirable sampling inlets for particle mass concentrations, a condensation particle counter for number concentration (P-Trak Model 8525, TSI Inc., Shoreview, MN), a handheld optical particle counter for size distribution by number (AeroTrak^{TM} Model 8220, TSI Inc., Shoreview, MN, or HHPC-6, Hach Ultra, Grants Pass, Oregon), and a surface area monitor for deposited alveolar SA concentration (AeroTrak^{TM} Model 9000, TSI Inc., Shoreview, MN).

The DustTrak is a light-scattering laser photometer to measure aerosol mass concentration. The intensity of the scattered light is a function of the particle mass concentration, the size distribution of the aerosol, and the composition of the aerosol drawn. It can measure size-selective particle concentrations corresponding to the respirable fraction, PM2.5, or PM1.0 using various sampling inlet conditioners such as impactors or cyclones.

The P-Trak is a real-time condensation particle counter (CPC) that counts single particles with diameters from 0.02 µm to greater than 1.0 µm after growing them by condensation in a super-saturated alcohol atmosphere. The range of the instrument is from 0 to 500,000 particles/cm^3.

A handheld optical particle counter (OPC) was also used. An OPC simultaneously

counts particles larger than 0.3 µm in diameter in six different size bins to give particle size distributions by number. The size bins were 0.3 to 0.5 µm, 0.5 to1.0 µm, 1.0 to 2.5 µm, 2.5 to 4.0 µm, 4.0 to 10.0 µm, and >10.0 µm. It detects single particles and their pulse intensity to simultaneously count and size particles into the size bins via light scattering.

The surface area monitor measured the SA of particles that have the ability to be deposited in the tracheobronchial (TB) or alveolar regions of the human lung (Shin *et al.* 2007). The particles in the sampled aerosol are charged with unipolar positive ions by diffusion in a mixing chamber. The electric charges on the particles were measured in an electrometer and were proportional to the SA of lung deposited particles based on the ICRP (International Commission on Radiological Protection) lung deposition model (1994) for a reference worker. For this study, the monitor was set on the alveolar deposition mode.

For easy portability, a mobile sampling cart was used to transport the instruments to each sampling location. A plastic mannequin was placed on the top section of the sampling cart to hang sampling tubes at breathing zone height. The photometers and an OPC were placed on the top shelf; the SA monitor and CPC were positioned on the middle shelf. All instruments were battery-operated with attached conductive sampling tubing measuring no longer than 1 m in length and 0.95 cm in diameter. The inlets of sampling tubes were set close together. Electronic data from each device were downloaded to a laptop computer and then exported to text files for further analysis.

Mapping measurements

Each workplace was divided into a grid based on its size. To reduce temporal variability, an entire set of mapping measurements was completed within a two hour period. Two minutes were required to obtain measurements at each grid point. The first minute was used for sampling and the second minute was used to move the sampling cart to the next location. In two hours, a maximum of sixty grid points could be measured. The equation

$$\frac{Total\ area\ of\ a\ workplace(m^2)}{60\ data\ points} = basic\ measurement\ unit(m^2\ /\ point) \qquad (1)$$

was used to determine the spacing between sampling points in each workplace. In the restaurant, the spacing of the mapping measurements was every 13 m^2. However, finer resolution (1.4 m^2) was used near the generation sources and a coarser grid (52 m^2) was applied in the seating area. In the die casting facility, measurements were taken every 52 m^2.

Before measurements commenced in each facility, colored tape was applied to the floor at each grid point to mark the sampling points. Colored tape was also applied to the cart at the center of each shelf's front surface. Prior to sampling, the center of the cart and the grid point were aligned. For consistent sampling, sampling inlet directions were recorded using an arrow on the map during the first set of measurements and this orientation was maintained for all the three days of measurement. The sampling inlets faced the nearest generation source.

There are two primary temporal scenarios for mapping measurements: workplaces having a regular and constant job schedule through the entire shift as in a die casting

facility, and workplaces having distinctive peak/off-peak time such as a kitchen in a restaurant. In the former case, the measurement can be made at anytime. In the latter case, measurements should be taken at around the time of the peak particle levels. Therefore, measurements were conducted in the restaurant during the lunch rush (11:00 am – 1:00 pm) and were started at the same time on each of the three measurement days to ensure consistent measurements.

All instruments were synchronized with standard time on a computer just before every sampling event. The P-trak and the Aerotrak were programmed to turn on and off automatically. The DustTraks and the OPC were turned on and off manually. All instruments were checked for normal operation and zero-calibrated prior to each sampling event.

Particle maps were created using the various concentration measurements for the three days. Arithmetic average concentrations were used to construct the particle maps. Gray coded contour plots were generated and used to construct an easy to read concentration map and to help visualize the nanoparticle concentrations by different metrics using mapping software (Surfer 8.0, Golden, CO).

Statistical analysis

The geometric mean (GM) and geometric standard deviation (GSD) were calculated for each area within a workplace. A one-way ANOVA (analysis of variance) test was used to determine if the GM of each metric was different between areas. A Duncan's multiple range test was performed to determine the areas that were significantly

different. For a non-parametric test, exposure concentrations at each sampling point were changed to ranks in ascending order for each metric. An ANOVA test was performed to test the hypothesis that exposure rankings may differ by various metrics, using an interaction term with areas and different exposure metrics. This test shows whether all metrics had the same mean exposure rankings between (or among) different areas. Statistical analyses were conducted using SAS 9.1 (SAS Institute Inc., Cary NC).

Results

Fig. 2 and 3 show the aerosol concentrations by each metric in the restaurant and die cast factory, respectively. The "+" marks represent the sampling grid locations. Tables 1 and 2 present the summary of particulate matter measurements by various exposure metrics during the mapping measurements in the restaurant and die casting facility. In Table 2, the column named "rank" is the exposure rankings by each exposure metric for three groups. Also in Table 2, the group code from the Duncan multiple range tests tells us which groups are significantly different from one another.

Restaurant

In the restaurant, concentrations for all metrics in the kitchen were higher than those in the serving area. The SA concentrations in the kitchen were 3.4 times higher in the serving area, and the serving area was significantly more homogeneous than in the kitchen. The GSDs of SA in kitchen and serving area were 3.62 and 1.13, respectively.

The ANOVA test showed that variability between the two areas was greater than that within each area ($p=0.012$). This indicated that SA concentration could be an appropriate exposure metric to classify the two groups.

The fine particle number concentrations demonstrated similarity to the SA concentrations. The GM of fine particle number concentration in the kitchen was 9,120 particles/cm^3, which was 4.7 times higher than in the serving area. The fine particle number concentration was found to be significantly different between the kitchen and serving area. The concentration in the serving area was more evenly distributed than in the kitchen area.

The coarse particle number, respirable mass, and PM1.0 concentrations were 2-2.7 times higher in the kitchen than the serving area. Although they showed smaller differences between the two areas than those for SA and fine particle number concentrations, they did show significant differences between the serving and kitchen areas (each $p<0.01$).

All maps in Figure 2 exhibit greater concentrations in the kitchen than in the serving area as the summary statistics showed in Table 1. Relatively homogeneous distributions occurred within the serving area where there were no incidental nanoparticle sources. The concentration peaks for all metrics were found to be in the same location near the oven in the kitchen and appeared similar to one another. However, the coarse particle number concentrations had multiple peaks in the kitchen and seemed more evenly distributed throughout the whole facility as compared to the concentrations for the other metrics.

Die cast facility

Table 2 shows that SA concentrations were highest in the die cast area followed by trim/repair and machining. The fine particle number concentrations exhibited the same trend as the SA concentrations. The spatial distribution of SA and fine particle number concentration (Fig. 3-(a) and (b)) showed similar patterns to each other. The SA and fine particle number concentrations in the die cast area were approximately two times greater than those in the trim and machining areas. The exposure rankings were the same for SA and fine particle number concentrations. The variability of these two exposure metrics between the three areas was greater than the variability within each area ($p<0.01$).

The coarse particle number concentrations showed the same ranks as the SA and fine particle number concentrations. However, they were much more uniform throughout the whole facility (Fig. 3-(c)). This metric did not show significant differences between the three areas ($p=0.37$).

The mass concentrations had different patterns than number and SA concentrations. Respirable mass and PM1.0 concentrations were highest in the machining area, which showed the lowest SA and fine particle number concentrations, followed by the die cast area and the trim/repair area. A nonparametric test showed that the mean exposure rankings were different depending on the exposure metrics chosen ($p<0.001$). This result confirmed that all metrics did not have the same exposure rankings in the die casting facility. ANOVA analysis showed that the GM of respirable mass concentration in the three locations was marginally different ($p=0.06$) and that the GM of PM1.0 was not significantly different ($p=0.36$). Respirable mass and PM1.0 particle maps (Fig. 3 (d) and (e)) showed high concentration peaks in the machining area as well as in the die cast area,

where SA and fine particle number concentrations also showed peaks.

Discussion

We carefully obtained aerosol measurements at pre-determined grid locations in the restaurant and die casting plant. We calculated the GM and GSD for each area in each workplace that was distinguished by process. The appropriateness of different exposure metrics (which is related to the agreement of concentration peaks with the nanoparticle source and with the nanoparticles' exposure levels) was evaluated using exposure rankings, statistical differences among groups, and concentration ratios between groups.

In the die casting plant, exposure rankings differed by exposure metric. The die cast facility had multiple particle generation sources: machining, die casting, melting, trimming, and welding. During thermal processes such as metal pouring and melting, nano-size particles formed through nucleation and coagulation likely dominated particle number concentrations (Chang *et al*. 2005). A broader size range of particles can be generated from the milling and turning machines in the machining area because these processes generate larger particle sizes. Based on the particle generation characteristics in each area, the highest incidental nanoparticle level was expected in the die cast area. Thus, fine particle number and SA concentrations, which are dominated by nanoparticles, were highest in the die cast area, but mass concentrations were the highest in the machining area. In addition, SA and fine particle number concentrations were significantly different between the three groups, but mass and coarse particle number concentrations were not.

Although mass and coarse particle number concentration metrics did not serve as good indicators of incidental nanoparticle levels in the die casting facility, these metrics did indicate the incidental nanoparticle sources in the restaurant. The restaurant had relatively simple particle generation characteristics: incidental nanoparticle sources were located only in the kitchen and no particle sources existed in the serving area. In the restaurant, all exposure metrics showed concentration peaks around combustion sources in the main cooking area and the same exposure rankings were shown for all metrics with significant differences between the two groups (all $p<0.05$).

In the restaurant, the concentration ratio between groups can be a useful way to evaluate each metric. The concentration ratios of kitchen to serving area were different depending on the exposure metric. The concentration ratios for SA and fine particle number were higher than those for mass or coarse particle number. This indicates SA and fine particle number are more sensitive to incidental nanoparticle exposure than mass or coarse particle number concentrations.

More distinct concentration ratios occurred in the kitchen. The concentrations of incidental nanoparticles showed large spatial variation at different sampling locations in the cooking area because the combustion sources were located in the oven and grill areas. The dishwashing area and storage rooms did not have incidental nanoparticle sources. The kitchen was subdivided into three sections: the oven, grill, and dishwashing/storage areas. The 16 sampling locations in the kitchen were each assigned to one of these sections, and the GM and concentration range for the different exposure metrics were calculated for each section as shown in Table 3. All metrics showed the same exposure rankings: the oven area was the highest followed by the grill area and

dishwashing/storage room area. The three sections within the kitchen were significantly different ($p<0.01$), suggesting that the kitchen group needs to be split into more specific SEGs.

The concentration ratios between the oven area and dishwashing/storage room differed based on exposure metric. The ratios for SA and fine particle number concentrations were 23 and 17, respectively. However, the ratios for coarse particle number, respirable mass, and PM1.0 were lower: 2.9, 4.3, and 5.0, respectively. The concentration ratios between the oven and grill areas and between the grill area and dishwashing/storage room showed similar patterns: higher ratios for SA and fine particle number and lower ratios for coarse particle number and mass concentrations. This indicates SA and fine number concentrations are more appropriate for exposure to incidental nanoparticles than mass or coarse particle number concentration.

Cooking activities are known to produce incidental nanoparticles from combustion sources. In particular, gas burning generates more particles than electric cooking appliances and most particles generated from gas burning were in the nanometer size range (15-40 nm) (Dennekamp *et al*. 2001). Gas burning cooking appliances were used in the restaurant. Incidental nanoparticles from natural gas burning do not contribute much to mass concentration, but they dominate particle number or surface area concentrations. Therefore, particle number or SA concentrations may be better metrics to assess incidental nanoparticle exposure levels.

Peters *et al.* (2006) observed findings similar to this study. When a direct-fired gas heater was on, the ultrafine particle number concentration (10-300 nm) increased substantially, but respirable mass concentration showed little change. They also identified

natural gas burners as the main combustion particle sources contributing to incidental nanoparticle number concentrations.

The choice of exposure metric is critical. If inappropriate exposure metrics are used, the probability of misclassification will increase and may result in a less accurate dose-response relationship (Flegal *et al*. 1991). This study confirms that SA and fine particle number concentrations are better at differentiating airborne nanoparticle exposures than mass concentration. Biological relevance is another way to evaluate the appropriateness of an exposure metric. Several toxicological studies have shown that a large surface area and number of particles per unit mass of incidental nanoparticles contributed to more inflammatory response or oxidative stress in the lung (Li *et al*., 1996, Stone *et al*., 1998). Increased SA concentration was linearly related to increased oxidative stress by free radical generation and proinflammatory responses in the lung (Oberdörster 2000, Tran *et al*., 2000, Brown *et al*., 2001, Stoeger *et al*., 2006).

Mapping techniques can be a useful tool for the pre-survey phase of an exposure assessment. Visual aerosol maps can convey spatial information for aerosol contaminants effectively and help prioritize control measures (Evans *et al*. 2008), and locate unexpected sources of contaminants.

At the stage of basic characterization for occupational exposure assessment of contaminants, the mapping approach can be utilized as a pre-survey tool. Before a detailed exposure assessment is completed to obtain the exposure profile of each SEG, mapping measurement results can serve as a useful preliminary estimation. Especially for contaminants such as engineered nanoparticles, industry experience is scarce. Thus, it is difficult to draw conclusions about exposure levels and spatial distributions based on

typical methods used such as qualitative information gathering and industrial hygienists' professional judgments. Particle concentration maps using measurements for multiple metrics can help industrial hygienists gain a broader understanding of workplace exposures to nanoparticles during the initial characterization phase. As a more detailed sampling strategy is formed, initial estimation of exposure levels from mapping can be used to establish sampling filter change schedules and to check if test site concentration levels are compatible with the operating ranges of the test instruments.

An additional use for mapping is to help classify SEGs. As mentioned earlier, SEGs could be a basic unit for occupational epidemiology studies or routine exposure assessment. Accurately determining SEGs is critical to obtain the best results from an epidemiological study or judge if an exposure profile is acceptable or not for management purpose. In the die casting facility, the three locations of the plant represented suitable SEGs when SA or fine particle number concentrations were used to determine SEGs. However, in the restaurant, finer SEGs are required rather than two SEGs (kitchen and serving area) to reflect significant concentration variability within the kitchen.

SEGs can be selected by an observational approach (Mulhausen and Damiano, 1998) or by a sampling approach (Rappaport *et al*. 1995). The observational approach is a practical way to classify SEGs. However, assigning SEGs by this approach lacks objectivity because industrial hygienists made judgments based on their training and experience. Since most industrial hygienists' judgments are not calibrated to the newer metrics such as SA and particle number, this may result in significant biases. Exposure profiles of SEGs could be calculated better using mapping measurements by including

worker movement among different locations. Here, information about the time spent at each location would also be needed. If mapping results can be combined with the traditional observational approach, classifying SEGs by the observational approach would be enhanced by monitoring data and would achieve greater accuracy with less effort and expense compared to the sampling approach. The probability of SEG misclassification using the observational approach would decrease.

Evans *et al*. (2008) considered mapping to be too labor intensive to be a routinely used in industrial hygiene. However, nanoparticle exposure assessment is a relatively new field for industrial hygienists. We lack the benefits of a vast amount of industry knowledge when it comes to nanoparticle exposure. In addition, there are no available devices for personal sampling of nanoparticles. In this case, classifying SEGs using mapping results could be more valuable compared to assessing exposures only with existing personal sampling methods.

Limitations of the mapping approach are that it is based on short term sampling and area sampling. Due to short sampling times, exposure estimation of SEGs based on the mapping measurement alone may not suffice. A process that occurs infrequently, such as welding in a maintenance area, may not be captured by mapping measurements. The aerosol monitoring results for mapping can not be a substitute for personal sampling.

Conclusions

In this study, particle concentrations for various exposure metrics were measured at multiple locations in a restaurant and a die casting factory. These measurements were

used to construct particle concentration maps and to evaluate the appropriateness of various exposure metrics for nanoparticle exposure. Exposure rankings, statistical differences between groups, and concentration ratios between groups were compared with different exposure metrics.

SA and fine particle number concentrations were found to be more appropriate exposure metrics for reducing exposure misclassification for nanoparticle exposures than mass concentration. The exposure rankings for SA and fine particle number concentrations agreed with incidental nanoparticle sources and distribution throughout the workplaces. These metrics showed larger concentration ratios between groups than mass concentrations.

As a pre-survey tool, the mapping technique can be used to understand aerosol generation source characteristics and spatial distributions in workplaces. The mapping approach can also help assign SEGs for an exposure assessment. This methodology can provide valuable information to environmental health specialists.

Acknowledgements

We thank TSI Inc. for the instrumentation and technical support for this study. We are also grateful for the financial support from 3M Company and Midwest Center for Occupational Health and Safety (MCOHS). Also we thank the staffs of the Campus Club at the University of Minnesota and the QX Inc.

References

Brook, R.D., Franklin B., Cascio W., Hong Y., Howard, G., Lipsett M., 2004. Air pollution and cardiovascular disease: a statement for healthcare professionals from the Expert Panel on population and prevention science of the American Heart Association. Circulation 109, 2655-2671.

Brown, D.M., Wilson M.R., MacNee W., Stone V., Donaldson K., 2001. Size-dependent proinflammatory effects of ultrafine polystyrene particles: a role for SA and oxidative stress in the enhanced activity of ultrafines. Toxicology and Applied Pharmacology 175, 191-199.

Chang, M.–C.O., Chow J.C., Watson J.G., Glowacki C., Sheya S.A., Prabhu A., 2005. Characterization of fine particulate emissions from casting processes. Aerosol Science and Technology 39, 947-959.

Dasch, J., D'Arcy J., Gundrum A., Sutherland J., Johnson J., Carlson D., 2005. Characterization of Fine particles from machining in automotive plants. Journal of Occupational and Environmental Hygiene 2, 609-625.

Dennekamp, M., Howarth S., Dick C.A.J., Cherrie J.W., Donaldson K., Seaton A., 2001. Ultrafine particles and nitrogen oxides generated by gas and electric cooking. Occupational and Environmental Medicine 58, 511-516.

Dick, C.A., Brown D.M., Donaldson K., Stone V., 2003. The role of free radicals in the toxic and inflammatory effects of four different ultrafine particle types. Inhalation Toxicology 15, 39-52.

Dockery, D.W., Pope C.A., Xu X., Spengler J.D., Ware J.H., Fay H.E., 1993. An association between air pollution and mortality in six U. S. cities. New England Journal of Medicine 329, 1753-1759.

Evans, D.E., Heitbrink W.A., Slavin T.J., Peters T.M., 2008. Ultrafine and respirable particles in an automotive grey iron foundry. Annals of Occupational Hygiene 52, 9-21.

Flegal, K.M., Keyl P.M., Nieto F.J., 1991. Differential misclassification arising from

nondifferential errors in exposure measurement. American Journal of Epidemilolgy 134, 1233-1241.

Gwinn, M.R., Vallyathan V., 2006. Nanoparticles: Health Effects-Pros and Cons, Environmental Health Perspectives 114, 1818-1825.

Heitbrink, W.A., Evans D.E., Ku B.K., Maynard A.D., Slavin T.J., Peters T.M., 2009. Relationships among particle number, surface area, and respirable mass concentrations in automotive engine manufacturing. Journal of Occupational and Environmental Hygiene 6, 19-31.

Hinds W.C., 1999. Aerosol technology: properties, behavior, and measurement of airborne particles. (2^{nd} ed.), Wiley-Interscience, New York.

International Commission on Radiological Protection (ICRP), 1994. International Commission on Radiological Protection Publication 66 Human Respiratory Tract Model for Radiological Protection, New Youk, Elsevier Science Ltd.

Li, X.Y., Gilmour P.S., Donaldson K., MacNee W., 1996. Free radical activity and pro-inflammatory effects of particulate air pollution (PM_{10}) *in vivo and in vitro*. Thorax 51, 1216-1222.

Maynard A.D., Aitken R.J., 2007. Assessing exposure to airborne nanomaterials: Current abilities and future requirements. Nanotoxicology 1, 26-41.

Mulhausen J.R., Damiano J., 1998. A strategy for assessing and managing occupational exposures, AIHA Press, Fairfax USA.

Nel A., Xia T., Madler L.V., Li N., 2006. Toxic Potential of Materials at the Nanolevel. Science 311, 622-627.

O'Brien, D.M., 2003. Aerosol mapping of a facility with multiple cases of hypersensitivity pneumonitis: Dempnstration of mist reduction and a possible dose/response relationship. Applied Occupational and Environmental Hygiene 18, 947-952.

Oberdörster G., 2000. Toxicology of ultrafine particles: *in vivo* studies. *Phil. Trans. R. Soc. Lond. A.* 358, 2719-2740.

Peters, M.T., Heitbrink W.A., Evans D.E., Slavin T.J., Maynard A.D., 2006. The mapping of fine and ultrafine particle concentrations in an engine machining and assembly facility. Annals of Occupational Hygiene 50, 249-257.

Pope, C.A., Dockery D.W., Kenner R.E., Villegas G.M., Schwartz J., 1999. Oxygen saturation, pulse rate and particulate air pollution: a daily time-series panel study. American Journal of Respiratory Critical Care Medicine 159, 365-372.

Pope, C.A., Burnett R.T., Thurston G.D., Thun M.J., Calle E.E., Krewski D., 2004. Cardiovascular mortality and long-term exposure to particulate air pollution: epidemiological evidence of general pathophysiological pathways of disease. Circulation 109, 71-77.

Ramachandran G., Paulsen D., Watts W., Kittelson D., 2005. Mass, surface area and number metrics in diesel occupational exposure assessment. Journal of Environmental Monitoring 7, 728-735.

Shin W.G., Pui D.Y.H., Fissan H., Neumann S., Trampe A., 2007. Calibration and numerical simulation of Nanoparticle Surface Area Monitor (TSI Model 3550 NSAM). Journal of Nanoparticle Research 9, 61-69.

Stoeger, T., Reinhard C., Takenaka S., Schroeppel A., Karg E., Ritter B., 2006. Instillation of Six Different Ultrafine Carbon Particles Indicates a Surface Area Threshold Dose for Acute Lung Inflammation in Mice. Environ Health Perspective 114, 328-333.

Stone, V., Shaw J., Brown D.M., MacNee W., Faux S.P., Donaldson K., 1998. The role of oxidative stress in the prolonged inhibitory effect of ultrafine carbon black on epithelial cell function. Toxicology *in Vitro* **12,** 649-59.

Sun, Q, Wang A., Natanzon A., Duquaine D., Brook R.D., 2005. Long-term air pollution exposure and acceleration of atherosclerosis and vascular inflammation in an animal model. Journal of American Medical Association 294, 3003-3010.

Tran C.L., Buchanan D., Cullen R.T., Searl A., Jones A.D., Donaldson K., 2000. Inhalation of poorly soluble particles. II. Influence of particle surface area on inflammation and clearance. *Inhalation Toxicology* 12, 1113-1126.

Table 1. Summary of the aerosol concentrations by various exposure metrics in the restaurant

Area	n*	Surface area ($\mu m^2/cm^3$)	Number (particles/cm^3)		Mass (mg/m^3)	
			Fine	Coarse	respirable mass	PM1.0
		GM (GSD†)	GM (GSD)	GM (GSD)	GM (GSD)	GM (GSD)
Kitchen	16	29.5 (3.62)	9,117 (3.41)	18 (1.62)	0.010 (1.81)	0.008 (1.98)
Serving	15	8.9 (1.13)	1,943 (1.11)	7 (1.13)	0.005 (1.21)	0.003 (1.17)
p‡		0.012	<0.01	<0.01	<0.01	<0.01

*n**: number of sampling locations
GSD†: GSD of the averaged concentrations at each sampling location within each area
p‡: comparing serving area and kitchen areas using a general linear model.

Table 2. Summary of the aerosol concentrations by various exposure metrics in the die cast facility

Area	n*	Surface area ($\mu m^2/cm^3$)			Number ($particles/cm^3$)						Mass (mg/m^3)					
					Fine (0.02-1.0 μm)			Coarse (0.3->5 μm)			respirable mass			PM1.0		
		GM (GSD)	Ra -nk	Group code‡	GM (GSD)	Ra -nk	Group code	GM (GSD)	Ra -nk	Group code	GM (GSD)	Ra -nk	Group code	GM (GSD)	Ra -nk	Group code
Machining	9	978 (1.09)	3	B	122,610 (1.06)	3	C	1190 (1.07)	3	A	2.072 (1.12)	1	A	1.804 (1.12)	1	A
Trim	10	1207 (1.49)	2	B	165,699 (1.41)	2	B	1200 (1.11)	2	A	1.391 (1.86)	3	B	1.163 (1.97)	3	A
Die cast	26	2253 (1.66)	1	A	283,888 (1.18)	1	A	1240 (1.09)	1	A	1.912 (1.42)	2	AB	1.596 (1.43)	2	A
***p*†**		<0.001			<0.001			0.37			0.06			0.36		

*n**: number of sampling locations

p†: comparing sampling areas from a general linear model

Group code‡: grouping codes from Duncan's multiple range tests for multiple comparisons.

Table 3. Summary of the aerosol concentrations by various exposure metrics in the kitchen in the restaurant

Area	N*	Surface area ($\mu m^2/cm^3$)	Number (particles/cm^3)		Mass (mg/m^3)	
			Fine	Coarse	respirable mass	PM1.0
		GM (range)	GM (range)	GM (range)	GM (range)	GM (range)
Oven	3	273.4 (110.7-1,020.9)	55,420 (30,672-179,269)	35 (32-39)	0.030 (0.018-0.059)	0.025 (0.014-0.059)
Grill	6	27.7 (19.1-25.6)	12,076 (5,582-30,138)	20 (17-24)	0.009 (0.008-0.012)	0.008 (0.007-0.009)
Dishwasher /storage	7	11.9 (8.5-18.10)	3,304 (2,626-5,167)	12 (6-15)	0.007 (0.005-0.009)	0.005 (0.003-0.007)
$p^{\dagger}$		<0.01	<0.01	<0.01	<0.01	<0.01

n^{*}: number of sampling locations

$p^{\dagger}$: comparing sampling areas from a general linear model.

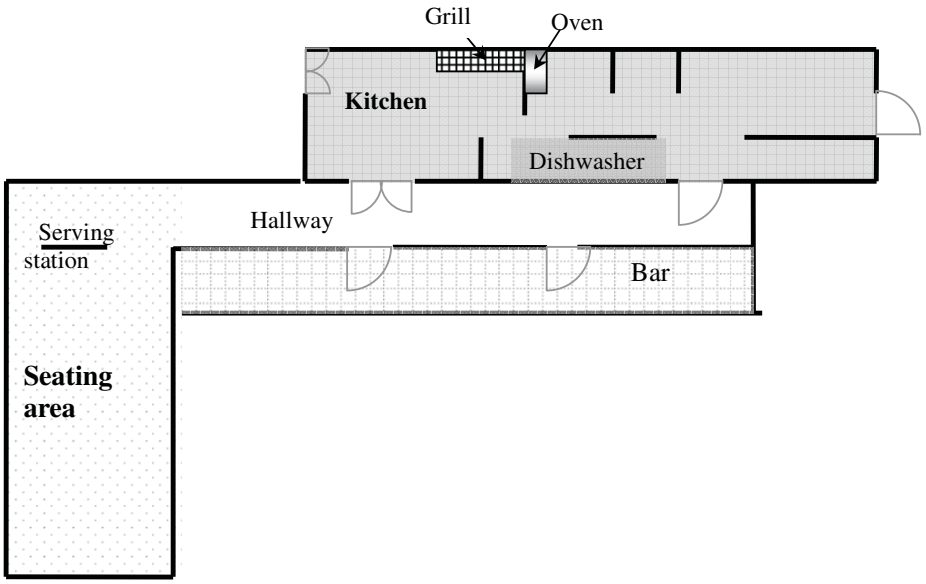

(a) Restaurant

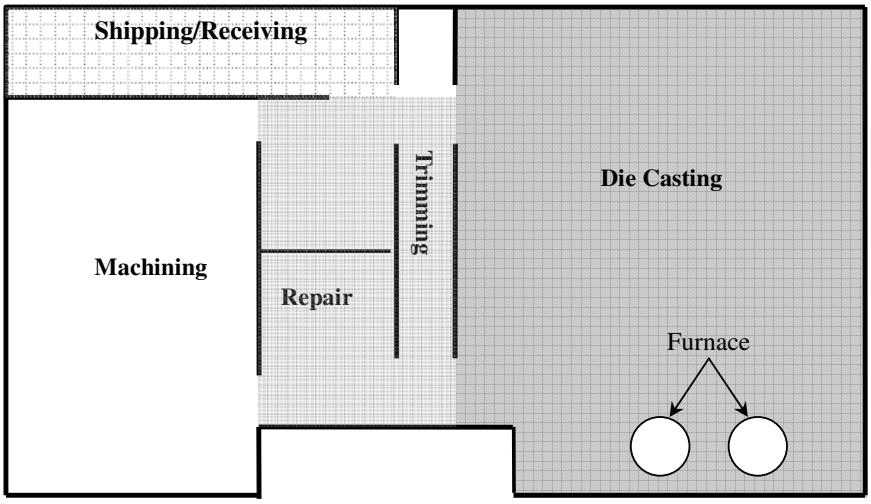

(b) die casting facility

Figure 1. Floor plans.

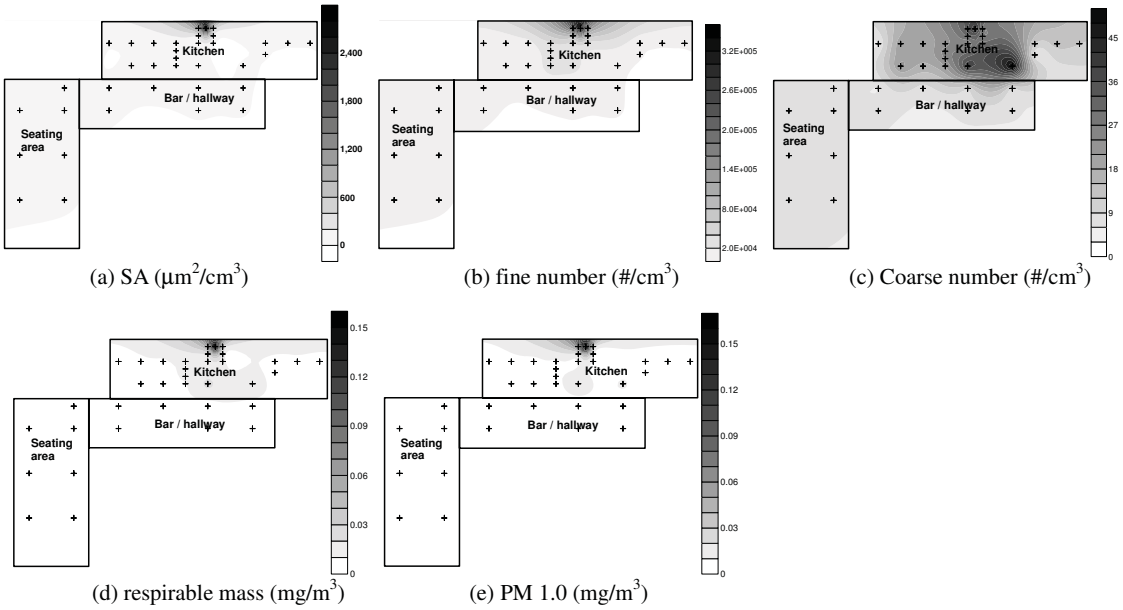

(a) SA ($\mu m^2/cm^3$) (b) fine number ($\#/cm^3$) (c) Coarse number ($\#/cm^3$)

(d) respirable mass (mg/m^3) (e) PM 1.0 (mg/m^3)

Figure 2. Aerosol concentration maps in the restaurant (+: sampling location).

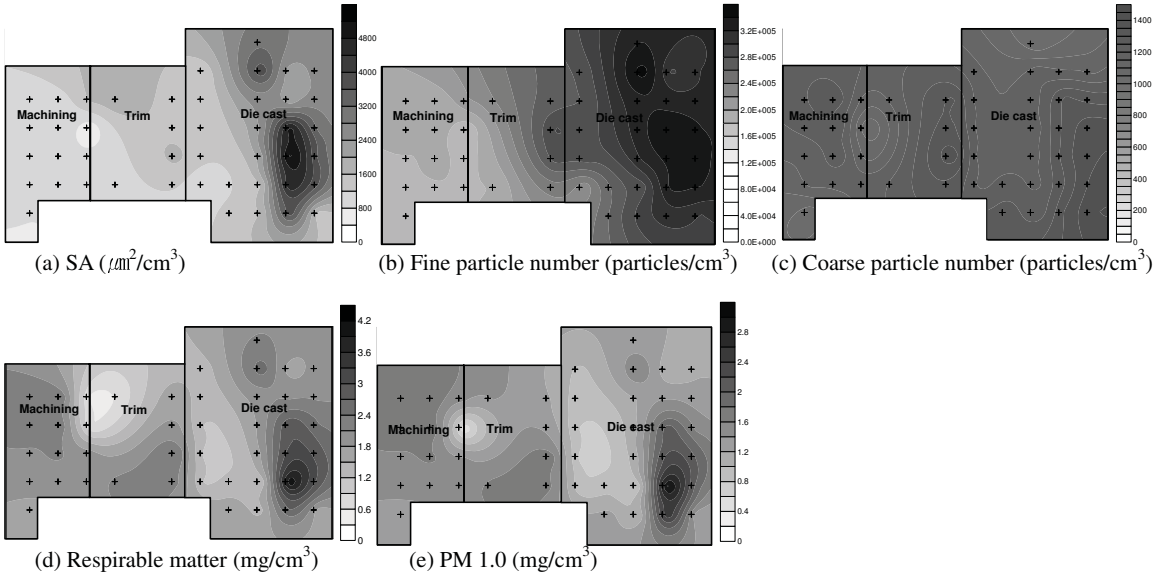

(a) SA ($\mu m^2/cm^3$) (b) Fine particle number ($particles/cm^3$) (c) Coarse particle number ($particles/cm^3$)

(d) Respirable matter (mg/cm^3) (e) PM 1.0 (mg/cm^3)

Figure 3. Aerosol concentration maps in the die casting factory (+: sampling location).

Chapter III

Comparing exposure zones by different exposure metrics using statistical parameters: contrast and precision

Recently, the appropriateness of using the "mass concentration" metric for ultrafine particles has been questioned and surface area (SA) or number concentration metrics have been proposed as alternatives. To find appropriate exposure metrics for classifying exposure categories in workplaces generating nanoparticles, exposure concentrations were measured in high and low exposure zones in a restaurant, an aluminum die-casting factory, and a diesel engine lab using SA, number, and mass concentration metrics. Predetermined exposure classifications were compared by each metric using statistical parameters and concentration ratios which were calculated from the different exposure concentrations. In the restaurant, SA and fine particle number concentrations showed significant differences between the high and low exposure zones and they had higher contrast (the ratio of between-group variance to the sum of the between-group and within-group variances) than mass concentrations. Mass concentrations did not show significant differences. In the die cast facility, concentrations of all metrics were significantly greater in the high zone than in the low zone. SA and fine particle number concentrations showed larger concentration ratios between the high and low zones and higher contrast than mass concentrations. None of the metrics were significantly different between the high and low exposure zones in the diesel engine lab. Instead of mass concentration, the use of fine particle number and SA concentration is recommended to classify exposure zones from the results of this study. That exposure categories depended on the exposure metric chosen has significant implications for epidemiological studies.

1. **Introduction**

Traditionally, mass concentration has been used as the metric for exposure assessment of airborne particles and the basis for regulation. Recently, however, the appropriateness of the "mass concentration" metric for nano-sized particles has been questioned. The concern is that exposure assessment that rely on mass concentration could underestimate ultrafine particle toxicity. This is because these particles do not contribute much to total mass concentration despite their high numbers. No scientific agreement exists for appropriate exposure metrics for nano-sized particles (Paik *et al*., 2008, Maynard and Aitken, 2007).

New exposure metrics for the nano-sized particles have been proposed. McCawley *et al*. (2001) showed that particle number concentration was a more appropriate metric than mass concentration for relating beryllium particle exposure to chronic beryllium disease and found no correlation between mass and number concentration. Peters *et al*. (1997) found that a decrease of peak expiratory flow among 27 nonsmoking asthmatics had stronger association with number concentration than mass concentration.

Surface area (SA) concentration has been highlighted as a biologically more relevant metric for the effective dose than mass concentration because the adverse health effects of nanoparticles may be associated with surface reactivity (Brown *et al*., 2001, Li *et al*., 1996, Oberdörster, 2000, Tran *et al*., 2000). Schwartz and Marcus (1990) compared daily air pollution measurements expressed as mass concentrations to mortality and found a nonlinear relationship between them. Using the same data set, but converting the mass concentrations into SA concentrations, Maynard and Maynard (2002) showed a linear

relationship between the particle SA and mortality. This indicates that SA may be a more suitable metric than mass for ambient aerosol exposure. Although these studies suggest that SA or number concentration is a better metric than mass concentration, further investigation is required to confirm its appropriateness in occupational and environmental settings through epidemiological studies.

The choice of the most appropriate exposure metric will be critical. In epidemiological studies, groups of workers are split into different exposure categories based on exposure information such as exposure concentration, job profile, and duration of exposure, to name a few. If exposure concentration by a less relevant exposure metric is used to determine exposure categories, workers could be misclassified into incorrect categories resulting in a less exposure-response association (Flegal *et al*., 1991).

The efficiency of an exposure metric to detect an exposure–response relationship in an epidemiologic study can be assessed using statistical parameters such as contrast between groups, and precision within a group (Kromhout and Heederik 1995). Contrast and precision can be derived from, the estimates of variance between-groups (S^2_{BG}), within-group (S^2_{WG}), and within-location distribution (S^2_{WL}) for a set of measurements. Contrast (ε) in exposure levels between groups was calculated as follows:

$$\varepsilon = \frac{S^2_{BG}}{S^2_{BG} + S^2_{WG}} \ . \qquad (1)$$

If the contrast approaches the value 1, it indicates that each group based on this exposure metric is a unique exposure group. On the contrary, if the contrast approaches the value 0, grouping based on this exposure metric is not effective. The precision (π) of each group's mean exposure is defined as:

$$\pi = \frac{1}{\sqrt{\left(S_{WG}^2 / n_1 + S_{WL}^2 / n_2\right)}} \quad (2)$$

where n_1 is the number of locations and n_2 is the number of measurements in a group. Precision is a measure of uniformity within each group. Higher precision indicates that exposure concentrations from each location within a group are relatively similar to each other compared to the case of lower precision.

In this study, exposure assessments were carried out in three workplaces generating incidental nanoparticles. Simultaneous real-time measurements of particle SA, number, and mass concentrations were obtained. The ability of various exposure metrics to distinguish between exposure categories were assessed using contrast and precision, exposure ranking, and concentration ratios between different exposure categories.

2. **Methods**

2.1 Sampling strategy

The study was conducted in three workplaces - a restaurant, a diesel engine lab, and a die cast facility - where incidental nanoparticles were being generated. In a previous study, we obtained aerosol measurements in the restaurant and the die cast facility to construct particle maps based on different exposure metrics and to identify exposure groups based on exposure levels (Park *et al*. 2009). In that study, concentrations for all metrics in the kitchen of the restaurant were significantly higher than in the serving area. The kitchen area was identified as the high exposure zone and the serving area was

identified as the low exposure zone. In the die casting plant, exposure rankings and the statistical significance of differences among the three primary areas of the facility varied based on the exposure metrics chosen. The fine particle number concentration was chosen to create three exposure zones because this metric is dominated by the nano-size range. The die casting, trim/repair, and machining areas were identified as the high, medium, and low exposure zones, respectively.

For the diesel engine lab, two exposure zones were chosen based on the activities being conducted. The lab was the high exposure zone and the office area was the low exposure zone.

For the exposure assessment, two exposure zones were selected for each facility. Because there are currently no SA or number concentrations instruments suitable for full-shift personal worker sampling, area sampling was used as a surrogate to measure personal exposures. This was done using real-time instruments for the various exposure metrics of interest at three or four locations for every exposure zone. Sampling time was approximately 4 to 6 hours with 3-minute averaging times for each instrument. Two sets of samples were taken at each of the six or seven workplace locations.

2.2 Descriptions of workplaces

2.2.1 Restaurant

The restaurant had two major job categories: cooking and serving. The cooking workers spent most of their time in the kitchen. The serving workers spent the majority of their time in the serving areas such as the serving station and seating area.

The high exposure zone contained an oven area, grill area, and a dishwashing area (Figure 1). Most entrees were prepared in the oven area. Some foods were warmed up and made-to-order in the grill area. The oven area had gas burners, flat top grills, and gas convection ovens that generated combustion particles. The grill area was for serving food to customers during lunch time. The deep fryers, flat top grills, and gas grill were located in the corner of the grill area. The dishwashing area was located adjacent to the oven area and was divided by a wall that had a door which was open most of the time. The restaurant was ventilated by HVAC (heating, ventilation, and air conditioning) systems, and canopy hoods were installed above cooking appliances to draw air away.

The serving area did not have any combustion sources and included a serving station, a bar, a general seating area, private rooms, and a hallway. Three representative locations for this zone were selected: the serving station, the bar, and the seating area.

2.2.2 Diesel engine lab

The diesel engine lab was in the Department of Mechanical Engineering at the University of Minnesota (Figure 2). It had two sections: a lab area and an office area. Seven diesel engines were located in the lab area where students and researchers performed their experiments. When they were not conducting experiments in the lab area, the students spent their time in the office area. When an experiment was being performed, researchers turned on fans, drawing outdoor air from windows on one side through the lab to windows on the other side. Diesel engine experiments were performed infrequently according to research needs. Because only one engine was operating at a time during the

days of this study, the nanoparticle source was clearly identified. Therefore, no mapping measurements were performed to establish exposure zones. The office area included a study room, teaching assistants (TA) office, and prep room. The prep room was right next to the lab area, separated by a wall, but contained no diesel engines.

2.2.3 Die casting facility

The die casting facility produced aluminum alloy products. The plant was divided into three sections by walls containing passage ways on either side. As indicated in Figure 3, the sections were the die casting, trim/repair, and machining areas. Aluminum was melted in the furnaces and delivered to each die casting machine by forklift trucks. In the trim/repair area, castings were trimmed in trim presses and stacked. Dies were also repaired in the tool repair section. In the machining area, the trimmed castings were finished using milling, broaching, and turning machines. The die cast facility had four job categories: die casting, trimming, machining, and maintenance groups. Most workers in each job category spent more than 90% of their time in their corresponding work area. However, some workers in the trimming group worked in the die casting area because two of the seven trim presses were located there. The exposure zones were ranked based on mapping of the fine particle number concentrations. The die cast area was the high exposure zone, the trim/repair area was the medium zone, and the machining area was the low exposure zone. Two die cast machines and one trim press were selected for the investigation because workers near these machines were in the high exposure zone. In the machining area, trimmed castings were finished through milling, turning, or broaching

processes that used metalworking fluids (MWFs). Two milling machines and one turning machine were chosen for the low exposure zone.

2.3 Particle Measurement

Real-time measurements of particle mass, number, and SA concentrations and size distribution by number, as well as gravimetric filter measurements for calibration of the real-time mass monitor, were obtained simultaneously. Three aerosol photometers (DustTrak Model 8520 TSI Inc., Shoreview, MN) with PM2.5, PM1.0 and respirable sampling inlets were used for mass concentration.

The DustTrak measurements were calibrated to the average aerosol concentration from the corresponding gravimetric measurements for the respirable and PM2.5 fraction. The gravimetric PM2.5 and respirable mass concentrations were obtained using a PM2.5 sampler (PEM^{TM} Model 200, MSP Inc., Minneapolis, MN) and a nylon cyclone (Dorr-Oliver 10 mm cyclone, Sensidyne, Clearwater, FL). Pumps drew air through sampling inlets at 4.0 and 1.7 L/min, respectively. Filters were weighed before sampling using a microbalance with a sensitivity of 5 μg in a weighing room where the temperature and humidity were environmentally controlled. After sampling, filters were equilibrated in the weighing room and then reweighed.

The DustTrak measurements were recalculated using a specific calibration factor for each measurement as follows:

$$\text{Calibration factor} = \frac{\text{Time - Integrated gravimetric concentration}}{\text{Time - Integrated DustTrak concentration}} \quad (3)$$

Each DustTrak measurement was multiplied by this factor to estimate the true mass

concentration. No gravimetric sampling was conducted for PM1.0. The calibration factor for PM1.0 was calculated using the concentration ratio between PM2.5 and PM1.0 and the gravimetric PM2.5 concentration as following:

$$\text{PM1.0 Calibration factor} = \frac{\text{Gravimetric PM2.5 concentration}}{\text{Time - Integrated DustTrak PM1.0}} \times \frac{\text{Size - Integrated PM1.0}}{\text{Size - Integrated PM2.5}} \qquad (4)$$

Integrated PM2.5 and PM1.0 concentrations were calculated from size distribution measurements, obtained from a scanning mobility particle sizer (SMPS Model 3034, TSI Inc., Shoreview, MN) and an optical particle counter (AeroTrak^{TM} Model 8220, TSI Inc., Shoreview, MN, or HHPC-6, Hach Ultra, Grants Pass, Oregon). The gravimetric mass concentration and integrated DustTrak concentrations were highly correlated (R^2= 0.84 for respirable matter and 0.97 for PM2.5) and the mean calibration factors for respirable matter, PM2.5, and PM1.0 were 0.307, 0.348, and 0.367 with standard errors of 0.01, 0.03 and 0.01, respectively.

For each run, blank samples (20% of total samples) were weighed at the same time as the sampled filters. The detection limit was 0.024 mg/m^3 and calculated as three times the standard deviation of the field blank weight gains divided by the sampled air volume.

The surface area monitor (AeroTrak^{TM} Model 9000, TSI Inc., Shoreview, MN) measured the surface area concentration of the particles that had the ability to be deposited in tracheobronchial or alveolar regions of the human lung (Shin *et al*. 2007). For this study, the monitor was set for alveolar deposition.

For number concentration, a condensation particle counter (P-Trak Model 8525, TSI Inc., Shoreview, MN) was utilized. The P-Trak is a real-time condensation particle

counter (CPC) that counts single particles 0.02 µm in diameter to greater than 1.0 µm. The particle counts from the P-trak will be referred to henceforth as fine particle number concentration in this study. An optical particle counter (OPC) was used to measure size distribution by number. The OPC simultaneously counts and sizes particles into six channels (0.3-0.5 µm, 0.5-0.7 µm, 0.7-1.0 µm, 1.0-2.0 µm, 2.0-5.0 µm, and greater than 5.0 µm) via light scattering. Particle counts from summing all size bins will be referred to henceforth as coarse particle number concentrations.

The SMPS was used to obtain information on particle size distribution by number based on the electrical mobility diameter. The SMPS can measure particles between 10 and 487 nm in diameter in up to 32 size channels.

For easy portability, a mobile sampling cart was used to carry the instruments. A mannequin was placed on the top section of the sampling cart to locate sampling tubes from the different instruments at breathing zone height. The inlets of sampling tubes were set closely together. All instruments were connected to a wall outlet using AC power. Data from each device were downloaded to a laptop computer.

2.4 Data analysis

All statistical analyses were conducted using SAS 9.1 (SAS Institute Inc. Cary NC). The real-time instrument data were organized into three-minute averages. To compare aerosol concentrations representing different exposure metrics from the simultaneous measurements, data were needed from all seven real-time instruments. If a time point did not have any one of the seven instrument readings, it was excluded from

analysis. More than 90% of time intervals had all seven measurements and were used for the analysis.

Concentrations for all exposure metrics were approximately log-normally distributed. The geometric means (GM) were calculated for each location and each zone. Significant mean differences between high and low zones by each metric in each workplace were detected using t-tests. Data taken from the same location were auto-correlated. To correct for the auto-correlation in the real-time measurements, general linear models with compound symmetry covariance structure were used. Such models are more appropriate to compare high and low exposure zone measurements than models assuming independence among different measurements. The level of statistical significance for all analyses was 0.05.

The two-way random effects ANOVA (analysis of variance) model (Kromhout and Heederik, 1995) was constructed using "Proc mixed random statements" to estimate variance components for exposure variability: within-location, within-group, and between-group as follows:

$$Y_{ijk} = \ln X_{ijk} = \mu_y + \alpha_i + \beta_{ij} + \varepsilon_{ijk} \quad (5)$$

for *i=high and low zones, j=1-4th locations, and k=1-240 time points*, where X_{ijk} = exposure concentration of the i^{th} zone's j^{th} location at the k^{th} time point,

μ_y = mean of Y_{ijk}, α_i= random deviation of the i^{th} group's true exposure ($\mu_{y,i}$) from μ_y,

β_{ij} = random deviation of the j^{th} location's true exposure ($\mu_{y,ij}$) from $\mu_{y,i}$,

ε_{ijk}= random deviation of the i^{th} group's j^{th} location's exposure on the k^{th} time point from its true exposure, μ_{yij}.

This model assumed that α_i, $\beta_{,ij}$, and ε_{ijk} are normally distributed and can be expressed

as $\alpha_i \sim N(0, \sigma_{BG}^2)$, $\beta_{ij} \sim N(0, \sigma_{WG}^2)$, and $\varepsilon_{ijk} \sim N(0, \sigma_{WL}^2)$. The distribution of X_{ijk} is log-normal. The variance components of the samples - S_{BG}^2, S_{WG}^2, and S_{WL}^2 - were used as estimates of the variance components in the population - $\sigma_{BG}^2, \sigma_{WG}^2$, and σ_{WL}^2 - and they were used to calculate standard deviation for distributions between-group (S_{BG}), within-group (S_{WG}), and within-location (S_{WL}). The exponential values of the standard deviations were the corresponding geometric standard deviations GSD_{BG}, GSD_{WG}, and GSD_{WL}.

The number concentration obtained by summing the counts in all size channels of the SMPS was assumed as the reference number concentration (N_{Ref}) for particles in the 10 to 500 nm size range. To compare N_{Ref} with the P-Trak and an OPC, the new number concentration (N_{UFP}) for particles 20-500 nm was calculated as:

$$N_{UFP} = N_{P-Trak} - \sum_{k=2}^{3} N_{OPC,k} \quad (6)$$

3. Results

3.1 Aerosol concentrations and exposure ranks by different metrics

The aerosol concentrations measured for various exposure metrics and exposure ranks in the three workplaces are summarized in Table 1. The column named “rank” lists the exposure rankings for each location within a workplace according to each exposure metric.

3.1.1 Restaurant

SA and fine particle number concentrations were the highest in the oven area followed by the grill and dishwashing area. These concentrations were significantly higher than those in the low exposure zone. In the high exposure zone, the coarse particle number concentrations were significantly higher than in the low exposure zone. Respirable mass concentration was higher in the low exposure zone than in the high zone. PM2.5 and PM1.0 concentrations showed no significant difference between the zones.

The top three rankings based on SA and fine and coarse particle number concentrations were all from the high exposure zone. In marked contrast, the top three high rankings were all from the low zone for respirable mass concentration.

Figure 4 presents the ratios of the mean concentrations of the high and low exposure zones for each concentration metric in the three workplaces. In the restaurant, the highest ratios were observed for SA and fine particle number concentrations. The coarse particle number concentration ratio was lower. The ratios of respirable mass and PM2.5 concentrations were less than 1.

3.1.2 Diesel engine lab

Table 1 shows that SA and fine particle number concentrations were highest near Engine 1 followed by the Engine 3 and 2. PM2.5 was highest in the prep room. Rankings based on SA and fine particle number concentration tracked each other, but coarse particle number and mass concentrations did not show any similarity. As shown in Figure 4, the ratios of SA and fine particle number concentrations were higher than those of

mass concentrations.

3.1.3 Die cast facility

In the die casting facility, all concentrations were significantly higher in the high exposure zone than in the lower exposure zone. The top three ranks of SA, respirable matter, PM1.0, and fine and coarse particle number concentrations came from the high exposure zone. However, the highest three ranks of PM2.5 were not all from the high exposure zone. The ratio of concentrations in the high and low exposure zones was highest for SA (Figure 4).

3.2 Exposure variability for different exposure metrics

The contrast and precision of different exposure metrics and exposure variability from the two-way ANOVA are presented in Table 2.

3.2.1 Restaurant

In the restaurant, the GSD_{BG} for SA and fine and coarse particle number concentrations were higher than those for mass concentrations. SA, respirable mass, and fine and coarse particle number concentration showed high contrast, but PM2.5 and PM1.0 had low contrast. Respirable mass concentration showed high contrast, but the concentrations were lower in the high exposure zone than in the low exposure zone. Fine particle number concentration showed relatively high contrast but the lowest precision.

3.2.2 Diesel engine lab

No statistically significant difference in GSD_{WL}, GSD_{WG}, and GSD_{BG} was observed for SA and fine and coarse particle number concentrations. As shown in Table 2, GSD_{WG} was slightly greater than GSD_{BG} for all metrics. PM2.5 and PM1.0 had the lowest contrast. The other metrics showed higher contrasts ranging between 0.21 and 0.39.

3.2.3 Die cast facility

GSD_{BG} was substantially greater than GSD_{WG} for all metrics except PM2.5 and PM1.0. Fine particle number concentration had the highest contrast and precision. SA concentration showed a similar contrast but lower precision compared to the fine particle number concentration. PM 2.5 and PM1.0 had the lowest contrast and precision in this facility.

3.3 Particle size distribution by number for particles less than 500 nm in diameter

The reference number concentration (N_{Ref}) measured by the SMPS and corresponding number concentrations calculated from the P-Trak and OPC (N_{UFP}) are summarized in Table 3. The size distribution parameters, count median diameter (CMD) and GSD, obtained from the SMPS measurement are also included.

N_{Ref} was greater than N_{UFP} in all locations of the three workplaces. Figure 5 shows N_{UFP} versus N_{Ref} from all time points. At lower concentrations, N_{UFP} was close to N_{Ref} with little variation. However, at high levels, N_{UFP} underestimated the number concentration.

4. Discussion

4.1 SA and fine particle number concentrations: more appropriate metrics for assessing incidental nanoparticles

Based on the exposure assessment of this study, SA and fine particle number concentrations are more sensitive measures of nanoparticle exposure than mass concentrations, which can not always be a substitute or surrogate metric for the others. The restaurant had relatively simple particle generation characteristics: incidental nanoparticle sources located only in the kitchen and no particle source in the serving area. The high exposure zone had significantly higher concentration than the low exposure zone in terms of SA and fine and coarse number concentrations. However, mass concentrations did not differ between the two zones for any of the mass concentrations. If mass concentration is used for toxicological research or epidemiologic studies, researchers may fail to obtain the association between exposure to nanoparticles and related health outcomes.

Within the high exposure zone, the strength of particle sources varied by location. For SA and fine particle number concentrations, the oven area was highest followed by

the grill and the dishwashing areas. However, coarse particle number concentration, which represented particles larger than 300 nm in diameter that were not produced by combustion sources, was highest in the dishwashing area. Although the dishwashing area had no nanoparticle generation sources, incidental nanoparticles transported from the grill and oven areas could agglomerate in this area. In addition, particles could grow by condensation of water vapor in the high humidity environment, causing a higher coarse particle number concentration in the dishwashing area than in the oven and grill areas.

When differences among the three locations in the high exposure zone were tested, SA and fine particle number concentrations showed significant differences ($p=0.02$ and 0.003, respectively) but coarse particle number concentration did not ($p=0.43$). This indicates that SA and fine particle number concentrations reflected spatial distribution of incidental nanoparticles better than coarse particle number concentrations. This suggests that the high exposure zone should be classified finer.

Although the diesel engine lab was assumed to have distinct particle generation conditions like the restaurant, no exposure metrics were significantly different between the two zones, unlike the restaurant. Seven engines were located in the lab but only one engine at a time was operating during our measurements. Outdoor air was provided to the lab through the entire period of our experiments and each engine was equipped with a local ventilation system to remove exhaust from the work area. In the restaurant, on the other hand, the oven and grill areas had many cooking appliances and most of them were used simultaneously. All cooking appliances were installed with canopy hoods to exhaust emissions from cooking, but during the peak time they were not efficient enough to remove all the particles being generated.

Concentrations for all metrics in the die casting facility were high because this facility was operated for 20 hours a day with two shifts and, due to cold weather, general ventilation through the doors with outside air did not occur. The die casting facility generated a broad size range of particles from the multiple particle generation sources. In the high exposure zone, nano-sized metal oxide particles were produced by furnaces and die cast machines (Chang *et al.*, 2005). In the low exposure zone, sub-micrometer particles to larger particles were generated by machining processes (Thornburg and Leith, 2000).

All concentrations in the die casting facility were significantly greater in the high exposure zone than in the low exposure zone, but the ratio of SA between high and low exposure zones was higher than those of other exposure concentration metrics.

4.2 Using contrast and precision for exposure grouping

Kromhout and Heederik (1995) developed contrast and precision to assess exposure grouping schemes in the rubber industry. In this study, these statistical parameters were used to assess the capability of different exposure metrics to classify exposure categories.

Contrast is the ratio of between-group variance to the sum of between-group and within-group variability. It is an excellent tool to detect an exposure-response association in epidemiological analysis (Kromhout and Heederik, 1995) and provides information about statistical differences between high and low zones in this study. Precision is a measure of how close exposure concentrations are within a zone and within a location.

From the epidemiologic point of view, higher contrast and precision indicates better exposure classification to find an exposure-response relationship.

In the die casting facility, the contrast and precision for fine particle number and SA concentrations were highest indicating the most efficient metrics to differentiate between the two exposure zones. However, precision of fine particle number concentration was much higher than that of SA. Fine particle number concentrations were saturated in the high exposure environment such as die casting machines (Figure 5) and this may cause less variability of fine particle concentrations within a location and zone.

In the diesel engine lab, no metric was observed to be efficient in differentiating between the two zones. Small between-group variability may cause low contrast indicating a higher probability of overlap between the distributions of exposure concentration of the two zones. In case of low contrast, comparing precision from different metrics may not be useful.

In the restaurant, SA, respirable mass, and fine and coarse particle number concentration metric had higher contrast than PM2.5 and PM1.0. In terms of precision, coarse particle number and respirable mass concentrations were better than SA and fine particle number concentrations. The concentrations of incidental nanoparticles showed large spatial variations in the cooking area as mentioned earlier. In addition, there was large time variation in the cooking area due to peak periods of service. The lower precision for the SA and fine particle concentration metrics reflected larger variation by location and time in the high exposure zone.

As described before, the SA and fine number concentrations in the dishwashing area were significantly lower than in other areas located in the high exposure zone,

leading to lower precision for these metrics. In response, the dishwashing area was reassigned to the low exposure zone and the statistical analyses were repeated with results shown in Table 4. The alternate classification yielded higher contrast and precision for fine particle number and SA concentrations. This occurred because the GSD_{WG} of SA and fine particle number concentration decreased while the GSD_{BG} for these metrics increased dramatically. However, contrast decreased for coarse particle number and mass concentrations with the reclassification and these metrics were clearly not useful for classifying exposure groups. In the restaurant, SA and fine particle number concentration metrics appear to be more efficient at differentiating nanoparticle exposures than the other metrics after regrouping.

The application of statistical parameters can be a useful methodology to evaluate various exposure metrics from the epidemiologic point of view. SA and fine particle number metrics were found to be more efficient for nanoparticle exposure assessment than mass concentration metrics.

4.3 Reducing measurement error in the P-Trak

A P-Trak is a handheld version of an optical particle counter and designed for a qualitative investigation. In a high concentration environment, an instrument using optical sensors can experience coincidence errors. That is, more than one particle can pass through the sensing region at a time and then can be counted as a single particle (Hameri *et al*., 2002).

At extremely high concentrations such as near die casting machines or when the

gas oven was open, significant underestimation (a factor of 3 lower than N_{Ref}) of N_{UFP} was observed. As shown in Figure 5, these large differences started to occur at approximately 2×10^5 particles/cm^3, which was lower than the manufacturer's maximum concentration of 5×10^5 particles/cm^3.

N_{UFP} and N_{Ref} concentrations in the die cast facility both showed statistically significant differences between the high and low exposure zones, but the N_{Ref} ratio was 7.8, which was much greater than the ratio of 3.1 using N_{UFP}. These data also show that the P-Trak underreported the fine particle number concentrations in the high zone of the die casting plant due to coincidence errors. This error could cause weaker association between exposure and related health outcomes than actually exists.

An accurate measurement as well as the choice of appropriate exposure metrics is essential in exposure assessment. The use of a dilution system with a particle counter will improve the performance of the P-Trak and the measurement error will decrease (Knibbs *et al.*, 2007; Peters *et al.*, 2005).

5. Conclusions

Multi-metric aerosol monitoring was performed in three workplaces generating incidental nanoparticles to assess the efficiency of different metrics to classify exposure categories and to find more appropriate exposure metrics for nanoparticle exposure. In a workplace with a distinct source of nanoparticles, SA and fine particle number concentrations were better metrics to describe the nanoparticle generation than mass and coarse particle number concentrations. They had higher contrasts and comparable

precisions relative to the other metrics. However, in the case of a distinct nanoparticle generation source situation with low workload or infrequent activity such as the diesel engine lab in this study, none of the metrics were found to be useful. Contrasts of all metrics were low. In a plant having multiple particle generation sources with high exposure levels, all exposure metrics showed significant mean difference between the high and low exposure zones, but SA and fine particle number concentrations showed higher concentration ratios with higher precision and contrast than mass and coarse number concentrations. Therefore, in the workplaces generating nanoparticles, SA and fine particle number concentration metrics appear to be more appropriate metrics for classifying exposure zones than mass concentrations. The choice of appropriate exposure metrics is critical for epidemiological studies to establish better exposure to response relationships. Efforts to reduce measurement error will also improve the ability to find associations in these studies.

6. Acknowledgements

We thank TSI Inc. for the instrumentation and technical support for this study. We are also grateful for the financial support from 3M Company and the Midwest Center for Occupational Health and Safety (MCOHS). Also we thank the staffs the Campus Club and the Center for Diesel Research in Department of Mechanical Engineering at the University of Minnesota and the QX Inc.

References

Brown, D.M., Wilson M.R., MacNee W., Stone V., Donaldson K., 2001. Size-dependent proinflammatory effects of ultrafine polystyrene particles: a role for SA and oxidative stress in the enhanced activity of ultrafines. Toxicology and Applied Pharmacology 175, 191-199.

Chang, M.–C.O., Chow J.C., Watson J.G., Glowacki C., Sheya S.A., Prabhu A., 2005. Characterization of fine particulate emissions from casting processes. Aerosol Science and Technology 39, 947-959.

Flegal, K.M., Keyl P.M., Nieto F.J., 1991. Differential misclassification arising from nondifferential errors in exposure measurement. American Journal of Epidemiology 134, 1233-1241.

Hameri K., Koponen I.K., Aalto P.P., Kulmala M., 2002. The particle detection efficiency of the TSI 3007 condensation particle counter. Journal of Aerosol Science; 33 1463-1469.

Knibbs L.D., de Dear R.J., Morawska L., Coote P.M., 2007. A simple and inexpensive dilution system for the TSI 3007 condensation particle counter. Atmospheric Environment 41, 4553-4557.

Kromhout H., Heederik D., 1995. Occupational epidemiology in the rubber industry: implications of exposure variability. American Journal of Industrial Medicine 27, 171-185.

Li, X.Y., Gilmour P.S., Donaldson K., MacNee W., 1996. Free radical activity and pro-inflammatory effects of particulate air pollution (PM_{10}) *in vivo and in vitro*. Thorax 51, 1216-1222.

Maynard A.D., Aitken R.J., 2007. Assessing exposure to airborne nanomaterials: Current abilities and future requirements. Nanotoxicology 1, 26-41.

Maynard, A.D., Maynard R.L., 2002. A derived association between ambient aerosol surface area and excess mortality using historic time series data. Atmospheric Environment 36, 5561-5567.

McCawley M.A., Kent M.S., Berakis M.T., 2001. Ultrafine beryllium number concentration as a possible metric for chronic beryllium disease risk. Applied Occupational Environmental Hygiene 16, 631-638.

Oberdörster G., 2000. Toxicology of ultrafine particles: *in vivo* studies. *Phil. Trans. R. Soc. Lond. A.* 358, 2719-2740.

Paik S.Y., Zalk D.M., Swuste P., 2008. Application of a pilot control banding tool for risk level assessment and control of nanoparticle exposures. Annals of Occupational Hygiene 52, 419-428.

Park J.Y., Ramachandaran G., Raynor P.C., Olson Jr G.M., 2009. Determination of workplace nanoparticle exposure rankings by spatial mapping of particle mass, number, and surface area concentrations. Journal of Occupational Environmental Hygiene (in proceeding).

Peters A., Wichmann H.E., Tuch T., Heinrich J., Heyder J., 1997. Respiratory effects are associated with the number of ultrafine particles. American Journal of Respiratory Critical Care Medicine 155, 1376-1383.

Peters, M.T., Heitbrink W.A., Evans D.E., Slavin T.J., Maynard A.D., 2006. The mapping of fine and ultrafine particle concentrations in an engine machining and assembly facility. Annals of Occupational Hygiene 50, 249-257.

Schwartz J., Marcus A., 1990. Mortality and air pollution in London: A time series analysis. American Journal of Epidemiology 131, 185-194.

Shin W.G., Pui D.Y.H., Fissan H., Neumann S., Trampe A., 2007. Calibration and numerical simulation of Nanoparticle Surface Area Monitor (TSI Model 3550 NSAM). Journal of Nanoparticle Research 9, 61-69.

Thornburg J., Leith D., 2000. Mist Generation During Metal Machining. Journal of Tribology 122, 544-549.

Tran C.L., Buchanan D., Cullen R.T., Searl A., Jones A.D., Donaldson K., 2000. Inhalation of poorly soluble particles. II. Influence of particle surface area on inflammation and clearance. *Inhalation Toxicology* 12, 1113-1126.

Table 1. Aerosol concentrations and exposure ranks for all metrics in the restaurant, diesel engine lab, and die casting plant

Workplace	Zone	location	Surface area		Number (#/cm^3)				Mass (mg/m^3)					
			µm^2/cm^3	Rank	Fine (0.02->1 µm)	Rank	Coarse (0.3->5 µm)	Rank	Respirable	Rank	PM2.5	Rank	PM1.0	Rank
Restaurant	High	dishwasher	18.8	3	2,843	3	74	1	0.032	5	0.035	2	0.028	1
		Grill	52.2	2	23,929	2	41	3	0.029	6	0.016	6	0.010	6
		Oven	128.6	1	77,074	1	69	2	0.036	4	0.020	3	0.015	3
		Mean[a]	**48.6**		**16,914**		**54**		**0.032**		**0.022**		**0.016**	
	Low	Bar	7.1	5	1,412	6	10	5	0.044	1	0.018	4	0.014	4
		Serv station	5.5	6	1,318	5	10	5	0.040	2	0.018	4	0.013	5
		Sitting area	8.8	4	1,757	4	19	4	0.038	3	0.036	1	0.023	2
		Mean	**6.4**		**1,417**		**11**		**0.041**		**0.023**		**0.016**	
		p	0.003		0.01		0.005		0.06		0.85		0.89	
Diesel Engine Lab	High	Engine1	89.8	1	42,700	1	40	2	0.033	5	0.017	6	0.013	5
		Engine2	30.6	3	8,126	3	57	1	0.060	1	0.039	2	0.029	1
		Engine3	48.4	2	20,426	2	33	4	0.038	2	0.016	7	0.012	7
		Engine4	16.2	7	5,693	6	29	5	0.037	3	0.023	4	0.016	4
		Mean	**35.5**		**11,709**		**38**		**0.043**		**0.023**		**0.018**	
	Low	Prep room	20.3	4	6,479	4	27	6	0.037	3	0.041	1	0.026	2
		Study area	18.4	6	6,188	5	22	7	0.032	6	0.030	3	0.023	3
		TA office	20.1	5	5,487	7	34	3	0.025	7	0.021	5	0.013	5
		Mean	**23.4**		**6,345**		**28**		**0.035**		**0.032**		**0.023**	
		p	0.21		0.26		0.19		0.25		0.29		0.38	
Die Cast Facility	High	Die cast1	2,306.3	3	308,908	2	1,833	3	0.419	3	0.236	4	0.147	3
		Die cast2	2,502.5	2	321,629	1	3,370	1	0.898	1	0.450	2	0.335	2
		Trim press	2,778.3	1	298,082	3	2,193	2	0.872	2	0.502	1	0.376	1
		Mean	**2,458.2**		**311,670**		**2,434**		**0.645**		**0.339**		**0.255**	
	Low	Turning	345.9	6	92,315	6	782	6	0.119	6	0.095	6	0.125	5
		Milling1	649.7	4	103,094	5	868	5	0.284	4	0.243	3	0.183	4
		Milling2	448.9	5	107,659	4	1,107	4	0.150	5	0.149	5	0.110	6
		Mean	**431.5**		**99,678**		**823**		**0.155**		**0.135**		**0.101**	
		P	<0.001		<0.001		0.01		0.001		0.03		0.03	

Within each metric, the first three or four are given different shades, [a]: antilog of the least square mean of the logarithms of concentrations.

Table 2. GSD_{WL}, GSD_{WG} , and GSD_{BG}, and contrast, and precision for all exposure metrics

Workplace /exposure metric	GSD_{WL}	GSD_{WG}	GSD_{BG}	Contrast, ϵ	Precision, π
Restaurant					
Surface area	2.14	2.02	3.77	0.78	2.7
Fine number	1.99	3.31	4.89	0.64	1.9
Coarse number	1.89	1.55	2.96	0.86	3.8
RPM	1.49	1.09	1.16	0.74	8.0
PM2.5	1.56	1.41	1.00	0.00	5.2
PM1.0	1.68	1.46	1.00	0.00	4.6
Diesel engine lab					
Surface area	1.62	1.76	1.42	0.28	3.9
Fine number	1.69	2.13	1.48	0.21	3.1
Coarse number	1.41	1.29	1.23	0.39	7.0
RPM	1.32	1.26	1.17	0.31	8.2
PM2.5	1.47	1.36	1.07	0.04	6.1
PM1.0	1.43	1.38	1.00	0.00	6.2
Die cast facility					
Surface area	1.40	1.27	3.25	0.96	6.9
Fine number	1.19	1.07	2.21	0.99	16.2
Coarse number	1.70	1.34	2.07	0.86	4.9
RPM	1.50	1.55	2.54	0.82	4.5
PM2.5	1.59	1.65	1.72	0.54	4.0
PM1.0	1.60	1.65	1.72	0.54	4.0

Table 3. Ultrafine particle number concentrations measured by SMPS (N_{REF}) and calculated from a P-Trak and an OPC (N_{UFP})

ID	Zone	Location	N_{Ref} (10-487 nm, particles/cm^3)				N_{UFP} (20-300 nm, particles/cm^3)		
			CMD (GSD)	Mean	5%	95%	Mean	5%	95%
Restaurant	High	dishwasher	57.0 (2.19)	2,860	1,200	8,770	2,680	1,130	8,550
		Grill	32.2 (1.83)	25,000	9,300	75,200	23,800	8,840	59,000
		Oven	25.5 (2.13)	87,610	11,800	526,000	77,000	13,200	260,000
		Mean[a]		**18,100**			**16,700**		
	Low	Bar	76.2 (2.13)	1,480	1,170	1,960	1,400	1,100	1,190
		Serv station	68.3 (2.06)	1,320	394	4,060	1,310	394	4,000
		Sitting area	82.2 (2.09)	1,780	851	4,550	1,740	790	4,590
		Mean		**1,430**			**1,420**		
		P		0.009			<.001		
Diesel Engine Lab	High	Engine1	27.4 (1.83)	50,600	13,500	631,000	42,600	14,400	292,000
		Engine2	30.5 (2.20)	13,100	7,500	23,500	7,140	3,230	16,200
		Engine3	30.1 (1.97)	24,500	14,000	53,900	20,300	11,200	45,700
		Engine4	34.3(2.29)	6,100	3,380	11,400	4,990	2,840	8,630
		Mean		**15,600**			**11,700**		
	Low	Office	40.1 (2.10)	7,590	5,420	11,500	6,270	4,360	10,000
		Study area	38.2 (2.08)	7,330	3,840	28,200	6,160	3,060	24,200
		TA office	45.5(2.08)	6,100	3,780	10,900	5,450	3,290	10,000
		Mean		**7,180**			**6,320**		
		p		0.16			0.26		
Die Cast Facility	High	Die cast1	38.0 (1.78)	845,600	511,000	1,510,000	307,000	280,000	370,000
		Die cast2	37.7 (1.92)	919,000	347,000	1,840,000	318,000	263,000	404,000
		Trim press	44.4 (1.93)	901,000	689,000	1,160,000	296,000	281,000	312,000
		Mean		**891,000**			**309,000**		
	Low	Turning	42.2 (2.11)	104,000	56,000	216,000	91,000	53,700	151,000
		Milling1	62.7 (2.51)	113,000	97,000	130,000	102,000	89,400	118,000
		Milling2	43.2 (2.22)	126,000	104,000	251,000	107,000	89,400	171,000
		Mean		**114,000**			**99,000**		
		p		<.001			<.001		

Table 4. GSD_{WL}, GSD_{WG}, and GSD_{BG}, and contrast, and precision for all exposure metrics in the restaurant after regrouping

Exposure metric	GSD_{WL}	GSD_{WG}	GSD_{BG}	Contrast, ϵ	Precision, π
Surface area	2.13	1.78	4.64	0.88	3.1
Fine number	2.02	1.68	9.52	0.95	3.3
Coarse number	1.90	2.44	1.52	0.18	2.4
RPM	1.47	1.14	1.08	0.28	7.8
PM2.5	1.56	1.39	1.12	0.10	5.3
PM1.0	1.68	1.43	1.19	0.19	4.7

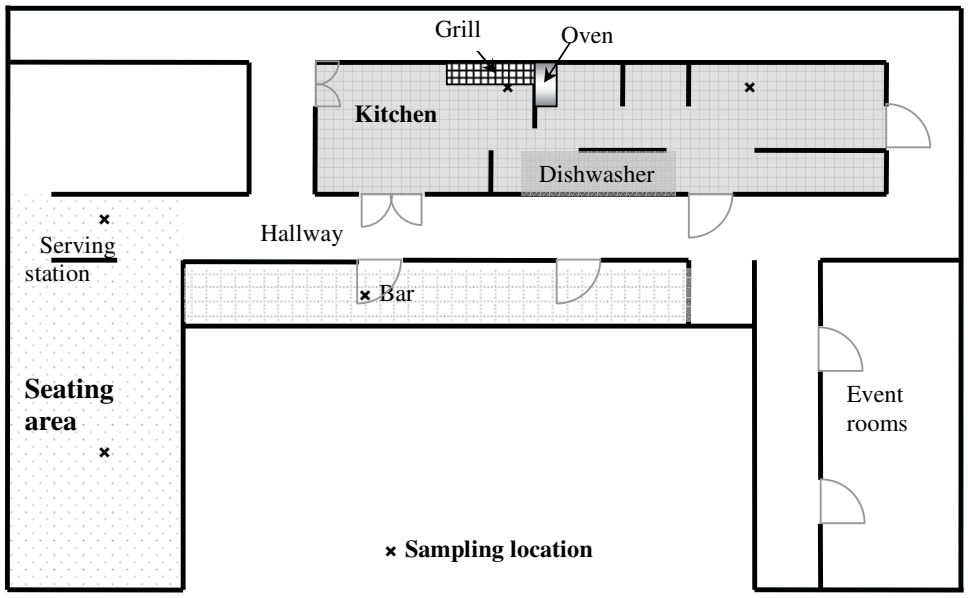

Figure 1. Floor plan of the restaurant (sampling locations are indicated on the diagram).

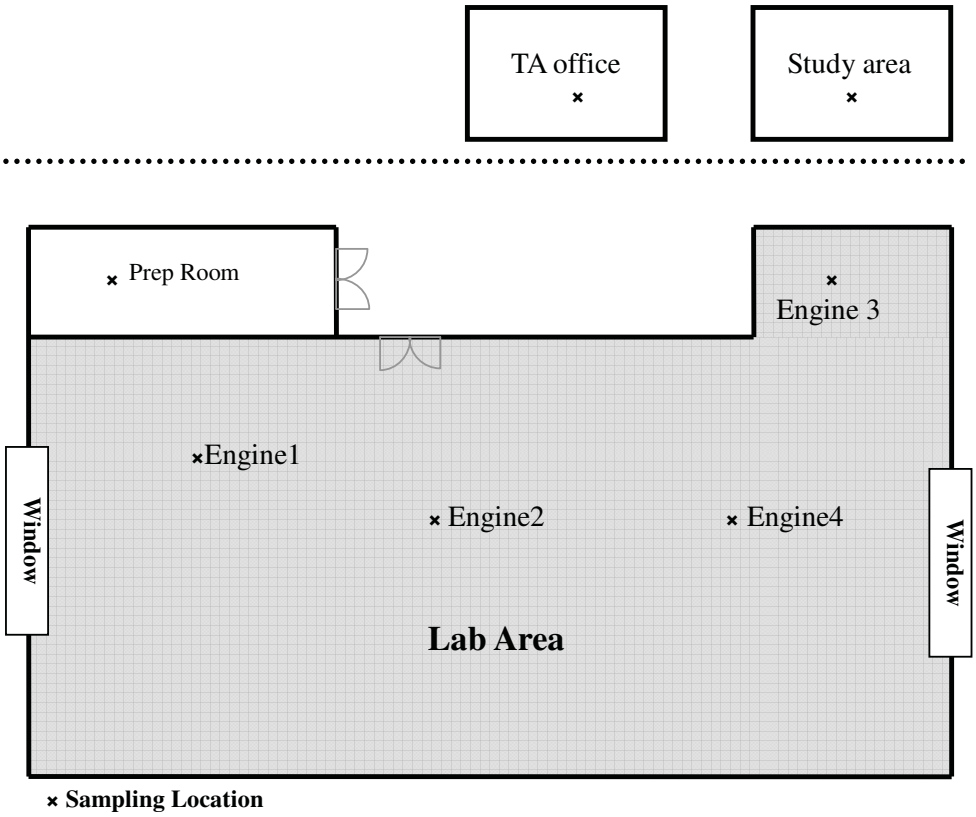

Figure 2. Floor plan of the diesel engine lab (sampling locations are indicated on the diagram).

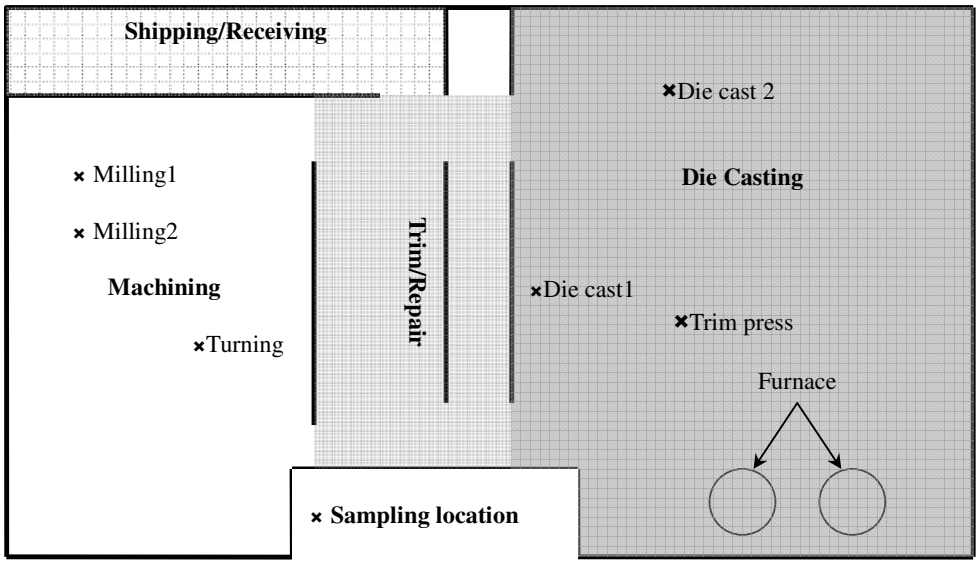

Figure 3. Floor plan of the die casting plant (sampling locations are indicated on the diagram).

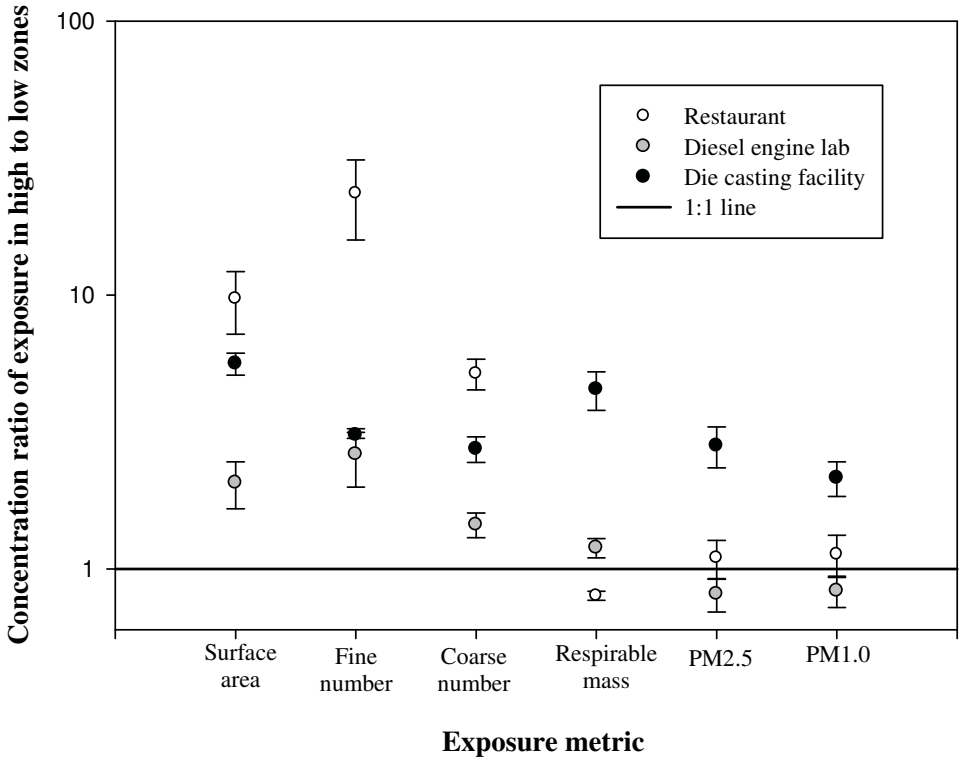

Figure 4. Ratio of high zone and low zone for mass, number, and SA concentrations in the three workplaces.

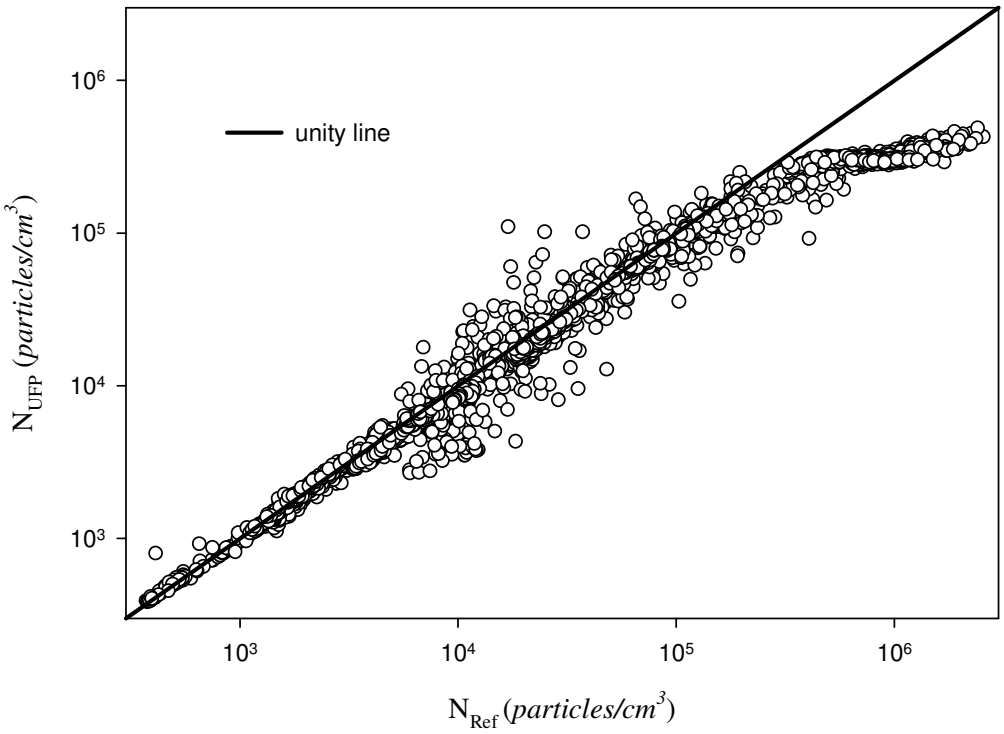

Figure 5. Relationships between N_{Ref} and N_{UFP}.

Chapter IV

Comparison of two estimation methods for surface area concentration using number concentrations and mass concentration of combustion-related ultrafine particles

Published In:

Atmospheric Environment, 2009; 43: 502-509

Recent research has suggested that the adverse health effects caused by nanoparticles are associated with their surface area (SA) concentrations. In this study, SA was estimated in two ways using number and mass concentrations and compared with SA (SA_{meas}) measured using a diffusion charger (DC). Aerosol measurements were made twice: once starting in October 2002 and again starting in December 2002 in Mysore, India in residences that used kerosene or liquefied petroleum gas (LPG) for cooking. Mass, number, and SA concentrations and size distributions by number were measured in each residence. The first estimation method (SA_{PSD}) used the size distribution by number to estimate SA. The second method (SA_{INV}) used a simple inversion scheme that incorporated number and mass concentrations while assuming a lognormal size distribution with a known geometrical standard deviation. SA_{PSD} was, on average, 2.4 times greater (range=1.6–3.4) than SA_{meas} while SA_{INV} was, on average, 6.0 times greater (range=4.6–7.7) than SA_{meas}. The logarithms of SA_{PSD} and SA_{INV} were found to be statistically significant predictors of the logarithm of SA_{meas}. The study showed that particle number and mass concentration measurements can be used to estimate SA with a correction factor that ranges between 2 and 6.

1. Introduction

Ultrafine particles are defined as particles smaller than 100 nm in diameter. As these particles have a larger surface area (SA) per unit mass and also more atoms on their surface than fine or coarse particles (Welland and Porter, 2005), they may have increased surface reactivity in technical applications and biological activity in the human body.

Since the hypothesis of a possible causal relationship between adverse health effects and exposure to ultrafine particles was first proposed, many papers have been published to support this assertion (Schwartz *et al.*, 1996; Fairley, 1999; Wichmann *et al.*, 2000; Oberdörster and Utell, 2002).

Traditionally, mass concentration has been regarded as most appropriately associated with ill health for particle exposure assessment. As the adverse health effects of ultrafine particles have been investigated, researchers have questioned the appropriateness of mass concentration measurements for ultrafine particles' exposure (e.g., Kent *et al.*, 2001; McCawley *et al.*, 2001). Exposure assessment using mass concentration may not reflect the toxicity of ultrafine particles because these particles do not contribute much to total mass concentration even when they dominate the particle number concentration. Therefore, alternative exposure metrics for the ultrafine and fine particles have been proposed. McCawley *et al.* (2001) showed that particle number concentration was a more appropriate metric for chronic beryllium disease and found no correlation between mass and number concentration. Peters *et al.* (1997) found that a decrease in peak expiratory flow among twenty-seven non-smoking asthmatics was more associated with number concentration than mass.

SA concentration has been proposed as biologically more relevant to the effective dose than other exposure metrics because the adverse health effects of ultrafine particles may be associated with surface reactivity and the portion of the size distribution that contributes most to SA does not contribute much to the mass concentration (Li *et al.*, 1996; Oberdörster, 2000; Tran *et al.*, 2000). Several toxicological studies have shown that inflammatory responses in the lung caused by ultrafine and fine particles (Tran *et al.*,

2000; Brown *et al.*, 2001) and translocation to the lymph nodes (Tran *et al.*, 2000) were proportional to SA deposited regardless of particle composition, size, or shape. Driscoll (1996) demonstrated that overload tumors were best correlated with SA, and not number or mass concentration.

Only a few devices to measure SA concentrations directly are available commercially. The first device developed for SA measurement was the epiphaniometer, which can measure active SA. However, it is not suitable for workplaces because it has a radioactive source (Maynard, 2003). TSI Inc. (Shoreview, MN) developed a portable nanoparticle SA monitor suitable for workplaces that measures the SA of particles likely to be deposited in the tracheobronchial or alveolar regions of the respiratory system rather than total aerosol SA (Fissan *et al.*, 2006). The LQ1-DC diffusion charger (Matter Engineering, Switzerland) consists of an aerosol diffusion charger and an electrometer to measure the attachment rate of unipolar ions to particles that in turn is directly related to active SA. The portable diffusion charger (DC) also can be utilized in occupational settings. While the SA of monodisperse particles which were smaller than 100 nm was comparable to the geometric SA, it underestimated SA for particles larger than 100 nm in diameter (Ku and Maynard, 2005).

Alternative methods can be used to estimate SA based on particle size distribution statistics. Woo *et al.* (2001) tried estimating aerosol SA concentrations with two methods based on indirect size distribution modeling using measurements of number, charge, and mass concentration and direct aerosol size distribution measurement by an SMPS (Scanning Mobility Particle Sizer) and an LPS (laser particle sizer). The authors obtained optimal values for three parameters defining a lognormal size distribution by

minimizing the difference between measured signals and expected values. They then calculated the total SA concentration by integrating the lognormal size distribution function. The estimated total SA concentration was compared with SA concentrations obtained from the SMPS–LPS system. The calculated SA concentration from the parametric measurements was higher by a factor of 2 than the SA obtained from the particle size distribution measurement, although there was a high degree of correlation between them (R^2=0.91). However, the devices used for measurement in that study are not widely and easily used in occupational and ambient environments for exposure assessment.

Maynard (2003) developed an SA estimation method using mass and number concentration measurements by assuming a lognormal particle size distribution with a specific geometric standard deviation (GSD). When compared to actual SA concentrations determined by integrating known size distributions obtained from published papers (McCawley *et al.*, 2001; Zimmer and Maynard, 2002), SA concentrations estimated using his algorithm were between 0.95 and 1.45 times the actual values for a unimodal size distribution when the GSD value was set equal to 1.8 and were between 1.66 and 3.06 times actual concentrations for a bimodal size distribution using GSD= 1.8 for both modes of the size distribution. However, Maynard's estimates correlated well with the measurements (R^2=0.98). This study provided a positive prospect for estimating SA concentration based solely on measurements routinely made in occupational health.

In this paper, two estimation methods are described and applied to estimate SA concentrations based only on number and mass measurements, and using only devices

easily available in the field. These estimates are compared with SA concentrations measured directly. The objective of this study is to determine if estimated SA concentrations can be used to predict the actual SA concentrations measured with a direct-reading instrument.

2. Methods

2.1. Study design

This work is part of a larger study dealing with women's exposure to particulate matter in India reported in Andresen *et al.* (2005). Cooking is primarily a woman's role in India and cooking heaters are considered one of the major ultrafine particle sources in Indian homes. Therefore, exposure measurements were performed in Mysore, India in residential homes that used kerosene or liquefied petroleum gas (LPG) as cooking fuels. Sampling was conducted in kitchens twice: once starting in October 2002 and again beginning in December 2002. In the first period, the assessments were conducted in seven homes (three kerosene, four LPG). In the second period, assessments were conducted in ten homes (five kerosene, five LPG).

2.2. Instrumentation

Four real-time instruments for particle mass, number, and SA concentrations and size distribution by number and one gravimetric sampler for calibration of the real-time mass monitor were used simultaneously in each location. All devices were used as area

samplers for 24 h and were placed near the combustion sources at table-top level.

The DustTrak (Model 8520, TSI, Shoreview, MN) with PM2.5 inlet was used for mass concentration. It measures scattered light which is a function of particle mass concentration, size distribution, and composition. The DustTrak measurements were calibrated to the average aerosol concentration from the gravimetric measurements. The gravimetric PM2.5 concentrations were obtained using a PM2.5 sampler (PEM_ Model 200, MSP Inc., Minneapolis, MN) that collected particles on Teflon filters by inertial impaction. Air pumps drew air through sampling inlets at 10 L min/1. Filters were weighed before and after sampling using a microbalance with a sensitivity of 5 mg in a weighing room where the temperature and humidity were environmentally controlled. After sampling, filters were equilibrated in the weighing room and then reweighed. For each run, blank samples were weighed at the same time as the sampled filters. The detection limit was calculated as three times the standard deviation of the field blank weight gains divided by the sampled air volume. The DustTrak measurements were recalculated using a specific calibration factor for each measurement as follows:

$$\text{Calibration Factor} = \frac{24-\text{hour average gravimetric concentration}}{24-\text{hour time integrated DustTrak concentration}} \quad (1)$$

Each DustTrak measurement was multiplied by this factor to estimate the true mass concentration. The gravimetric concentration and integrated DustTrak concentrations were highly correlated (R^2=0.93) and the mean calibration factor was 0.216 with a standard error of 0.021.

The CPC 3007 (TSI, Shoreview, MN), a real-time single-particle counting instrument, was used for measuring number concentration of ultrafine particles by

condensational growth and optical detection. The LQ1-DC (Matter Engineering, Switzerland) was used to measure the aerosol active SA. It measures the attachment rate of unipolar ions sticking to the surface of particles. The HHPC-6 (Hach Ultra, Grants Pass, OR) is an optical particle counter which has a laser beam and photodetector installed in it to simultaneously count and size particles into six channels via light scattering. It was used for size distribution by number. All real-time instrument data were organized into two-min averages.

The average relative humidity in sampling seasons I and II was 40% and 22% respectively, and not high enough to significantly affect the performance of the DustTrak (e.g., Ramachandran *et al.*, 2003) or the CPC 3007 (TSI, Inc).

2.3. Surface area estimation methods

2.3.1. Estimation method based on particle number size distribution (SA_{PSD})

Particle number concentration can be measured by the CPC 3007 and the HHPC-6. The CPC 3007 is a size-integrating counter detecting particles 0.01–1.0 mm in diameter. The HHPC-6 counts particles into 6 size ranges: 0.3–0.5 mm, 0.5–0.7 mm, 0.7–1.0 mm, 1.0–2.5 mm, 2.5–5.0 mm, and >5.0 mm. The ultrafine particle count (N_{UFP}, 0.01–0.3 mm) can, therefore, be calculated using the first three size intervals of the HHPC-6 and the CPC count:

$$N_{UFP} = N_{CPC} - \sum_{k=1}^{3} N_{HHPC\,6,k} \qquad (2)$$

where k is the index for the size intervals of the HHPC-6.

The counts in the first five size intervals of the HHPC-6 and the N_{UFP} are used to calculate total SA concentrations. Under the assumption that the particles are log-normally distributed, the log median diameter ($d_{med\,i}$) is chosen as the representative diameter for each interval:

$$d_{med\,i} = 10^{(\log d_{\max i} + \log d_{\min i})/2} \quad (3)$$

where $d_{max\,i}$ and $d_{min\,i}$ are the upper and lower limits of the i^{th} interval.

Using $d_{med\,i}$, the SA concentration of each interval (SA_i) is obtained as

$$SA_i = N_i \cdot \pi \cdot d_{med\,i}^2 \quad (4)$$

in which N_i is the number concentration in the i^{th} interval from the CPC 3007 and HHPC-6 measurements.

The total particle SA concentration for this method, SA_{PSD}, is the sum of the SA from each interval.

$$SA_{PSD} = \sum_{i=1}^{6} SA_i \quad (5)$$

2.3.2. Estimation method based on Maynard algorithm (SA_{INV}) (Maynard, 2003)

This method assumes that the particle size distribution is unimodal and lognormal and described by the count median diameter (CMD), GSD, and the total number concentration (N). The size distribution function can be expressed as

$$f(CMD, GSD, d) = N\Phi(CMD, GSD, d) \quad (6)$$

where F is the normalized lognormal function.

For instruments that function over a certain size range, the expected number

concentration (N_{exp}) and the expected mass concentration (M_{exp}) can be expressed as

$$N_{\exp} = N \int_{d_{\min j}}^{d_{\max j}} \Phi(CMD, GSD, d)\mathrm{d}d \tag{7}$$

$$M_{\exp} = M \int_{d_{\min j}}^{d_{\max j}} \Phi(MMD, GSD, d)\mathrm{d}d \tag{8}$$

in which M is the total mass concentration, MMD is the mass median diameter, and $d_{min\,j}$ and $d_{max\,j}$ are the lower and upper limits of the j^{th} measurement. The CMD and MMD are related by the Hatch–Choate equation:

$$MMD = CMD\, e^{3\ln^2 GSD} \tag{9}$$

To reconstruct the aerosol size distribution, three unknowns need to be determined: these can be either the CMD, GSD and N or the MMD, GSD and M. If three independent measurements are taken, aerosol size distribution can be approximated by minimizing the χ^2 function:

$$\chi^2(CMD, GSD, N) = \sum_{j=1}^{n} \left(\frac{C_j - m_j}{\sigma_j} \right)^2 \tag{10}$$

where C_js are expected (or calculated) values, m_js are measured values from aerosol instruments, and σ_j is the measurement error (*i.e.*, the standard deviation of measured values and calculated values). If GSD is fixed, just two measurements (e.g., number and mass concentrations) will be needed. If these two measurements are taken on the same aerosol, and each measured value is equal to each calculated (expected) value, their relation will be expressed as follows:

$$\frac{N_{\exp}}{M_{\exp}} = \frac{N_{meas}}{M_{meas}} \tag{11}$$

and the χ^2 will be equal to 0. When Eqs. (7) and (8) are substituted into Eq. (11), the expression

$$\frac{N}{M} = \frac{N_{meas} \int_{d_{\min j}}^{d_{\max j}} \Phi(MMD, GSD, d)\mathrm{d}d}{M_{meas} \int_{d_{\min j}}^{d_{\max j}} \Phi(CMD, GSD, d)\mathrm{d}d} \tag{12}$$

is obtained. In addition, the total mass and number concentrations are related as

$$M = N \cdot \rho \cdot \left(\frac{\pi}{6} d_{\overline{m}}^3 \right) \tag{13}$$

in which $d_{\overline{m}}$ is the diameter of average mass; if the particles are assumed to be spherical dm is calculated as

$$d_{\overline{m}} = CMD \cdot e^{1.5 \ln^2 GSD} \tag{14}$$

The ratio (N/M) can be expressed as follows:

$$\frac{N}{M} = \frac{6}{\pi\rho} \cdot \left(CMD \cdot e^{1.5 \ln^2 GSD} \right)^{-3} \tag{15}$$

If GSD is fixed, Eqs. (12) and (15) can be solved iteratively by changing CMD to obtain N/M. Once N/M is determined, CMD and N can be calculated. In this study, GSD was set to 1.8 as in Maynard (2003). With GSD fixed, the remaining size distribution parameters can be determined using two independent measurements of total particle number concentration and total particle mass concentration. In this study, the CPC 3007 and

DustTrak were used for number and mass concentration measurements, respectively.

Once the parameters of the size distribution have been determined, the diameter of average SA ($d_{\bar{s}}$) can be calculated using the Hatch–Choate equation:

$$d_{\bar{s}} = CMD \cdot e^{ln^2 GSD} \quad (16)$$

and total aerosol SA concentration estimated using this method is given by:

$$SA_{INV} = N \cdot \pi \cdot d_{\bar{s}}^2 \quad (17)$$

2.4. Statistical analysis

Statistical analysis was conducted using SAS 9.1 (SAS Institute Inc., Cary, NC). The study design included two sampling periods – I (October and November) and II (December and January), and two types of cooking fuel – kerosene and LPG. Therefore, the associations between measured and estimated SA concentrations needed to be adjusted for the effects of sampling period and cooking fuel.

As described earlier, the measurements used for the statistical analysis were two-minute averages obtained using the four different real-time devices. Data taken from the same residence were auto-correlated. To correct for the auto-correlation in the realtime measurements, general linear models with compound symmetry covariance structure were used. Such models were more appropriate to compare estimated SA with SA_{meas} than models assuming independence among different measurements and could adjust for the effects of sampling period and fuel type. Data within each sampling period were tested for fuel type differences and data within each fuel type were tested for sampling

period differences. Linear regression models were constructed to see the effects of these two variables on the association between log-transformed measured (SA_{meas}) and estimated SA (SA_{PSD}, and SA_{INV}) concentrations. Interaction terms were included to examine the effect of each variable on the association between measured and estimated SA (SA_{est}). In order to compare calculated SA and estimated SA for each time period, data are needed from all four real-time instruments. If a time point did not have any one of the four instrument readings for some reason, it was excluded. Only 39% of data had all four measurements at each data point and were used for the analysis. In the model equation, all data analysis results were interpreted at the median time in monitoring. The level of statistical significance for all analyses was 0.05.

3. Results and discussion

3.1. Aerosol concentrations using different metrics

The particulate matter concentrations measured using various exposure metrics by each category are summarized in Table 1. Fine particle number concentration was measured by CPC 3007 covering a diameter range of 0.01 to >1.0 whereas coarse particle number concentration used the HHPC-6 to detect particles 0.3 to >5 mm in diameter. All exposure metrics were approximately log-normally distributed.

The two-minute average concentrations for kerosene and LPG homes and for sampling period I and II were statistically compared using t-tests. Concentrations using all exposure metrics in kerosene homes were slightly higher than those in LPG homes,

but no fuel type differences were statistically significant (mass: p= 0.26; fine particle number: p= 0.33; coarse particle number: p= 0.40; and SA: p= 0.81). In addition to the two-min average concentrations, the averaged concentrations for the entire sampling time at each home showed no differences as a function of fuel type for all metrics (mass: p=0.15; fine particle number: p= 0.29; coarse particle number: p=0.23; and SA: p=0.42) and the gravimetric mass measurements that were conducted for DustTrak calibration presented similar trends (p=0.36).

Andresen *et al.* (2005) reported on gravimetric measurements made in the same residences and found that 24-h average exposure to PM2.5 in homes using kerosene was significantly higher than in LPG homes. Mass concentrations in the Andresen *et al.* study were also lower than the 24-h average respirable particulate matter concentrations measured by Balakrishnan *et al.* (2004) in Indian households using the same fuels. In the Balakrishnan *et al.* study, the geometric mean mass concentrations from kerosene and LPG kitchens were 0.203 and 0.073 mg/m^3, respectively. As mentioned previously, only 39% of our data were utilized for the statistical analyses. Thus, our data do not represent 24-h exposures. This might explain some of the difference of our results from others. Raiyani *et al.* (1993) measured total suspended particulate concentrations of 0.520 and 0.500 mg/m^3, respectively, in kerosene and LPG households in India during cooking time. These differences were not significant.

In all metrics except the fine particle number concentration, values from sampling period II were significantly higher than those from sampling period I. Mass (p=0.01) and SA (p= 0.02) concentrations showed significant sampling period differences but coarse particle number concentrations did not (p=0.65). For the fine particle number

concentrations, levels in sampling period I were higher than those in sampling period II, but not in a statistically significant manner ($p=0.65$).

Table 2 shows the mean exposure concentrations for the different exposure metrics and their rankings when classified by sampling period and fuel type. Exposure rankings by mass and SA concentrations were similar to each other. However, rankings by fine number concentrations were different. This indicates the importance of choosing the metric most relevant to adverse health effects caused by exposure to ultrafine particles. The choice of the exposure metric will be important in classifying similar exposure groups (SEG) by exposure levels for epidemiological studies and in establishing a sampling strategy for exposure assessments.

To see the temporal trends of the exposure metrics depending on the usage of cooking heaters during the sampling, all measured metrics were normalized by dividing by the average concentration for each measurement. As an example, Fig. 1 shows the normalized exposure concentrations plotted in a home with a kerosene cooker in sampling period II. From ~12:00 to ~13:00 when lunch was prepared, higher normalized concentrations were seen, while lower concentrations were observed between lunch and dinner time.

The SA concentration and mass concentration showed good correlation even though during the peak time, the mass concentration increased less than the SA concentration. The SA concentration and fine number concentration also showed good agreement between each other. However, normalized concentrations for the coarse particle number concentrations were significantly lower than those for SA and fine particle number concentrations during the cooking time. The normalized coarse particle

number concentrations showed similar trends to those for mass concentrations, most likely because coarse particles are not only from combustion sources but also from general dusts, and contribute more heavily to mass concentrations.

3.2. The association between measured and estimated surface area concentrations

Table 3 shows mean measured and estimated SA by sampling period and fuel type. By categories of sampling period and fuel type, the SA estimated using particle number size distribution data (SA_{PSD}) was between 1.6 and 3.4 times the SA measured using the diffusion charger (SA_{meas}). Likewise, the SA estimated using the Maynard algorithm (SA_{INV}) was between 4.6 and 7.7 times SA_{meas}. For both estimation methods, the ratios of estimated to measured SA were generally closer to unity as SA_{meas} increased. Although the ratios of SA_{INV}/SA_{meas} were greater than the ratios of SA_{PSD}/SA_{meas}, exposure rankings based on SA_{INV} were more similar to those based on SA_{meas} than rankings based on SA_{PSD}. The exposure ranks by SA_{PSD} were similar to those by fine particle number concentration in Table 2 while the exposure ranks of SA_{INV} were different from those of fine number concentration and SA_{PSD}.

Comparisons of measured SA and estimated SA concentrations in a kerosene home and an LPG home are shown in Fig. 2. SA_{PSD} was around two times higher but well correlated with SA_{meas}. SA_{INV} was around five times higher than SA_{meas}. The three metrics had similar temporal patterns.

The relationships between the logarithm of SA_{meas} and the logarithms of SA_{PSD}

and SA_{INV} are shown in Fig. 3. Correlation coefficients are not appropriate to describe auto-correlated data. However, they can be useful as a tool for exploratory data analysis that needs to be followed by more rigorous statistical analysis. The correlation coefficients for the relationship between log [SA_{meas}] and log [SA_{PSD}], and log [SA_{meas}] and log [SA_{INV}] were 0.85, and 0.91, respectively, which indicates a strong correlation between log-[SA_{meas}] and both log [SA_{PSD}] and log [SA_{INV}]. The correlation of SA_{meas} with SA_{INV} was slightly higher, although SA_{INV} overestimated SA_{meas} much more than SA_{PSD} did.

Calculation of SA_{PSD} is based on measurements made by two instruments, an integrated measurement of particle number by a CPC for particles <1.0 mm and size selective measurement for particles in the range 0.3 to >5 mm. As mentioned previously, SA_{PSD} was obtained from summing up the product of number concentration of each channel and the log median diameter SA for that channel. Thus, SA_{PSD} can potentially be influenced by the number concentration and log median diameter for each size channel. The log median diameters of particles from each size interval were the same in all cases because each size channel was fixed. Fine particle number concentrations were sensitive to the usage of cooking stoves and had similar trends to those for SA concentrations. However, coarse particle number concentrations over time were relatively constant (Fig. 1(b)). Therefore, the most important factor for determining SA_{PSD} is the fine particle number concentration.

We assumed 100% counting efficiency in all six size bins. However, the counting efficiency of the first size bin (0.3–0.5 mm) from instrument's specification is 50% at 0.3 mm and 95% at 0.5 mm. The lower counting efficiency could cause

overestimation in N_{UFP} which is the first size channel in calculating SA_{PSD} and underestimation in the second size channel for SA_{PSD}. The percentage of particles in 0.3–1.0 mm from N_{CPC} was less than 0.8% on average (range= 0.3–1.7%) of the total CPC concentration, which is not significant. When the collection efficiency of the first size bin was assumed to be 50% and 75%, SA_{PSD} increased by 15% and 7%, respectively. Although the estimated SA increased slightly, the exposure ranks remained the same as those based on the original SA_{PSD}.

Another source of error could come from coincidence at high particle number concentration in the OPC. According to the manufacturer's specifications, at a concentration of approximately 70 particles/cm^3, 5% of particles could be lost due to coincidence. While our coarse particle concentration was frequently greater than 70 particles/cm^3, the errors due to this are likely not significant because, as noted earlier, coarse particles are a miniscule fraction of the total particle count. An error of the order of 5–10% in the coarse particle count will not significantly change SA_{PSD}.

A third source of error is the response function of the OPC. The OPC response is a complex function of particle size distribution, wavelength of light and the refractive index of the particles. If the instrument is calibrated using a test aerosol such as PSL spheres that mainly reflect and refract light, then its response to cooking fuel aerosol containing carbon particles that mainly absorb light (imaginary component of refractive index) could be different.

Although beyond the scope of this paper, these errors could be estimated using Mie theory. Thus the several instrument limitations described above may contribute to differences between SA_{meas} and SA_{PSD}.

3.3. Sensitivity of estimated SA_{PSD} concentrations to exponent of d in Eq. (3)

For estimating SA based on size distribution, the same SA calculation was applied to all six size channels. In the free molecular regime, active SA is known to be proportional to d^2 regardless of the particle composition (Adachi *et al.*, 1985). Hence, for particles below 100 nm in diameter, the LQ1-DC measures the total geometric SA of the particles without being dependent on the chemistry of the particles (Siegman *et al.*, 1998; Zhiqiang *et al.*, 2000). However, the active SA dependence on particle size diminishes from to 'd^2' to 'd' through the transition regime to the continuum regime (Baron and Willeke, 2001). Ku and Maynard (2005) showed that the diffusion charger's response for particles smaller than 80 nm in diameter was proportional to d^2 but decreased to $d^{1.5}$ for particles 80–200 nm in diameter. As the diameter increased further, active SA measured by the diffusion charger became proportional to d.

To investigate this instrument limitation further, we recalculated an SA proportional to $d^{1.0}$, and then to $d^{1.5}$ to approximately match the diffusion charger response for size channels greater than 300 nm. Table 4 presents the estimated SA calculated by the new equations applied to particle sizes greater than 300 nm. $SA_{2.0}$ in Table 4 is equal to SA_{PSD} in Table 3. The ratios of estimated to measured SA are much closer to unity, moving from 2.4 for $SA_{2.0}$ to 1.5 for $SA_{1.0}$ for these new equations compared to the original method while correlation between measured SA and new estimated SA concentrations was equally good. Our measurements were conducted in residential homes where there may have existed significant numbers of coarse particles

which could have led to an underestimation of the concentration by the diffusion charger. This may especially be the case during off-peak times when the relative contribution of coarse particles to the SA may be higher than peak concentrations which are dominated by ultrafine combustion particles. This may cause bigger deviation between SA_{PSD} and SA_{meas} measured by the diffusion charger.

3.4. Sensitivity of estimated SA_{PSD} concentrations to median diameter in Eq. (3)

According to the manufacturer, the LQ1-DC can measure the SA of particles from a few nm to greater than 10 mm. The detection range is not precisely determined. For the estimation of SA_{PSD}, number concentrations from six size channels (10–300 nm, 300–500 nm, 500–700 nm, 700 nm–1 mm, 1–2 mm, 2–5 mm) were used. The lower limit of 10 nm for the first channel is an educated guess, with some uncertainty associated with it. Thus, the assumed log median diameter of the first channel is 55 nm. However, if the log median diameter were smaller or larger than this assumed value, estimated SA based on size distribution could be influenced substantially. To determine the sensitivity of SA_{PSD} to a lower detection limit for the first channel, different log median diameters (45 nm, 50 nm, and 60 nm) for the first channel were assumed (Table 5). SA_{55} in Table 5 is equal to $SA_{1.5}$ in Table 4. In this calculation, the SA for size channels greater than 300 nm was calculated using '$d^{1.5}$', instead of '$d^{2.0}$'. Reducing the log median diameters of the first channel and applying $d^{1.5}$ for SA calculation decreased the estimation errors from ~140% to ~3% on average. This finding shows that SA_{PSD} is critically dependent on the method used to select the representative diameter for the first size channel.

3.5. Sensitivity of estimated SA_{INV} concentrations to assumed values for geometric standard deviations (GSDs)

The second estimation method (SA_{INV}) is based on a simple inversion method that uses number and mass concentration measurements to estimate aerosol SA concentrations while assuming a lognormal aerosol size distribution with a fixed value of GSD=1.8. This assumed value of GSD might be responsible for the overestimation of the SA by this method.

Table 6 presents SA estimation based on the Maynard method assuming different values of GSD between 1.5 and 3.0. $SA_{1.8}$ in Table 6 is equal to SA_{INV} in Table 3. As GSD increases, estimation errors decreased significantly, indicating that the Maynard method is very dependent on the assumed GSD value. If the full size distribution by mass had been measured using an impactor or the full size distribution by number had been measured with real-time instruments, the actual GSD would be known, and a better SA estimation could be obtained.

4. Conclusions

SA concentrations were estimated based on number and mass concentrations using aerosol instruments routinely used in environmental and occupational measurements and compared with SA directly measured using a diffusion charger.

Particle concentrations in homes using kerosene as a cooking fuel were slightly

higher than those in homes using LPG, but the differences were not statistically significant. Mass and SA concentrations in sampling period II were significantly higher than those in sampling period I ($p < 0.05$) but no significant sampling period difference was observed for fine and coarse particle number concentrations ($p > 0.05$).

SA estimated using particle size distribution by number (SA_{PSD}) was approximately two times greater than directly measured SA (SA_{meas}) but well correlated with SA_{meas}. This difference may be due to the diffusion charger's detection characteristics that led to an underestimation of SA for particles larger than 100 nm. SA_{PSD} was sensitive to the power of d to which measurement might be proportional and to the diameter chosen to represent the first size interval. The estimated SA using a simple inversion method (SA_{INV}) was about six times greater than SA_{meas} even though it was better correlated with SA_{meas} than was SA_{PSD}. This estimation requires assuming a lognormal distribution and a value for the GSD, and these assumptions might be responsible for the overestimation. This method was very dependent on the assumed GSD levels. Each method was found to be a good predictor of SA_{meas} statistically. The exposure ranks by SA_{INV} were similar to those by SA_{meas} while the exposure ranks by SA_{PSD} kept a similar trend to those by fine particle number concentration. Even though SA_{INV} overestimated SA_{meas}, the method can be used with a correction factor to estimate SA_{meas}.

References

Adachi M., Kousaka Y., Okuyama K., 1985. Unipolar and Bipolar Diffusion Charging of Ultrafine Aerosol Particles. Journal of Aerosol Science 16, 109-123.

Andresen P.R., Ramachandran G., Pai P., Maynard A.D., 2005. Women's personal and indoor exposures to PM2.5 in Mysore, India: Impact of domestic fuel usage. Atmospheric Environment 39, 5500-5508.

Balakrishnan K., Sambandam S., Ramaswamy P., Mehta S., Smith K.R., 2004. Exposure assessment for respirable particulates associated with household fuel use in rural districts of Andhra Pradesh, India. Journal of Exposure Analysis and Environmental Epidemiology supplement 1, S14-S25.

Baron P.A., Willeke K., 2001. Aerosol measurement: Principles, techniques, and Applications, 2nd ed. Wiley-Interscience, New York, pp. 404-406.

Brown, D.M., Wilson M.R., MacNee W., Stone V., Donaldson K., 2001. Size-dependent proinflammatory effects of ultrafine polystyrene particles: A role for surface area and oxidative stress in the enhanced activity of ultrafines. Toxicology and Applied Pharmacology 175**,** 191-199.

Driscoll K.E., 1996. Role of inflammation in the development of rat lung tumors in response to chronic particulate exposure. Inhalation Toxicology 8 (suppl. 1), 139-153.

Firley D., 1999. Daily mortality and air pollution in Santa Clara County, California: 1989-1996. Environmental Health Perspective 107, 637-641.

Fissan H., Neumann S., Trampe A., Pui D.Y.H., Shin W.G., 2006. Rationale and principle of an instrument measuring lung deposited nanoparticle surface area. Journal of Nanoparticle Research 9, 53-59.

Kent M.S., Robins T.G., Madl A.K., 2001. Is total mass or mass of alveolar-deposited airborne particles of beryllium a better predictor of the prevalence of disease? a preliminary study of a beryllium processing facility. Applied Occupational and Environmental Hygiene 16, 539-558.

Ku B.K., Maynard A.D., 2005. Comparing aerosol surface area measurements of monodisperse ultrafine silver agglomerates by mobility analysis, transmission electron microscopy and diffusion charging. Journal of Aerosol Science 36, 1108-1124.

Li X.Y., Gilmour P.S., Donaldson K, MacNee W., 1996. Free radical activity and pro-inflammatory effects of particulate air pollution (PM_{10}) in vivo and in vitro. Thorax 51, 1216-1222.

Maynard A.D., 2003. Estimating Aerosol Surface Area fro Number and Mass Concentration Measurements. Annals of Occupational Hygiene 47, 123-144.

McCawley M.A., Kent M.S., Berakis M.T., 2001. Ultrafine beryllium number concentration as a possible metric for chronic beryllium disease risk. Applied Occupational and Environmental Hygiene 16, 631-638.

Oberdörster G., 2000. Toxicology of ultrafine particles: in vivo studies. Philosophical transactions of the Royal Society of London A 358, 2719-2740.

Oberdörster, G., Utell M.J., 2002. Ultrafine Particles in the Urban Air: To the Respiratory Tract— And Beyond?. Environmental Health Perspectives 110, A440-A441.

Peters A., Wichmann H.E., Tuch T., Heinrich J., Heyder J., 1997. Respiratory effects are associated with the number of ultrafine particles. American journal of respiratory and critical care medicine 155, 1376-1383.

Raiyani C.V., Shah S.H., Desai N. Venkaiah M.K., Patel J.S., Parikh D.J., Kashyap S.K., 1993. Characterization and problems of indoor pollution due to cooking stove smoke. Atmospheric Environment 27A, 1643-1655.

Schwartz J., Dockery D.W., Neas L.M., 1996. Is daily mortality associated specifically with fine particles. Journal of Air Waste Management Association 46, 927-939.

Siegman K., Scherrer L., Siegman H.C., 1998. Physical and Chemical Properties of Airborne Nanoscale Particles and how to Measure the Impact on Human Health. Journal of Molecular Structure: THEOCHEM 458, 191-201.

Tran C. L., Buchanan D., Cullen R.T., Searl A., Jones A.D., Donaldson K., 2000. Inhalation of poorly soluble particles. II. Influence of particle surface area on

inflammation and clearance. Inhalation Toxicology 12, 1113-1126.

Welland M., Porter A., 2005. Why Nanoparticles Are Different. (http://www.royalsoc.ac.uk/downloaddoc.asp?id=2372)

Wichmann H.E., Spix C., Tuch T., Wolke G., Peters A., Heinrich J., Kreyling W.G., Heyder G., 2000. Daily mortality and fine and ultrafine particles in Erfurt, Germany. Part I: Role of particle number and particle mass. Research Report 98, Health Effects Institute, Cambridge, MA. (http://www.healtheffects.org/Pubs/st98.htm)

Woo K., Chen D., Pui D.Y.H., Wilson W.E., 2001. Use of Continuous Measurements of Integral Aerosol Parameters to Estimate Particle Surface Area. Aerosol Science and Technology 34, 57-65.

Zhiqiang Q., Siegmann K., Keller A., Matter U., Scherrer L., Siegmann H.C., 2000. Nanoparticle air pollution in major cities and its origin. Atmospheric Environment 34, 443-451.

Zimmer A.T., Maynard A.D., 2002. Investigation of the aerosols produced by a high-speed, hand-held grinder using various substrates. Annals of Occupational Hygiene 46, 663–672.

Table 1. Summary of the particulate matter concentrations using mass, fine and coarse particle number, and surface area exposure metrics. All measurements are two-minutes averages

Sampling period	Fuel type (number of homes)	Total Data points		PM2.5 mg/m^3	Number, #/cm^3		Surface area (SA), cm^2/m^3
					fine (0.01-1.0μm)	coarse (0.3- >5μm)	
I (October-November)	Kerosene (3)	579	Mean	0.044	42041	143.2	2.26
			SD	0.065	57278	101.7	3.48
			GM	0.030	25698	120.4	1.17
			GSD	1.99	2.45	1.73	2.85
	LPG (4)	987	Mean	0.037	22046	132.2	1.35
			SD	0.056	14804	100.0	1.48
			GM	0.023	18643	103.7	1.02
			GSD	2.27	1.75	2.00	1.93
II (December –January)	Kerosene (5)	1223	Mean	0.101	34021	187.1	3.43
			SD	0.118	37789	107.3	3.83
			GM	0.065	19278	161.4	2.01
			GSD	2.34	2.95	1.70	2.58
	LPG (5)	1638	Mean	0.059	21737	129.1	2.25
			SD	0.110	25283	81.6	2.22
			GM	0.039	15554	106.4	1.67
			GSD	2.09	2.21	1.92	2.08

Table 2. Means[a] and exposure ranks (highest to lowest) for the different exposure metrics

Sampling period	Fuel type	PM2.5		Number I (0.01-1.0μm)		Number II (0.3- >5μm)		Surface area (SA)	
		mg/m^3	Rank	$\#/cm^3$	Rank	$\#/cm^3$	Rank	cm^2/m^3	Rank
I	kerosene	0.025	3	23,949	1	100.6	4	0.88	4
	LPG	0.025	3	19,295	3	110.6	2	1.07	3
II	kerosene	0.071	1	21,947	2	171.1	1	2.34	1
	LPG	0.039	2	17,004	4	101.1	3	1.69	2

[a]: antilog of the least square mean of the logarithms of concentrations.

Table 3. Summary of measured SA (SA_{meas}) and estimated SA (SA_{PSD}, and SA_{INV}) concentrations

Sampling period	Fuel type	SA_{meas}	SA_{PSD}		SA_{INV}	
		cm^2/m^3	cm^2/m^3	SA_R[a]	cm^2/m^3	SA_R
I	Kerosene	0.88[b] (0.67-1.16)[c]	3.01 (2.39-3.79)	3.4	6.81 (5.41-8.57)	7.7
	LPG	1.07 (0.80-1.42)	2.81 (2.21-3.57)	2.6	6.29 (4.96-7.99)	5.9
II	Kerosene	2.34 (1.81-3.02)	4.34 (3.50-5.37)	1.9	12.31 (9.94-15.23)	5.3
	LPG	1.69 (1.31-2.18)	2.75 (2.22-3.40)	1.6	7.74 (6.25-9.57)	4.6

[a]: SA ratio: estimated SA divided by measured SA,
[b]: antilog of the least square mean of the logarithms of concentrations,
[c]: (antilog of the least square mean of the logarithms of concentrations ÷ antilog of the standard error of the logarithms of concentrations) to (antilog of least square mean × anti log of standard error of the logarithms of concentrations).

Table 4. SA_{SD} using different equation of SA for particles bigger than 300 nm

Sampling period	Fuel type	$SA_{2.0}$		$SA_{1.5}$		$SA_{1.0}$	
		cm^2/m^3	SA_R	cm^2/m^3	SA_R	cm^2/m^3	SA_R
I	Kerosene	3.01	3.4	2.28	2.6	2.25	2.6
	LPG	2.81	2.6	1.85	1.7	1.81	1.7
II	Kerosene	4.34	1.9	2.16	0.9	2.05	0.9
	LPG	2.75	1.6	1.64	1.0	1.59	0.9
Average		3.23	2.4	1.98	1.6	1.93	1.5

$SA_{1.5}$: $\pi \cdot d_1^{\,2} + \sum_{2}^{6} N_i \cdot \pi \cdot d_{med\,i}^{1.5}$, $d_1 = 55$ nm, $SA_{1.0}$: $\pi \cdot d_1^{\,2} + \sum_{2}^{6} N_i \cdot \pi \cdot d_{med\,i}$, $d_1 = 55$ nm.

Table 5. SA_{SD} using different diameters in the first size interval

Sampling period	Fuel type	SA_{60}		SA_{55}		SA_{50}		SA_{45}	
		cm^2/m^3	SA_R	cm^2/m^3	SA_R	cm^2/m^3	SA_R	cm^2/m^3	SA_R
I	Kerosene	2.73	3.1	2.25	2.6	1.91	2.2	1.55	1.8
	LPG	2.21	2.1	1.81	1.7	1.55	1.5	1.26	1.2
II	Kerosene	2.57	1.1	2.05	0.9	1.82	0.8	1.49	0.6
	LPG	1.95	1.2	1.59	0.9	1.36	0.8	1.11	0.7
Average		2.37	1.9	1.93	1.5	1.66	1.3	1.35	1.1

SA_{60}: $d_1 = 60$ nm, SA_{55}: $d_1 = 55$ nm (equation (2)), SA_{50} :, $d_1 = 50$ nm, SA_{45}:, $d_1 = 45$ nm.

Table 6. SA_{MA} using different GSD

Sampling period	Fuel type	$SA_{1.5}$		$SA_{1.8}$		$SA_{2.1}$		$SA_{2.4}$		$SA_{3.0}$	
		cm^2/m^3	SA_R	cm^2/m^3	SA_R	cm^2/m^3	SA_R	cm^2/m^3	SA_R	cm^2/m^3	SA_R
I	Kerosene	8.38	9.5	6.81	7.7	5.57	6.3	4.70	5.3	3.60	4.1
	LPG	7.69	7.2	6.29	5.9	5.17	4.9	4.38	3.8	3.38	3.0
II	Kerosene	14.68	6.3	12.31	5.3	10.29	4.4	8.84	4.1	6.99	3.2
	LPG	9.28	5.5	7.74	4.6	6.43	3.8	5.48	3.2	4.29	2.5
Average		10.01	7.1	8.32	5.9	6.86	4.8	5.85	4.1	4.57	3.2

$SA_{1.5}$: GSD = 1.5, $SA_{1.8}$: GSD = 1.8 (original calculation), $SA_{2.1}$: GSD = 2.1, $SA_{2.4}$: GSD = 2.4, $SA_{3.0}$: GSD = 3.0.

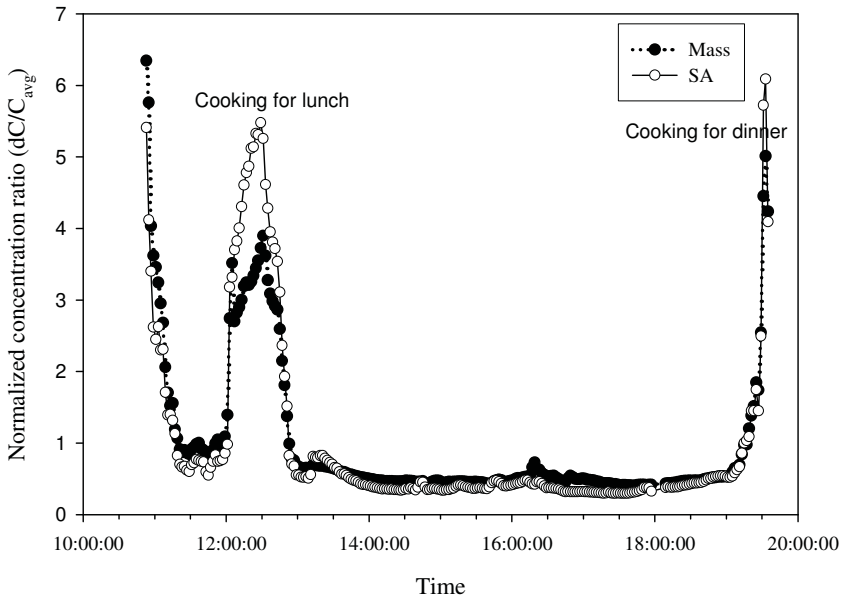

(a) Mass and SA concentrations vs. time

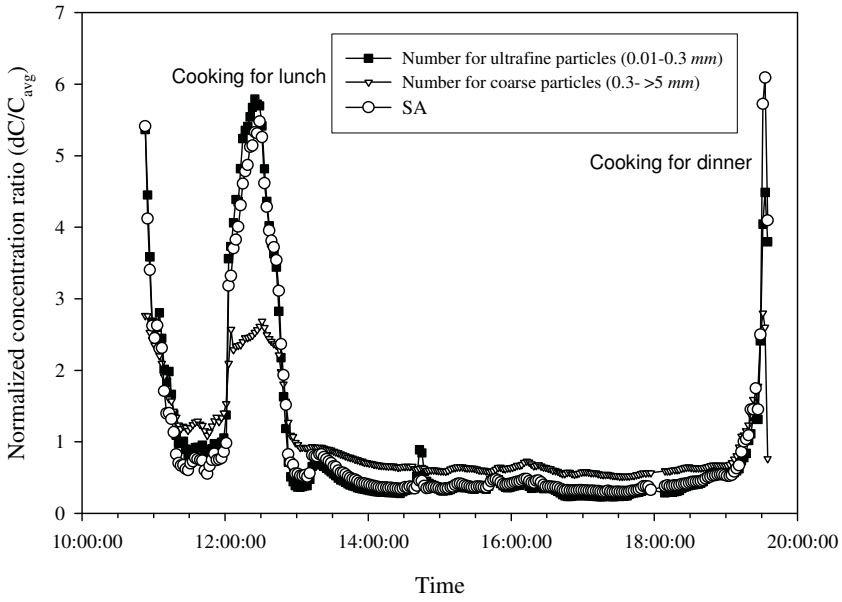

(b) Number concentration for ultrafine and coarse particles, and SA concentration vs. time

Figure 1. Normalized concentration for each metric in a home using a kerosene cooking heater.

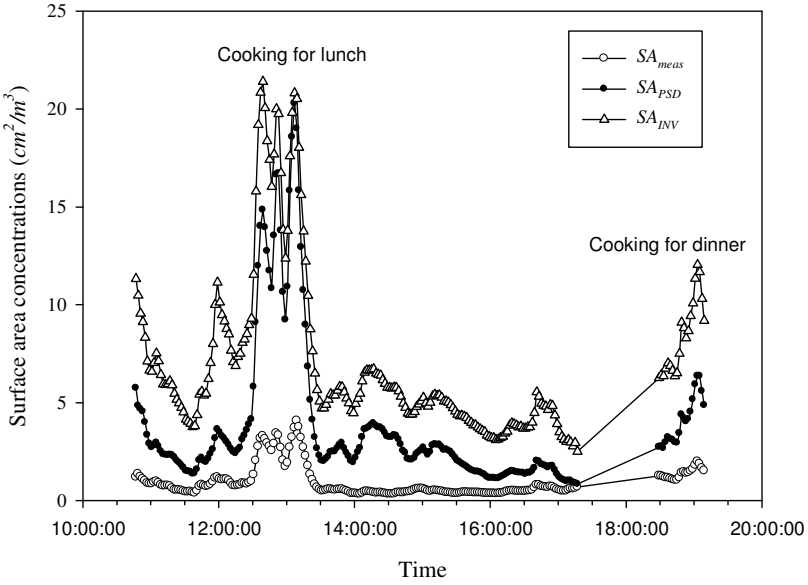

(a) Kerosene home

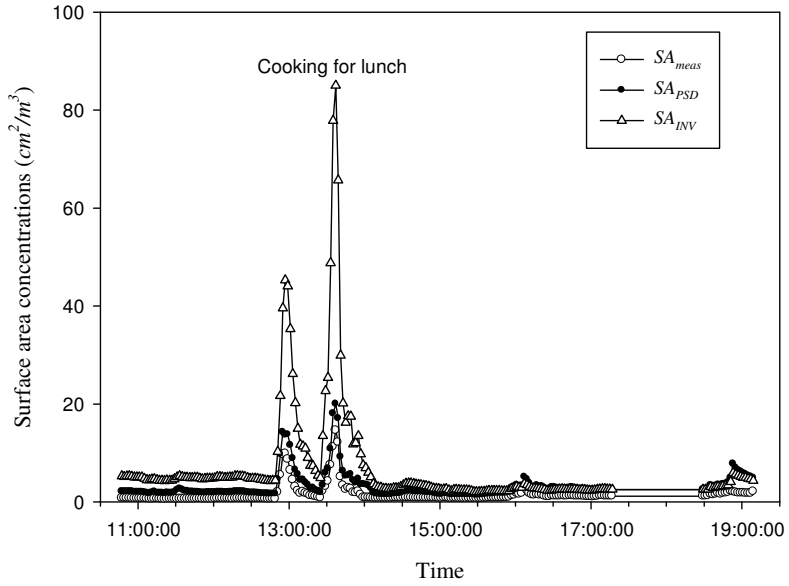

(b) LPG home

Figure 2. Comparison of measured SA and estimated SA concentrations in a household using (a) kerosene and (b) LPG using three different methods. SA_{meas} is obtained directly using a diffusion charger; SA_{PSD} is estimated from number size distribution data; SA_{INV} is estimated using the Maynard algorithm.

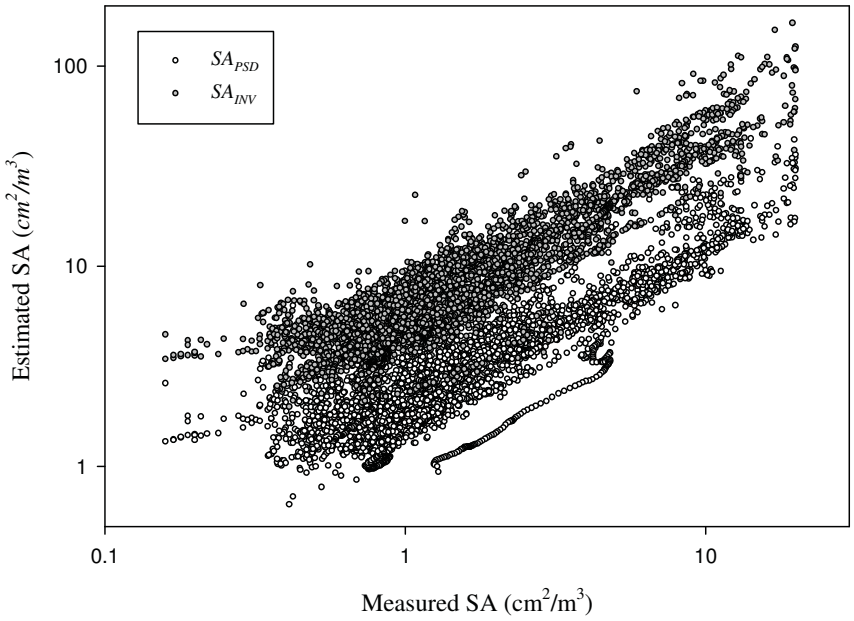

Figure 3. Relationship between 2-minute averages measured and estimated SA concentrations using two different methods.

Chapter V

Estimation of surface area concentration of workplace incidental nanoparticles based on number and mass concentrations

Airborne particle surface area (SA) concentration has been suggested as an appropriate exposure metric for nanoparticles, but few instruments are currently available to measure SA directly. In this study, SA concentration was estimated by three different methods using number and/or mass concentrations obtained from either two or three instruments that are commonly used in the field. The estimated SA were compared with a reference SA (SA_{REF}) calculated from the particle size distribution obtained from a scanning mobility particle sizer (SMPS) and an optical particle counter (OPC). The first estimation method (SA_{PSD}) used particle size distribution by number measured with a condensation particle counter and the OPC. The second method (SA_{INV1}) used an inversion routine based on measurements of PM1.0, PM2.5, and number concentrations to reconstruct assumed lognormal size distributions by minimizing the difference between measurements and calculated values. The third method (SA_{INV2}) utilized a simpler inversion method that used PM1.0 and number concentration measurements to construct a lognormal size distribution with an assumed geometric standard deviation. From the reconstructed size distributions, total SA concentrations were calculated numerically. To evaluate the methods, particle concentration measurements were made in a restaurant, an aluminum die-casting factory, and a diesel engine lab. In the restaurant and diesel engine lab, SA_{INV1} and SA_{INV2} were higher than SA_{REF}. However, in the die casting facility, estimated SA was generally lower than SA_{REF}. The estimated SA had qualitatively similar trends to the SA_{REF} within a workplace. This indicates that the methods used to estimate SA concentrations based on particle number and mass concentration measurements may be used to classify exposure groups.

1. Introduction

Although mass concentrations for nanoparticles are typically much lower than those for coarse particles, nanoparticles have much higher number concentrations and large surface area concentrations (SA) per unit mass. Because of increased toxicological and biological activity resulting from large number and SA concentrations, the interaction with cellular structures may increase in the human body and may cause increased toxicity or different biokinetic characteristics.

The first characteristic of nanosized particles related to their toxicity is size. The extremely small size of nanoparticles compared to cell structures can lead to an increased probability of ion interaction with cell structures (Bell, 2007 and Nel *et al.*, 2006). The higher proportion of nanoparticle surface atoms to that of coarser particles can allow a greater likelihood of interactions with biologically reactive groups on the cell surface that may cause oxidative stress by free radical generation and proinflammatory responses (Oberdörster *et al.*, 2005, Welland and Porter, 2005). Several toxicological studies have shown that the inflammatory responses in the lung by low-solubility and low-toxicity ultrafine particles and fine particles were proportional to SA deposited and have shown good dose-response relationships with SA (Oberdörster 2000, Tran *et al.*, 2000, Brown *et al.*, 2001, Faux *et al.*, 2003).

The SA dose in the above mentioned toxicological studies was calculated using the geometric SA measured by the Brunauer Emmett Teller (BET) gas adsorption method or transmission electron microscope (TEM) analysis. BET and TEM are potentially good reference methods for SA measurements. However, these measurements require a large

mass for each sample, are labor intensive, and are difficult to analyze. Further, they are not real-time measurements.

Only a few devices are currently available to measure SA concentration. The first device developed for SA measurement was the epiphaniometer that can monitor active SA. However, its use is not appropriate in occupational environments due to its radioactive source (Maynard, 2003).

The LQ1-DC diffusion charger (Matter Engineering, Switzerland) contains an aerosol diffusion charger and an electrometer to measure the attachment rate of unipolar ions to particles that is proportional to the active SA. Even though it underestimates the SA of particles with diameters larger than 100 nm, the measurements are comparable to the geometric SA for particles less than 100 nm (Ku and Maynard, 2005).

Recently, TSI Inc. has developed a nanoparticle SA monitor for use in occupational environments. This instrument measures SA of particles that have the ability to be deposited in the tracheobronchial (TB) or the alveolar regions of the human lung (Shin *et al.*, 2007). The particles in the sampled aerosol are charged with unipolar positive ions by diffusion in a mixing chamber. The electric charge on the particles is measured in an electrometer and is proportional to the SA concentration of lung-deposited particles based on the International Commission on Radiological Protection (ICRP) lung deposition model for a reference worker (ICRP, 1994).

SA concentration can also be estimated from aerosol measurements using particle size distribution characteristics. Woo *et al.* (2001) estimated SA concentrations using three measurements: number, mass, and charge. The size distribution parameters were determined by minimizing the difference between measured and theoretical values based

on an assumed particle size distribution and instrument performance. The calculated SA concentrations obtained by integrating the retrieved size distributions were systematically higher than those obtained from the measured particle size distribution, but the calculated SA correlated well with the measured SA. However, the instruments used in that study, an electrical aerosol detector and a research grade particle counter, are not widely available or easily usable in workplaces and the ambient environment for exposure assessment studies.

Maynard (2003) developed a SA estimation method based on mass and number concentration measurements by assuming a lognormal particle size distribution with a specific geometric standard deviation (GSD). Although the SA values estimated using this method were up to four times greater than the values calculated using measured size distributions, the correlation between them was high (R^2=0.98).

Park *et al.* (2009b) compared two SA estimating methods: (1) the simple inversion scheme to retrieve particle size distributions from number and mass concentrations developed by Maynard (2003) and (2) calculated from the particle size distribution by number found from crude size distribution measurements. The estimated SA concentrations were compared to the SA measured by an LQ1-DC diffusion charger. Estimated SA from the Maynard inversion and calculated SA based on the particle size distribution were 6 and 2.4 times higher, respectively, than the measured SA. Although Maynard's method overestimated measured SA concentrations, this estimation method showed better correlation with the measured SA than the size distribution method. Because the SA measured by the diffusion charger underestimates the geometric SA as the particle diameters increase (Ku and Maynard, 2005), the concentrations measured by

the diffusion charger are not an appropriate reference method for evaluating various SA estimation methods. Therefore, a better reference measurement should be selected.

If the particle size distribution is known, total aerosol SA concentration can be calculated using size distribution parameters assuming a spherical shape for particles. The particle size distribution can be retrieved from a set of discrete measurements through a mathematical inversion, a process to reconstruct unknown parameters of the size distribution from indirect measurements. It has been used for retrieving particle size distributions from cascade impactors, parallel diffusion batteries, and aerosol light scattering measurements (Fiebig *et al.* 2005, Ramachandran *et al.* 1996). Ramachandran and Vincent (1997) used a chi-square minimization of the differences between actual and calculated measurements assuming a log-normal particle size distribution to reconstruct continuous particle size distributions from discrete sets of personal cascade impactor measurements. From the reconstructed size distribution, the inhalable, thoracic, and respirable fractions were retrieved as well.

There is growing toxicological evidence that SA is an important health-related metric for nanoparticles exposure. Due to the limited availability of a SA measuring instrument, estimating aerosol SA with easy-to-use existing instruments is a practical solution prior to a broader use of SA monitors. In this study, SA estimating methods based on number and/or mass concentrations from readily available instruments were proposed and evaluated.

2. Methods

2.1 Overview

This study used three methods to estimate SA concentrations based on number and mass concentration measurements commonly used in field work. The first method used the particle size distribution directly measured by two hand-held aerosol instruments. The other two methods use the reconstructed particle size distribution by number through inversion schemes: a weighted least squares minimization with *a priori* assumption of log-normality based on three aerosol measurements (two mass fractions and one number concentration) and Maynard's algorithm based on two aerosol measurements (one mass fraction and one number concentration). The estimated SA concentrations calculated from these three methods were compared to the reference SA concentrations calculated from directly measured size distribution by number using the scanning mobility particle sizer (SMPS) and an optical particle counter (OPC) that together measure particle size distribution by number in the size range from 10 nm to 5 μm.

Three workplaces – a restaurant, a diesel engine lab, and a die cast facility – in which incidental nanoparticles are generated were selected for comparing SA concentrations determined from the estimation methods to concentrations from the reference method (Park *et al.*, 2009a). Measurements were made in two distinct high and low nanoparticle exposure zones in each facility, with three to four locations utilized within each zone. Two sets of samples were taken at each of the sampling locations. Each

sampling run lasted approximately 4 to 6 hours.

2.2. Instrumentation

Real-time measurements (for particle mass, number, and size distribution by number) and gravimetric filter measurements (for calibration of the real-time mass monitor) were made simultaneously. Three-minute averaging times were used for the real-time instruments.

Two aerosol photometers (DustTrak Model 8520 TSI Inc., Shoreview, MN) with PM2.5 and PM1.0 sampling inlets were used for mass concentration. The DustTrak is an aerosol monitor that measures mass concentration using the principle of light scattering. It can measure particle concentrations corresponding to PM2.5 or PM1.0 based on the sampling inlet chosen.

The DustTrak measurements were calibrated to the average aerosol concentration from the corresponding gravimetric measurements for the PM2.5 fraction. The gravimetric PM2.5 was obtained using a PM2.5 sampler (PEM^{TM} Model 200, MSP Inc., Minneapolis, MN). A pump drew air through the sampling inlet at 4.0 L/min. Filters were weighed before sampling using a microbalance with a sensitivity of 5 μg in a weighing room where the temperature and humidity were controlled. After sampling, filters were stored in the weighing room to allow them to reach equilibrium before reweighing.

For each run, blank samples (20% of total samples) were weighed at the same time as the sampled filters. The detection limit was 0.024 mg/m^3 and calculated as three times the standard deviation of the field blank weight gains divided by the sampled air

volume.

The PM2.5 concentrations of the DustTrak measurements were recalculated using a specific calibration factor for each measurement as follows:

$$Calibration\ factor\ for\ PM\,2.5 = \frac{Time\text{ - }Averaged\ PM\,2.5\ gravimetric\ concentration}{Time\text{ - }Integrated\ PM\,2.5\ concentration\ from\ DustTrak} \quad (1)$$

PM2.5 concentrations of the DustTrak were multiplied by this factor to estimate the true mass concentration. No gravimetric sampling was conducted for PM1.0. The calibration factor for PM1.0 was calculated using the concentration ratio between PM2.5 and PM1.0 and the gravimetric PM2.5 concentration as following:

$$PM1.0\ Calibration\ factor = \frac{Gravimetric\ PM\,2.5\ concentration}{\text{Time - }Integrated\ DustTrak\ PM1.0} \times \frac{Size\text{ - }Integrated\ PM1.0}{Size\text{ - }Integrated\ PM\,2.5} \quad (2)$$

Size-integrated PM2.5 and PM1.0 concentrations were calculated from size distribution measurements obtained from a SMPS (Model 3034, TSI Inc., Shoreview, MN) and an optical particle counter (Aerotrak™ Model 8220, TSI Inc., Shoreview, MN, or HHPC-6, Hach Ultra, Grants Pass, Oregon). The gravimetric concentration and integrated DustTrak concentrations were highly correlated (R^2= 0.97 for PM2.5) and the mean calibration factor for PM2.5 and PM1.0 were 0.348 and 0.367 with standard errors of 0.03 and 0.01, respectively.

A condensation particle counter (P-Trak Model 8525, TSI Inc., Shoreview, MN) was used to measure number concentration. The P-Trak is a single-particle counting instrument using the principle of vapor super-saturation and condensation on particles. It measures particles from 0.02 µm to greater than 1.0 µm in diameter. An OPC (AeroTrak™ Model 8220, TSI Inc., Shoreview, MN, or HHPC-6, Hach Ultra, Grants Pass, Oregon) was used to measure size distribution by number. Both OPCs

simultaneously count and size particles into six channels (0.3-0.5 µm, 0.5-0.7 µm, 0.7-1.0 µm, 1.0-2.0 µm, 2.0-5.0 µm, and greater than 5.0 µm) via light scattering. The SMPS was used to obtain information on particle size distribution by number based on the electrical mobility diameter. The SMPS can measure particles between 10 nm to 487 nm in diameter in up to 32 channels.

For easy portability, a mobile sampling cart was used to move the instruments. A mannequin was placed on the top section of the sampling cart to locate sampling tubes from the different instruments at breathing zone height. The inlets of sampling tubes were set closely together. All instruments were connected to a wall outlet using AC power. Data from each device were downloaded to a laptop computer.

2.3 SA estimation methods

2.3.1 Estimation method 1 based on particle size distribution by number (SA_{PSD})

This estimation method used the P-Trak and OPC. The P-Trak is a size-integrating particle counter that detects and counts all particles from 20 nm to 1 µm. The OPC counts particles in six different size bins: 0.3-0.5 µm, 0.5-0.7 µm, 0.7-1.0 µm, 1.0-2.5 µm, 2.5-5 µm, and >5 µm. The ultrafine particle count (N_{UFP}, 0.01-0.3 µm) was, therefore, calculated using the first three size bins of the OPC and the P-Trak count:

$$N_{UFP} = N_{P-Trak} - \sum_{k=1}^{3} N_{OPC,k} \quad (3)$$

where k is the index for the size intervals of the OPC.

The counts in the first five size bins of the OPC and the N_{UFP} were used to

calculate total SA concentrations. The log median diameter ($d_{med\,i}$) was chosen as the representative diameter for each interval:

$$d_{med\,i} = 10^{(\log d_{max\,i} + \log d_{min\,i})/2} \quad (4)$$

where $d_{max\,i}$ and $d_{min\,i}$ are the upper and lower limits of the i^{th} interval. Using $d_{med\,i}$, the SA concentration of each interval (SA_i) was obtained as

$$SA_i = N_i \, \pi \, d_{med\,i}^2 \quad (5)$$

in which N_i is the number concentration in i^{th} interval from the P-Trak and OPC measurements. The total particle SA concentration for this method, SA_{PSD}, was the sum of the SA from each interval:

$$SA_{PSD} = \sum_{i=1}^{6} SA_i \quad . \quad (6)$$

2.3.2 Estimation method 2 based on zeroth order minimization inversion method (SA_{INVI})

This estimation method was based on an inversion scheme that reconstructed the unknown size distribution from indirect measurements. Because the aerosol was assumed to be unimodal with a lognormal size distribution, it can be described by three unknown parameters: the median diameter, the GSD, and the total concentration. Thus, three independent measurements were needed to obtain the three unknown parameters. In this study, measurements of PM2.5 and PM1.0 (using DustTraks) and particle number concentrations (using the P-Trak) were used to reconstruct the particle size distributions. However, the instrument response functions (kernel function) of the three instruments

overlapped one another. Thus, the measurements were not completely independent causing the mathematical problem of reconstructing the size distribution to be an ill-posed one, *i.e.* many solutions exist that satisfy a given set of measurements.

An inversion procedure finds the best solution by imposing additional criteria that select one among the many possible solutions. In this study, by solving the system of Fredholm integral equations of the first kind, the particle size distribution was reconstructed from the three measurements. The measurement made by each instrument (C_i) was described as

$$C_i = \int_a^b K_k(d) f(d) \mathrm{d}d + \varepsilon_k \qquad i = 1,\ 2,\ and\ 3 \tag{7}$$

where K_i is the kernel function for the i^{th} instrument describing the instrument response, $f(d)$ is the particle size distribution function of mass or number for aerosol entering the instrument, a and b are the size limits within which the instrument responds to the particle size distribution, and ε_i are measurement errors. The instrument performance data were obtained from the manufacturer (Personal communication, A. Sreenath, TSI Inc.). The instrument response functions were found based on the performance data using curve-fitting (SigmaPlot 10.0, San Jose, CA)

$$K_{P-Trak} = \frac{0.93}{1 + e^{\frac{-(d-0.0172)}{0.0033}}} \tag{8}$$

$$\begin{aligned} \mathrm{K}_{\mathrm{DustTrak\ PM2.5}} &= (1 + \mathrm{e}^{\frac{-(\mathrm{d}-0.269)}{0.077}})^{-1} \ \text{for d} < 1.03\,\mu\mathrm{m} \\ &= (1 + \mathrm{e}^{\frac{(\mathrm{d}-2.518)}{0.145}})^{-1} \ \text{for d} > 1.03\,\mu\mathrm{m} \end{aligned} \tag{9}$$

$$K_{\text{DustTrak PM1.0}} = (1+e^{\frac{-(d-0.275)}{0.053}})^{-1} \text{ for } d < 0.62\,\mu m$$
$$= (1+e^{\frac{(d-1.070)}{0.068}})^{-1} \text{ for } d > 0.62\,\mu m \quad (10)$$

With the assumption that the particles are spherical, the diameter of average mass ($d_{\bar{m}}$) was calculated from the Hatch-Choate equation

$$d_{\bar{m}} = CMD \exp\left(1.5 \ln^2 GSD\right) \quad (11)$$

and the relationship between total number concentration (N) and total mass concentration (M) was

$$M = N\left(\frac{\pi}{6}\rho\, d_{\bar{m}}^3\right) \quad (12)$$

where ρ is the particle density. In this study, depending on the sources of incidental nanoparticles in each workplace, different particle densities were applied: 0.9 g/cm^3 for grease particles in the restaurant (Kuen *et al.*, 2008), 2.1 g/cm^3, for diesel engine emission particles in the diesel engine lab (Hougaard *et al.*, 2008), and 3.72 g/cm^3 for 96% aluminum oxide (Al_2O_3) particles in the die casting facility (Accuratus, 2009).

The inversion scheme used a weighted least squares optimization with zeroth-order regularization to fit a unimodal distribution function (Ramachandran and Vincent, 1997). The approach used an intermediate step to make initial estimates of the parameters of interest and provide an appropriate starting point for the optimization routine. The optimization routine itself minimized the expression

$$R = \sum_{i=1}^{n}\left(\frac{C_i - \int_a^b K_i(d)\cdot f(d)\mathrm{d}d}{E(\varepsilon_i)}\right)^2 - N \quad (13)$$

where N is the number of measurements used (N=3), and $E(\varepsilon_i)$ is the expected value of the measurement error. The optimization procedure found a solution for the particle size distribution of the total aerosol satisfying the measurements to just within experimental error.

It is important to know the expected measurement errors from each instrument. The DustTrak had two main sources of error, one originating from the DustTrak itself and the other from gravimetric measurements obtained for DustTrak calibration. The first kind of measurement error was calculated from the experiment results for DustTrak calibration against a reference photometer at TSI Inc. (Personal communication, A. Sreenath, TSI Inc.). The DustTrak was repeatedly calibrated in the range of mass concentration generated using an Emery oil aerosol. From the repeat calibration runs, we calculated the average mass concentration measured by the DustTrak and its standard deviation. The standard deviation divided by the average mass concentrations equaled the fractional error. This photometer error turned out to be less than 1%. The gravimetric error performed for the DustTrak calibration was assumed to be 10% in the worst case to meet National Institute for Occupational Health and Safety (NIOSH) gravimetry criteria (NIOSH 1994). The overall measurement error for the DustTrak was conservatively assumed to be 10% for this estimation method. The P-Trak's measurement error was also calculated from calibration tests performed at TSI Inc. The calibration error for the P-Trak was ~15%.

Because it is assumed *a priori* that the size distribution is a uni-modal log-normal distribution, the inversion routine needed to find the three parameters of the unimodal log-normal particle distribution (*i.e.*, count median diameter, GSD, and total number

concentration) that best expressed the measured data. Initial approximations for the three parameters were determined and then adjusted iteratively until Eq. (13) was minimized (*i.e.*, approaches zero). In this study, we set initial estimate of the total number concentration (N) to be equal to the measured P-Trak concentrations, the initial estimate of CMD to be 50 nm, and the initial estimate of GSD to be 2. The minimization was performed using the "Solver" function in Microsoft Excel^{TM}.(Microsoft, Redmond, WA)

Once the three parameters (CMD, GSD, N) for the lognormal number size distributions were determined, the total SA concentration (SA_{INV1}) was calculated by

$$SA_{INV1} = N \cdot \pi \cdot d_{\bar{s}}^{\,2} \tag{14}$$

where $d_{\bar{s}}$ is the diameter of the average SA obtained from the Hatch Choate equation.

$$d_{\bar{s}} = CMD \cdot \exp(\ln^2 GSD) \tag{15}$$

2.3.3 Estimation method 3 based on Maynard method (SA_{INV2})

Maynard (2003) proposed a SA estimation method that was a simplified version of the inversion theory approach described in the previous section. To completely characterize the size distribution, three unknowns need to be determined. In this method, only two measurements (number concentrations from the P-trak and mass concentration from the DustTrak with PM1.0 sampling inlet) were used to estimate SA while a value of GSD, a lognormal fit parameter, was fixed. In this study, a *GSD* of 1.8 was used to estimate SA. The detailed estimation process was described in Maynard (2003) and Park *et al.* (2009b).

2.3.4 Calculation of reference SA from the SMPS and OPC combination (SA_{REF})

For the reference SA concentration, the SMPS and OPC combination was used. The entire detection range of the SMPS (0.01-0.487 μm) and the middle four size bins of the OPC (0.5-5 μm) were used to construct the reference size distribution. The log median diameter ($d_{med\ i}$) was used as the representative diameter for each size channel. The total particle SA concentration for the reference, SA_{REF}, was the sum of the SA_i from each interval.

$$SA_{REF} = \sum_{l=1}^{32} N_{SMPS,i} \pi\, d_{med\,1}^2 + \sum_{k=2}^{4} N_{OPC,k} \pi d_{med\,k}^2 \qquad (16)$$

in which *l* represents the intervals on the SMPS.

2.4 Data analysis

The real-time instrument data were organized into three-minute averages. To compare all estimated SA concentrations simultaneously, all measurement data from the five real-time instruments used to estimate SA were needed. If a time point did not have any one of the five instrument readings, it was excluded from analysis. More than 90% of time intervals had all five measurements and were used for the analysis.

The geometric means (GM) of estimated SA, and size distribution parameters were calculated for each location and each zone. Significant differences between high and low zones by each SA concentration and total number concentration in each workplace were detected using t-tests. Data taken from the same location were auto-correlated. To correct for the auto-correlation in the real-time measurements, general linear models with compound symmetry covariance structure were used. Such models are more appropriate

to compare high and low exposure zone measurements than models that assume independence among different measurements. The level of statistical significance for all analyses was 0.05. All statistical analyses were conducted using SAS 9.1 (SAS Institute Inc., Cary NC).

3. Results

3.1 The association between reference SA and estimated SA

Table 1 presents SA_{REF}, estimated surface areas (SA_{PSD}, SA_{INV1}, SA_{INV2}), and the ratios of each estimated surface area to SA_{REF}. SA_{REF} were highest in the high and low exposure zones of the die casting facility and were lowest in the low exposure zone of the restaurant. All estimated SA concentrations had trends similar to those for SA_{REF}. In addition, the statistical mean differences between the two exposure zones in each workplace were similar to those for SA_{REF}: significant difference in the restaurant and die casting facility but no difference in the diesel engine lab.

The estimated SA based on particle number size distribution data (SA_{PSD}) was between 0.7 and 2.0 times higher than SA_{REF}. The SA_{PSD}/SA_{REF} significantly differed by the exposure groups and workplaces. In the restaurant, SA_{PSD} overestimated SA_{REF} in the high exposure group but underestimated SA_{REF} in the low exposure group. In the diesel engine lab, the SA_{PSD} were close to SA_{REF} in both exposure groups. In the die casting facility, SA_{PSD} underestimated SA_{REF} in both exposure groups. The relationship between the logarithm of SA_{REF} and the logarithms of SA_{PSD} is shown in Fig. 1-(a).

The SA_{INV1}/SA_{REF} and SA_{INV2}/SA_{REF} ratios were between 0.7-7.6 and 0.5-7.7, respectively. Both estimation methods overestimated SA in the restaurant and diesel engine lab. In the die casting facility where concentration levels were high, they underestimated SA_{REF}. The relationships between the logarithm of SA_{REF} and the logarithm of SA_{INV1} and SA_{INV2} are shown in Fig. 1-(b). SA_{INV1} and SA_{INV2} were similar to each other.

3.2 Size distribution parameters used for calculation of the reference SA and estimated SA

For SA calculation, particle size distributions were directly measured (for SA_{Ref} and SA_{PSD}) and were retrieved using inversion processes (for SA_{INV1} and SA_{INV2}). Table 2 summarizes the three parameters for size distribution by number (CMD, GSD, and total number concentration). The lognormal parameters used for SA_{REF} and SA_{PSD} were directly calculated based on the aerosol measurement of the SMPS-OPC and the P-Trak-OPC combination, respectively. However, lognormal parameters used for SA_{INV1} and SA_{INV2} calculation were reconstructed through the inversion processes based on the P-Trak and DustTrak measurements, described earlier.

The total number concentrations (N_{PSD}, N_{INV1}, and N_{INV2}) retrieved using the three estimation methods were comparable to the reference total number concentration (N_{REF}) in the restaurant, the diesel engine lab and the low exposure group of the die casting plant. However, in the high exposure group of the die casting plant, all total number concentrations were 2.2 to 3.2 times lower than the N_{REF}.

The CMDs from the reference size distribution varied by sampling location in the three workplaces. Small CMDs (~ 30 nm), were observed in the grill and oven areas in the restaurant and near the engines in the diesel engine lab. The CMDs in the dishwashing, bar, and seating areas in the restaurant and milling machine 1 in the die casting plant were ~ 60 nm, larger than in other locations. The CMDs calculated for SA_{PSD} were between 78 to 80 nm across all the sampling locations (*i.e.,* much narrower ranges and larger CMDs than those for SA_{REF}). The GSDs for the data used to calculate SA_{PSD} ranged from 1.06 and 1.38 and were lower than the GSDs for the reference. The CMDs retrieved for SA_{INV1} and SA_{INV2} were larger than those for SA_{REF} especially in the restaurant and the diesel engine lab. In the die casting plant, the CMDs estimated from the the weighted least squares minimization inversion routine were comparable to the reference CMDs.

4. Discussion

All estimated concentrations showed similar trends to the reference SA concentrations in the three workplaces, although the ratios that express the magnitude of these errors were different for all three estimation methods and differed by concentration levels and workplaces for a given method.

Estimated SA concentrations based on particle size distribution (SA_{PSD}) were comparable to the reference SA concentrations (SA_{REF}) in the restaurant and diesel engine lab but were underestimated significantly in the die casting facility. Estimated SA concentrations based on the two inversion processes (SA_{INV1} and SA_{INV2}) were a factor of

2.5 to 7.6 higher than SA_{REF} in the restaurant and diesel engine lab, respectively. In the die casting facility, however, these methods underestimated SA_{REF}.

Underestimation of SA by the three estimation methods in the die casting plant could be due to instrumental limitations of the P-Trak. The number concentrations measured by the P-Trak were compared to the number concentrations of the SMPS, for the same particle size range (0.02 to 0.3 μm). To obtain the number concentrations for particles 20-300 nm in diameter from the SMPS measurements (N_{SMPS}), the counts in the corresponding particle size bins of the SMPS were used. This was compared against N_{UFP}, the number concentrations of first size bin (0.02-0.3 μm) calculated as described earlier. Fig. 2 shows N_{SMPS} versus N_{UFP} using all time point data. As seen in Fig. 2, at lower concentrations (up to 5,000 particles/cm^3), N_{UFP} is close to N_{SMPS} with little variation. However, at extremely high concentrations such as near die casting machines or when the gas oven in the restaurant was open, N_{UFP} were on average a factor of 2.5 lower than N_{SMPS}.

The underestimated number concentrations may affect the particle size distributions. The estimated total number concentration is smaller and estimated CMD and GSD are larger than actual values. The changed size distribution parameters would make estimated SA concentrations smaller than the actual values.

The P-Trak's underestimation is most likely because of coincidence errors that can occur in an instrument using optical sensors in a high concentration environment. That is, several particles can pass through the sensing zone at the same time and be counted as a single particle (Hameri *et al.*, 2002). This results in SA_{PSD} underestimating SA_{REF} substantially in the high exposure group of the die casting plant. If a dilution system had

been attached to the P-Trak to keep particle concentrations passing through the sensing zone low, the measurement errors would have been smaller, and SA_{PSD} would have been closer to SA_{REF}. The use of a dilution system would have also improved the performance of the other two estimation methods (SA_{INV1} and SA_{INV2}).

For the calculation of SA_{PSD}, number concentrations from six size bins (0.02-0.3 μm, 0.3-0.5 μm, 0.5-0.7 μm, 0.7-1.0 μm, 1-2 μm, and 2-5 μm) were used. Importantly, the first channel contains ~ 99% of the total number of particles. Thus, the selection of the representative diameter for the first channel is critical.

The lower limit of the first size bin (20 nm) is the same as the lowest detection size of the P-trak according to the manufacturer's specifications. In our study, the geometric mean of the lower and upper limit of each size bin was chosen as the representative diameters for each bin. Thus, the assumed log median diameter of the first channel ($d_{med\ 1}$) was 77 nm. However, the true count median diameter of particles in the size range covered by this bin was probably different from this value and would vary depending on the ultrafine particle generation source and the characteristics of generated particles. To determine the sensitivity of this method to the lowest limit of the P-trak or the first size bin, different representative diameters (55, 65, and 85 nm) were assumed for this interval. The estimated SA concentrations based on these three diameters were 50%, 30 % lower and 20 % higher, respectively, than the SA_{PSD} obtained using 77 nm as the $d_{med\ 1}$. Thus, SA_{PSD} is highly sensitive to the value assumed for $d_{med\ 1}$.

In a previous study (Park *et al.*, 2009b), two of the same estimation methods (SA_{PSD} and SA_{INV2}) were applied to estimate SA from number and mass measurements. The values of SA_{PSD}/SA_{REF} in the current study (excluding the high exposure group of the

die casting plant) are lower than those found by Park et al (2009b). The particle counters used in the two studies are different. The lower limit for particle detection for the P-Trak in this study is 20 nm while the lower limit for and the CPC (Model 3007 TSI Inc., Shoreview, MN) in the previous study was 10 nm. Thus, in this study, all SA estimations were done without accounting for particles between 10 to 20 nm in diameter. The ratio of particle counts between 10 and 20 nm to total particle counts measured by the SMPS was estimated using the more detailed measurements. The percentage of particle counts in this range was 7 - 40 % and the SA percentage in the corresponding particle size range was between 0.2 - 6.6%. In other words, SA_{PSD} in this study may have been lower (up to 6.6%) than SA_{PSD} in the previous study and this may lead the smaller SA_{PSD}/SA_{REF} ratios in this study than those in the previous study.

In this study, the direct measurement of size distribution was used to calculate a reference SA concentration assuming a spherical particle shape. Park *et al.* (2009b) used the SA concentration measured by a diffusion charger as the reference. The active SA measured by the diffusion charger is close to the geometric SA for particles below ~100 nm in diameter for which the mean free path of ions is greater than the particle diameter. As a particle diameter increases, the active SA underestimates the geometric SA because it is proportional to the diameter of particles rather than the squared diameter of particles (Ku and Maynard, 2005). The difference between the SA concentration measured with the diffusion charger (SA_{Meas}) and the reference SA calculated from the SMPS as in this study depends on the ratio of particles bigger than 100 nm to the total particles. As the proportion of these larger particles becomes greater, the difference between SA_{Meas} and SA_{REF} increases. In the previous study, larger particle number concentrations (0.3->5 μm)

ranged from 129 to 187 particles/cm^3, which were greater than 11-54 particles/cm^3 observed in the current study. The ratios, SA_{PSD}/SA_{Meas} in the previous study were bigger than those (SA_{PSD}/SA_{REF}) in the current study, in part, because of the underestimated reference values in the previous study.

In all sampling locations, both estimation methods using inversion schemes overestimated the CMDs compared to the reference. In particular, in the restaurant and diesel engine lab, the CMDs were 2-3 times larger than the corresponding reference CMDs while the estimated total number concentrations were close to the reference concentration. The overestimated SA is a result of the over estimated CMD.

One of the parameters used to determine the calculated mass concentrations from the reconstructed size distribution by number is the particle density. To determine the effect of different particle densities on the two estimation methods using inversion schemes, different sets of particle density were applied to estimate SA: 0.2 g/cm^3 lower (0.7, 1.9, and 3.5 g/cm^3 for the restaurant, diesel engine lab, and die casting facility, respectively) and 0.2 g/cm^3 higher (1.1, 2.3, and 3.9 g/cm^3 for the restaurant, diesel engine lab, and die casting facility, respectively) than original particle densities assumed for each workplace.

When the two adjusted values of particle densities were used, the reconstructed particle number concentrations were similar to the originally estimated particle number concentrations for both estimation methods. However, the retrieved CMDs of these estimated size distributions decreased as higher particle densities were assumed. Thus, increasing particle densities resulted in decreased estimated SA in both methods.

The sensitivity of particle density to estimated SA was greater in the case of lighter

density particles. Particles in the restaurant were lightest (particle density=0.9 g/m^3) and the magnitude of the effects of the particle densities were the greatest in the restaurant (~ -15% for SA_{INV1} and ~ -13% for SA_{INV2}) followed by the diesel engine lab (~ -5% for both methods) and die casting facility (~- 2-3% for the both methods). The estimated SA in the die casting facility was not sensitive to the particle density.

The Maynard method (SA_{INV2}) is based on a simple inversion routine that uses number and mass concentration measurements. In this method, the GSD of size distribution was a fixed value of 1.8. This value is slightly lower than that observed in the reference size distributions. The value of GSD was changed to 2.0 which is close to the reference GSD to determine the effect of GSD on this estimation method. The newly obtained CMD were smaller and the total number concentrations (N_{INV2}) were higher than original parameters when the assumed value of GSD was 1.8. The newly estimated SA based on these CMD and total number concentrations slightly decreased (nearly 10%) but in some sampling locations did not change at all. Varying GSDs does not affect the sensitivity results of this method (SA_{INV2}).

5. Conclusions

SA concentrations were estimated from measurement of mass and number concentrations made by aerosol instruments commonly used by industrial hygienists in the field. The estimated SA concentrations were compared with the reference SA concentrations obtained from the SMPS and OPC combination.

All estimated SA had qualitatively similar trends to the SA_{REF} but the magnitude

of errors differed by workplaces and by estimation method chosen. In the restaurant and diesel engine labs, estimated SA were higher than SA_{REF} on average, but estimated SA were lower than SA_{REF} in the die casting facility. Due to significant coincidence error of the P-Trak in the high exposure levels, all estimated SA were likely underestimated in die casting facility. The use of a dilution system to the P-Trak will improve the ability of estimating SA in high exposure environments.

SA_{PSD} was found to be sensitive to the representative diameter and number concentrations of the first channel containing the smallest particle sizes. This could be a limitation of SA_{PSD}.

The reconstructed size distribution by number through the inversion processes showed comparable total particle number concentrations to the reference, but the CMDs were higher than the reference. This is responsible for the overestimation SA in the restaurant and diesel engine lab. The particle density was found to influence the SA estimating methods based on the inversion routines.

This research suggests that all estimation methods may be used as an interim solution for the purpose of classifying exposure zones within a workplace if the real-time measurements can be performed as accurately as possible.

6. Acknowledgements

We thank TSI Inc. for the instrumentation and technical support for this study. We are also grateful for the financial support from 3M Company and the Midwest Center for Occupational Health and Safety (MCOHS). Also we thank the Campus Club at the

University of Minnesota, QX Inc., and the Center for Diesel Research in Department of Mechanical Engineering at University of Minnesota. We acknowledge A. Sreenath's help with calibration data.

References

Accuratus, 2009. Aluminum Oxide, Al_2O_3. Available from URL http://www.accuratus.com/alumox.html. Accessed July 2009.

Bell T. E., 2007. Understanding risk assessment of nanotechnology

Available from URL http://www.nano.gov/Understanding_Risk_Assessment.pdf. Accessed June 2009.

Brown, D.M., Wilson M.R., MacNee W., Stone V., Donaldson K., 2001. Size-dependent proinflammatory effects of ultrafine polystyrene particles: a role for SA and oxidative stress in the enhanced activity of ultrafines. Toxicology and Applied Pharmacology 175, 191-199.

Faux S.P., Tran C.L., Miller B.G., Jones A.D., Montellier C., Donald K., 2003. *In vitro* Determinants of particulate toxicity: the dose-metric for poorly soluble dusts. Research Report RR154, HSE Books, Sudbury UK.

Fiebig M., Stein C., Schröder F., Feldpausch P., Petzold A., 2005. Inversion of data containing information on the aerosol particle size distribution using multiple instruments. Journal of Aerosol Science 36, 1353-1372.

Hameri K., Koponen I.K., Aalto P.P., Kulmala M., 2002. The particle detection efficiency of the TSI 3007 condensation particle counter. Journal of Aerosol Science; 33 1463-1469.

International Commission on Radiological Protection (ICRP), 1994. International Commission on Radiological Protection Publication 66 Human Respiratory Tract Model for Radiological Protection, New Youk, Elsevier Science Ltd.

Ku B.K., Maynard A.D., 2005. Comparing aerosol surface area measurements of monodisperse ultrafine silver agglomerates by mobility analysis, transmission electron microscopy and diffusion charging. Journal of Aerosol Science 36, 1108-1124.

Maynard A.D., 2003. Estimating Aerosol Surface Area fro Number and Mass Concentration Measurements. Annals of Occupational Hygiene 47, 123-144.

National Institute for Occupational Safety and Health (NIOSH), 1994. Particulates not otherwise regulated, total (0500). In *NIOSH Manual of Analytical Methods*, NIOSH, Cincinnati.

Nel A., Xia T., Madler L.V., Li N., 2006. Toxic Potential of Materials at the Nanolevel. Science 311, 622-627.

Oberdörster G., 2000. Toxicology of ultrafine particles: *in vivo* studies. *Phil. Trans. R. Soc. Lond. A.* 358, 2719-2740.

Oberdörster G., Oberdörster E., Oberdörster J., 2005. Nanotoxicology: An Emerging Discipline Evolving from Studies of Ultrafine Particles. Environmental Health Perspective 113, 823–839.

Park J.Y., Raynor P.C., G. Olson, Eberly, Ramachandran G., 2009a. Comparing exposure groups by different exposure metrics using statistical parameters: contrast and precision. Annals of Occupational Hygiene; (in preparation)

Park J.Y., Raynor P.C., Maynard A.D., Eberly L.E., Ramachandran G., 2009b. Comparison of two estimation methods for SA concentration using number concentration and mass concentration of combustion-related ultrafine particles. Atmospheric Environment 43, 502-509.

Ramachandran G., Vincent J.H., 1997. Evaluation of Two Inversion Techniques for Retrieving Health-Related Aerosol Fractions from Personal Cascade Impactor Measurements. American Industrial Hygiene Association Journal 58, 15 – 22.

Ramachandran G., Johnson E.W., Vincent J.H., 1996. Inversion techniques for personal cascade impactor data. Journal of Aerosol Science 27, 1083-1097.

Shin W.G., Pui D.Y.H., Fissan H., Neumann S., Trampe A., 2007. Calibration and numerical simulation of Nanoparticle Surface Area Monitor (TSI Model 3550 NSAM). Journal of Nanoparticle Research 9, 61-69.

Sreenath A. (TSI Inc.): personal communication.

Tran C.L., Buchanan D., Cullen R.T., Searl A., Jones A.D., Donaldson K., 2000.

Inhalation of poorly soluble particles. II. Influence of particle surface area on inflammation and clearance. *Inhalation Toxicology* 12, 1113-1126.

Welland M., and A. Porter (2005). Why Nanoparticles Are Different? Available from URL http://www.royalsoc.ac.uk/downloaddoc.asp?id=2372. Accessed July 2009.

Woo K., Chen D., Pui D.Y.H., Wilson W.E., 2001. Use of Continuous Measurements of Integral Aerosol Parameters to Estimate Particle Surface Area. Aerosol Science and Technology 34, 57-65.

Table 1. Summary of reference SA and estimated SA (SA_{PSD}, SA_{INV1}, SA_{INV2}) concentrations

Workplace	Group	location	SA_{REF} (cm^2/m^3)	SA_{PSD}		SA_{INV1}		SA_{INV2}	
				cm^2/m^3	SA_{PSD}/SA_{REF}	cm^2/m^3	SA_{INV1}/SA_{REF}	cm^2/m^3	SA_{INV2}/SA_{REF}
Restaurant	High	dishwasher	2.12	1.90	0.9	5.55	2.6	5.64	2.7
		Grill	2.11	4.88	2.3	8.40	4.0	6.48	3.1
		Oven	4.05	15.31	3.8	16.86	4.2	13.55	3.4
		Mean[a]	**2.56**	**5.12**	**2.0**	**9.06**	**3.6**	**7.74**	**3.0**
	Low	Bar	0.45	0.32	0.7	2.85	6.4	2.96	6.6
		Serv station	0.35	0.31	0.9	2.70	7.8	2.69	7.8
		Seating area	0.63	0.45	0.7	4.30	6.8	4.43	7.0
		Mean	**0.42**	**0.34**	**0.8**	**3.22**	**7.6**	**3.28**	**7.7**
		p	0.001	0.005		0.006		0.01	
Diesel Engine Lab	High	Engine1	3.36	8.34	2.5	9.33	2.8	6.24	1.9
		Engine2	1.96	1.85	0.9	5.50	2.8	4.46	2.3
		Engine3	2.28	4.21	1.9	5.13	2.3	4.10	1.8
		Engine4	1.12	1.19	1.1	3.22	2.9	2.66	2.4
		Mean	**2.00**	**2.62**	**1.3**	**4.92**	**2.5**	**4.05**	**2.0**
	Low	Prep room	1.31	1.42	1.1	4.25	3.3	3.96	3.0
		Study area	1.02	1.34	1.3	4.24	4.2	3.60	3.5
		TA office	1.23	1.24	1.0	2.61	2.1	2.47	2.0
		Mean	**1.40**	**1.39**	**1.0**	**3.60**	**2.6**	**3.57**	**2.5**
		p	0.15	0.19		0.20		0.55	
Die Cast Facility	High	Die cast1	84.83	68.35	0.8	52.85	0.6	42.47	0.5
		Die cast2	112.26	78.30	0.7	82.80	0.7	64.47	0.6
		Trim press	143.73	67.35	0.5	78.25	0.5	66.04	0.5
		Mean	**107.02**	**72.10**	**0.7**	**69.73**	**0.7**	**55.68**	**0.5**
	Low	Turning	21.04	22.90	1.1	19.92	0.9	15.59	0.7
		Milling1	53.64	23.93	0.5	29.90	0.6	27.43	0.5
		Milling2	29.07	25.86	0.9	25.96	0.9	21.47	0.7
		Mean	**28.97**	**24.19**	**0.8**	**24.10**	**0.8**	**19.86**	**0.7**
		p	0.0009	<.0001		0.0002		0.0005	

[*]: antilog of the least square mean of the logarithms of concentrations.

Table 2. size distribution parameters used to calculate reference SA (SA_{REF}) and estimated SA (SA_{PSD}, SA_{INV1}, SA_{INV2}) concentrations

ID	Group	Location	Size distributions for SA_{REF}		Size distributions for SA_{PSD}		Lognormal fit reconstructed for SA_{INV1}		Lognormal fit reconstructed for SA_{INV2}	
			CMD (GSD)	N_{REF}	CMD (GSD)	N_{PSD}	CMD (GSD)	N_{INV1}	CMD (GSD)	N_{INV2}
Restaurant	High	dishwasher	57 (2.23)	2,886	82 (1.38)	2,769	151 (1.99)	2,994	178 (1.8)	2,839
		Grill	31 (1.82)	25,030	78 (1.07)	23,866	54 (2.05)	29,817	63 (1.8)	26,372
		Oven	25 (1.61)	87,621	78 (1.06)	77,068	48 (2.03)	86,087	49 (1.8)	91,321
		Mean*		**19,434**		**16,929**		**19,434**		**18,684**
	Low	Bar	58 (2.13)	1,481	78 (1.15)	1,412	153 (1.98)	1,510	181 (1.8)	1,447
		Serv station	52 (2.06)	1,322	78 (1.14)	1,324	153 (2.00)	1,389	177 (1.8)	1,378
		Seating area	62 (2.09)	1,786	79 (1.19)	1,757	154 (2.07)	1,976	197 (1.8)	1,811
		Mean		**1,527**		**1,417**		**1,527**		**1,463**
		P		0.008		0.009		0.008		0.009
Diesel Engine Lab	High	Engine1	27 (1.83)	50,983	78 (1.06)	42,701	52 (1.89)	48,107	44 (1.8)	52,279
		Engine2	30 (2.20)	13,095	79 (1.17)	7,203	100 (1.90)	7,562	98 (1.8)	7,480
		Engine3	29 (1.97)	24,509	78 (1.08)	20,331	51 (2.02)	22,913	53 (1.8)	23,194
		Engine4	33 (2.29)	6,128	78 (1.14)	5,028	89 (1.94)	5,275	98 (1.8)	5,225
		Mean		**15,579**		**11,710**		**12,646**		**12,740**
	Low	Office	40 (2.10)	7,607	78 (1.12)	6,296	83 (2.10)	6,560	98 (1.8)	6,521
		Study area	38 (2.03)	7,332	78 (1.11)	6,188	91 (1.96)	6,569	94 (1.8)	6,425
		TA office	45 (2.08)	6,076	78 (1.14)	5,487	62 (2.21)	6,141	83 (1.8)	5,751
		Mean		**7,192**		**6,345**		**6,721**		**6,549**
		P		0.12		0.26		0.26		0.25
Die Cast Facility	High	Die cast1	37 (1.78)	845,653	78 (1.14)	309,048	42 (2.02)	347,895	42 (1.8)	384,707
		Die cast2	37 (1.92)	918,719	79 (1.18)	321,633	52 (2.01)	367,694	53 (1.8)	366,667
		Trim press	44 (1.93)	901,485	78 (1.15)	298,084	51 (2.05)	335,177	56 (1.8)	334,455
		Mean		**892,159**		**311,670**		**352,177**		**365,419**
	Low	Turning	42 (2.12)	104,193	79 (1.16)	91,739	49 (2.00)	101,567	48 (1.8)	108,141
		Milling1	63 (2.51)	113,254	79 (1.16)	103,095	51 (2.11)	118,214	62 (1.8)	112,857
		Milling2	42 (2.22)	126,473	79 (1.18)	107,814	49 (2.05)	121,879	53 (1.8)	123,766
		Mean		**113,721**		**99,688**		**111,680**		**114,394**
		P		<.001		<.001		<.001		<.001

*: antilog of the least square mean of the logarithms of concentrations.

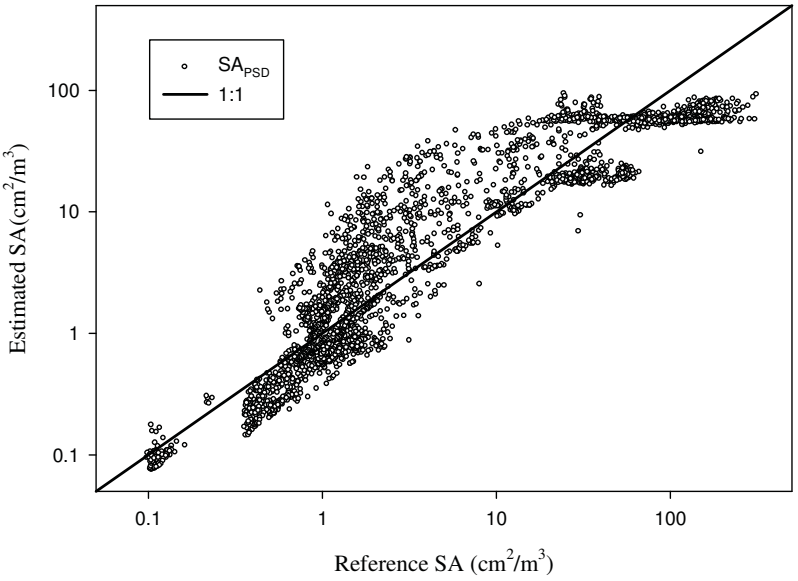

(a) SA_{REF} versus SA_{PSD}

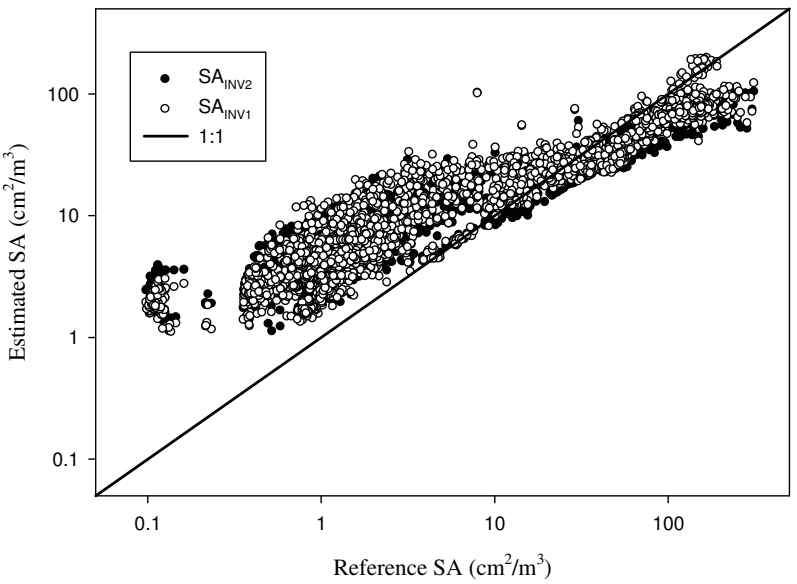

(b) SA_{REF} versus SA_{INV1} and SA_{INV2}

Figure 1. Relationship between reference and estimated SA concentrations using three different estimation methods.

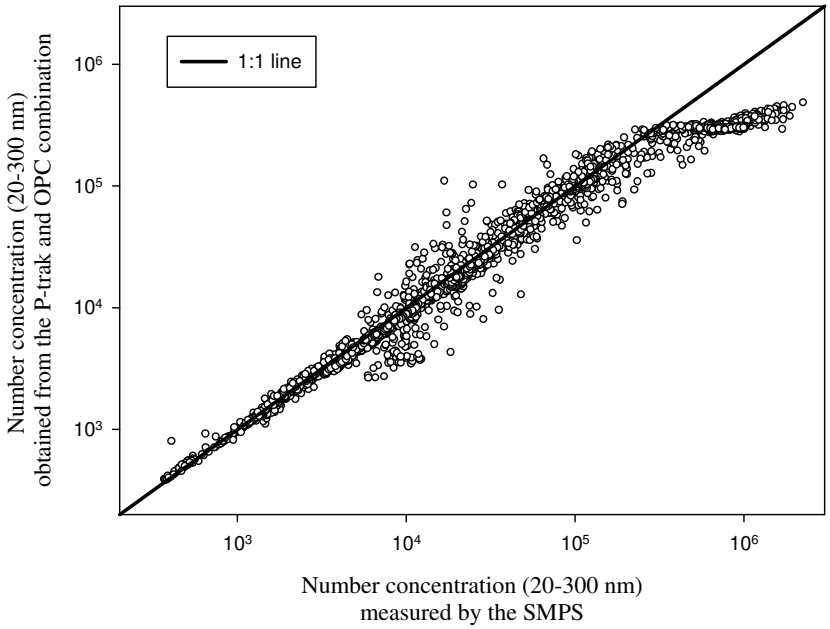

Figure 2. Relationship between the number concentrations (20-300 nm) obtained from the SMPS and calculated from the P-trak and OPC combination.

Chapter VI

Conclusions and Future Directions

Overall conclusions

The long-range goal of this research is to determine the most relevant exposure metrics for nanoparticle exposure assessment. In this study, measurements using multiple exposure metrics were conducted to find more appropriate exposure metrics for nanoparticle exposure that reduce exposure misclassification and to find SA estimation methods based on currently available measurements of aerosol number and mass concentrations. This section draws the following conclusions and summarizes implications regarding the findings of this research.

- Of the several types of short term measurements for aerosol concentration mapping using various metrics in the restaurant and the die casting facility, SA and fine particle number concentrations of nanoparticles are more related to concentration peaks and nanoparticle sources than mass concentrations. This indicates that SA and fine particle number concentration metrics reflect characteristics typical of nanoparticles, *i.e.*, high surface area and particle number per mass concentration. The mapping technique can be used to identify particle generation sources and understand contaminants' spatial distribution. Visual aerosol maps can convey spatial information for aerosol contaminants effectively and locate unexpected sources of contaminants. This can be a useful tool for the pre-survey phase of an exposure assessment especially for the case of nanoparticles where there is very little industry knowledge and professional judgment.

- SA or fine particle number concentrations are more efficient metrics than mass concentration for classifying workers into exposure categories or zones and and less likely to result in exposure misclassification. This suggests that researchers may fail to obtain the association between exposure to nanoparticles and related health outcomes, if a less relevant or appropriate exposure metric is chosen. The choice of appropriate exposure metric has significant implications for exposure groupings in epidemiological studies as well as for routine industrial hygiene exposure assessment.
- SA concentration can be estimated from number and/or mass concentration using relatively simple inversion techniques. These estimated SA concentrations are reasonably well correlated with to the reference SA concentrations and showed qualitatively similar trends, even though the magnitude of errors varied by workplace and the selected estimation method. This suggests that SA estimating methods can be used as interim solutions prior to a broader use of surface area monitoring instruments.

Future directions

Further research is needed for the following issues: i) exposure assessment using multiple metrics in workplaces manufacturing/handling engineered nanoparticles; ii) evaluation of the appropriateness of SA or fine particle number concentrations for engineered nanoparticle exposures; iii) validation of SA estimating methods depending on the morphology of engineered nanoparticles.

This research dealt with exposure to incidental nanoparticles because the accessibility to facilities manufacturing or handling with engineered nanoparticles was limited. Monitoring data of engineered nanoparticles in occupational settings is important for future risk assessment. However, there are a few peer-reviewed papers and most of them report on studies conducted in research laboratories. Naturally occurred nano-sized particles exist in the ambient and occupational environments, but it is difficult to distinguish them from engineered nanoparticles using routine instrumentation described in this research. Therefore, speciation of particles using Scanning Electron Microscopy (SEM) or Transmission Electron Microscopy (TEM) analysis should complement real-time measurements of number, SA, and mass concentrations. A multiple-metric sampling approach combined with speciation of particles will be more appropriate for exposure assessment for engineered nanoparticles.

Engineered nanoparticles are manufactured to have certain size, shape, and surface area characteristics and they have various morphological properties depending on their design (NIOSH, 2009). Their size distribution characteristics and relationships between different measurement metrics may be different those for incidental particles' due to their distinct morphology. Thus, the appropriateness of SA or fine particle number concentrations obtained in this research needs to be confirmed for engineered nanoparticles.

SA estimating methods based on number and/or mass measurements described in this study need to be investigated further. Engineered nanoparticles may differ from incidental particles in terms of their physical characteristics, including morphology, and thus, relationships between various exposure metrics may be different. These relationships need to be studied further. As long as the size distribution remains unchanged, the relationship between number, surface area, and mass will be fixed and if information on the relationships such as surface to mass or surface to number ratio is known, it can be utilized to estimate surface area (NIOSH, 2009; Maynard and Kuempel, 2005).

References

Maynard A.D., Kuempel E.D., 2005. Airborne nanostructured particles and occupational health. Journal of nanoparticle Research 7, 587-614.

National Institute for Occupational Safety and Health (NIOSH), 2009. Approaches to Safe Nanotechnology; An Information Exchange with NIOSH. Available from URL www.cdc.gov/niosh/topics/nanotech/nano_exchange.html. Accessed July 2009.

Bibliography

Accuratus, 2009. Aluminum Oxide, Al_2O_3. Available from URL http://www.accuratus.com/alumox.html. Accessed July 2009.

Adachi M., Kousaka Y., Okuyama K., 1985. Unipolar and Bipolar Diffusion Charging of Ultrafine Aerosol Particles. Journal of Aerosol Science 16, 109-123.

Aitken R.J., Creely K.S., Tran C.L., 2004. Nanoparticles: An occupational hygiene review. HSE Research Report 274. Available from URL http://www.hse.gov.uk/research/rrpdf/rr274.pdf. Accessed July 2009

Analytical Methods, NIOSH, Cincinnati.

Andresen P.R., Ramachandran G., Pai P., Maynard A.D., 2005. Women's personal and indoor exposures to PM2.5 in Mysore, India: Impact of domestic fuel usage. Atmospheric Environment 39, 5500-5508.

Balakrishnan K., Sambandam S., Ramaswamy P., Mehta S., Smith K.R., 2004. Exposure assessment for respirable particulates associated with household fuel use in rural districts of Andhra Pradesh, India. Journal of Exposure Analysis and Environmental Epidemiology supplement 1, S14-S25.

Baron P.A., Willeke K., 2001. Aerosol measurement: Principles, techniques, and Applications, 2nd ed. Wiley-Interscience, New York, pp. 404-406.

Bell T. E., 2007. Understanding risk assessment of nanotechnology. Available from URL http://www.nano.gov/Understanding_Risk_Assessment.pdf. Accessed June 2009.

Brook, R.D., Franklin B., Cascio W., Hong Y., Howard, G., Lipsett M., 2004. Air pollution and cardiovascular disease: a statement for healthcare professionals from the Expert Panel on population and prevention science of the American Heart Association. Circulation 109, 2655-2671.

Brouwer D.H., Gijsbers J.H.J., Lurvink M.W.M., 2004. Personal exposure to ultrafine particles in the workplace: exploring sampling techniques and strategies. Annals of Occupational Hygiene 48, 439-453.

Brown, D.M., Stone V., Findlay P., MacNee W., Donaldson K., 2000. Increased inflammation and intracellular calcium caused by ultrafine carbon black is independent of transition metals or other soluble components. Occupational and Environmental Medicine **57,** 685-691.

Brown, D.M., Wilson M.R., MacNee W., Stone V., Donaldson K., 2001. Size-dependent proinflammatory effects of ultrafine polystyrene particles: a role for SA and oxidative stress in the enhanced activity of ultrafines. Toxicology and Applied Pharmacology 175, 191-199.

Brown, D.M., Wilson M.R., MacNee W., Stone V., Donaldson K., 2001. Size-dependent proinflammatory effects of ultrafine polystyrene particles: a role for SA and oxidative stress in the enhanced activity of ultrafines. Toxicology and Applied Pharmacology 175, 191-199.

Chamberlain E.A.C., Makower A.D., Walton W.H., 1970. New gravimetric dust standards and sampling procedures for British coal mines. Inhaled particles III. Unwin Brothers Ltd., London, UK pp.111-124.

Chang, M.–C.O., Chow J.C., Watson J.G., Glowacki C., Sheya S.A., Prabhu A., 2005. Characterization of fine particulate emissions from casting processes. Aerosol Science and Technology 39, 947-959.

Dasch, J., D'Arcy J., Gundrum A., Sutherland J., Johnson J., Carlson D., 2005. Characterization of Fine particles from machining in automotive plants. Journal of Occupational and Environmental Hygiene 2, 609-625.

Dennekamp, M., Howarth S., Dick C.A.J., Cherrie J.W., Donaldson K., Seaton A., 2001. Ultrafine particles and nitrogen oxides generated by gas and electric cooking. Occupational Environmental Medicine 58, 511-516.

Dick, C.A., Brown D.M., Donaldson K., Stone V., 2003. The role of free radicals in the toxic and inflammatory effects of four different ultrafine particle types. Inhalation Toxicology 15, 39-52.

Dockery, D.W., Pope C.A., Xu X., Spengler J.D., Ware J.H., Fay H.E., 1993. An

association between air pollution and mortality in six U. S. cities. New England Journal of Medicine 329, 1753-1759.

Donaldson K., Stone V., 2003. Current hypotheses on the mechanisms of toxicity of ultrafine particles. Annl 1st Super Sanita 39, 405-10.

Donaldson K., Stone V., Clouter A., Renwick L., MacNee W., 2001. Ultrafine Particles. Occup Environ Med 58, 211-216.

Driscoll K.E., 1996. Role of inflammation in the development of rat lung tumors in response to chronic particle exposure. Inhalation Toxicology 8(suppl), 139–153.

Evans, D.E., Heitbrink W.A., Slavin T.J., Peters T.M., 2008. Ultrafine and respirable particles in an automotive grey iron foundry. Annals of Occupational Hygiene 52, 9-21.

Faux S.P., Tran C.L., Miller B.G., Jones A.D., Montellier C., Donald K., 2003. *In vitro* Determinants of particulate toxicity: the dose-metric for poorly soluble dusts. Research Report RR154, HSE Books, Sudbury UK.

Ferin J., Oberdörster G., Penney. D.P., 1992. Pulmonary retention of ultrafine and fine particles in rats. American Journal of Respiratory Cell Molecular Biology 6, 535-542.

Fiebig M., Stein C., Schröder F., Feldpausch P., Petzold A., 2005. Inversion of data containing information on the aerosol particle size distribution using multiple instruments. Journal of Aerosol Science 36, 1353-1372.

Firley D., 1999. Daily mortality and air pollution in Santa Clara County, California: 1989-1996. Environmental Health Perspective 107, 637-641.

Fissan H., Neumann S., Trampe A., Pui D.Y.H., Shin W.G., 2006. Rationale and principle of an instrument measuring lung deposited nanoparticle surface area. Journal of Nanoparticle Research 9, 53-59.

Flegal, K.M., Keyl P.M., Nieto F.J., 1991. Differential misclassification arising from nondifferential errors in exposure measurement. American Journal of Epidemiology 134, 1233-1241.

Gwinn, M.R., Vallyathan V., 2006. Nanoparticles: Health Effects-Pros and Cons.

Environmental Health Perspectives 114, 1818-1825.

Hameri K., Koponen I.K., Aalto P.P., Kulmala M., 2002. The particle detection efficiency of the TSI 3007 condensation particle counter. Journal of Aerosol Science; 33 1463-1469.

Heitbrink W.A., Evans D.E., Ku B.K., Maynard A.D., Slavin T.J., Peters T.M., 2009. Relationships among particle number, surface area, and respirable mass concentrations in automotive engine manufacturing. Journal of Occupational Environmental Hygiene 6, 19-31.

Hinds W.C., 1999. Aerosol technology: properties, behavior, and measurement of airborne particles. (2nd ed.), Wiley-Interscience, New York.

International Commission on Radiological Protection (ICRP), 1994. International Commission on Radiological Protection Publication 66 Human Respiratory Tract Model for Radiological Protection, New Youk, Elsevier Science Ltd.

International Organization for Standardization (ISO), 2008. ISO/TS 27687:2008 Terminology and definitions for nanoparticles.

Kent M.S., Robins T.G., Madl A.K., 2001. Is total mass or mass of alveolar-deposited airborne particles of beryllium a better predictor of the prevalence of disease? a preliminary study of a beryllium processing facility. Applied Occupational and Environmental Hygiene 16, 539-558.

Knibbs L.D., de Dear R.J., Morawska L., Coote P.M., 2007. A simple and inexpensive dilution system for the TSI 3007 condensation particle counter. Atmospheric Environment 41, 4553-4557.

Kreyling W.G., Semmer-Behnke M., Möller W., 2006. Health implications of nanoparticles. Journal of nanoparticle research 8, 543-562.

Kreyling W.G., Tuch T., Peters A., Pitz M., Heinrich J., Stolzel M., Cyrys J., Heyder J., Wichmann H.E., 2003. Diverging long-term trends in ambient urban particle mass and number concentrations associated with emission changes caused by the German unification. Atmospheric Environment 37, 3841-3848.

Kromhout H., Heederik D., 1995. Occupational epidemiology in the rubber industry:

implications of exposure variability. American Journal of Industrial Medicine 27, 171-185.

Ku B.K., Maynard A.D., 2005. Comparing aerosol surface-area measurements of monodisperse ultrafine silver agglomerates by mobility analysis, transmission electron microscopy and diffusion charging. Journal of Aerosol Science 36, 1108-1124.

Li X.Y., Gilmour P.S., Donaldson K, MacNee W., 1996. Free radical activity and pro-inflammatory effects of particulate air pollution (PM_{10}) in vivo and in vitro. Thorax 51, 1216-1222.

MacNee W., Donaldson K., 2003. Mechanism of lung injury caused by PM_{10} and ultrafine particles with special referance to COPD. European Respiratory Journal **21,** 47S-51S.

Maynard A.D., 2003. Estimating Aerosol Surface Area fro Number and Mass Concentration Measurements. Annals of Occupational Hygiene 42, 123-144.

Maynard A.D., Aitken R.J., 2007. Assessing exposure to airborne nanomaterials: Current abilities and future requirements. Nanotoxicology 1, 26-41.

Maynard A.D., Kuempel R.D., 2005. Airborne nanostructured particles and occupational health. Journal of nanoparticle Research 7, 587-614.

Maynard A.D., Stone V., 2005. Airborne nanostructured particles and occupational health. Journal of nanoparticle research 7, 587-614.

Maynard, A.D., Maynard R.L., 2002. A derived association between ambient aerosol surface area and excess mortality using historic time series data. Atmospheric Environment 36, 5561-5567.

McCawley M.A., Kent M.S., Berakis M.T., 2001. Ultrafine beryllium number concentration as a possible metric for chronic beryllium disease risk. Applied Occupational Environmental Hygiene 16, 631-638.

McMurry P.H., 2000. A review of atmospheric aerosol measurements. Atmospheric Environment 34, 1959-1999.

Monteiller, C., Tran L., MacNee W., Faux S., Jones A., Miller B., Donaldson K., 2007. The pro-inflammatory effects of low-toxicity low-solubility particles, nanoparticles and fine particles, on epithelial cells in vitro: the role of surface area. Occupational Environmental Medicine 63, 609-615.

Moshammer H., Neuberger M, 2003. The active surface of suspended particles as a predictor of lung function and pulmonary symptoms in Austrian school children. Atmospheric Environment **37,** 1737-1744.

Mulhausen J.R., Damiano J., 1998. A strategy for assessing and managing occupational exposures, AIHA Press, Fairfax USA.

National Institute for Occupational Safety and Health (NIOSH), 1994. Particulates not otherwise regulated, total (0500). In *NIOSH Manual of Analytical Methods*, NIOSH, Cincinnati.

National Institute for Occupational Safety and Health (NIOSH), 2009. Approaches to Safe Nanotechnology; An Information Exchange with NIOSH. Available from URL www.cdc.gov/niosh/topics/nanotech/nano_exchange.html. Accessed July 2009.

Nel A., Xia T., Madler L.V., Li N., 2006. Toxic Potential of Materials at the Nanolevel. Science 311, 622-627.

Nemmar, A., Hoet P.H.M., Vanquickenborne B., Dinsdale D., Thomeer M., Hoylaerts M.F., Vanbilloen H., Mortelmans L., Nemery B., 2002. Passage of inhaled particles into the blood circulation in humans. Circulation **105,** 411-414.

O'Brien, D.M., 2003. Aerosol mapping of a facility with multiple cases of hypersensitivity pneumonitis: Dempnstration of mist reduction and a possible dose/response relationship. Applied Occupational and Environmental Hygiene 18, 947-952.

Oberdörster G, Oberdörster O. E., Oberdörster J., 2005. Nanotoxicology: An Emerging Discipline Evolving from Studies of Ultrafine Particles. Environmental Health Perspectives 113, 823-839.

Oberdörster G., 2000. Toxicology of ultrafine particles: in vivo studies. Philosophical

transactions of the Royal Society of London A 358, 2719-2740.

Oberdörster, G., Ferin J., Gelein R., Soderholm S.C., Finkelstein J., 1992. Role of the alveolar macrophage in lung injury: Studies with ultrafine particles. Environmental Health Perspectives 97, 193-199.

Oberdörster, G., Ferin J., Lehnert B.E., 1994. Correlation Between Particle-Size, in-Vivo Particle Persistence, and Lung Injury. Environmental Health Perspectives 102(S5), 173-179.

Oberdörster, G., Sharp Z., Atudorei V., Elder A., Gelein R., Lunts A., Kreyling W., Cox C., 2002. Extrapulmonary translocation of ultrafine carbon particles following whole-body inhalation exposure of rats. Journal of Toxicology and Environmental Health Part A **65,** 1531-1543.

Oberdörster, G., Utell M.J., 2002. Ultrafine Particles in the Urban Air: To the Respiratory Tract— And Beyond?. Environmental Health Perspectives 110, A440-A441.

Paik S.Y., Zalk D.M., Swuste P., 2008. Application of a pilot control banding tool for risk level assessment and control of nanoparticle exposures. Annals of Occupational Hygiene 52, 419-428.

Park J.Y., Ramachandaran G., Raynor P.C., Olson Jr G.M., 2009. Determination of workplace nanoparticle exposure rankings by spatial mapping of particle mass, number, and surface area concentrations. Journal of Occupational Environmental Hygiene (in proceeding).

Park J.Y., Raynor P.C., G. Olson, Eberly, Ramachandran G., 2009. Comparing exposure groups by different exposure metrics using statistical parameters: contrast and precision. Annals of Occupational Hygiene; (in preparation)

Park J.Y., Raynor P.C., Maynard A.D., Eberly L.E., Ramachandran G., 2009. Comparison of two estimation methods for SA concentration using number concentration and mass concentration of combustion-related ultrafine particles. Atmospheric Environment 43, 502-509.

Peters A., Wichmann H.E., Tuch T., Heinrich J., Heyder J., 1997. Respiratory effects are

associated with the number of ultrafine particles. American journal of respiratory and critical care medicine 155, 1376-1383.

Peters, M.T., Heitbrink W.A., Evans D.E., Slavin T.J., Maynard A.D., 2006. The mapping of fine and ultrafine particle concentrations in an engine machining and assembly facility. Annals of Occupational Hygiene 50, 249-257.

Pope, C.A., Burnett R.T., Thurston G.D., Thun M.J., Calle E.E., Krewski D., 2004. Cardiovascular mortality and long-term exposure to particulate air pollution: epidemiological evidence of general pathophysiological pathways of disease. Circulation 109, 71-77.

Pope, C.A., Dockery D.W., Kenner R.E., Villegas G.M., Schwartz J., 1999. Oxygen saturation, pulse rate and particulate air pollution: a daily time-series panel study. American Journal of Respiratory Critical Care Medicine 159, 365-372.

Raiyani C.V., Shah S.H., Desai N. Venkaiah M.K., Patel J.S., Parikh D.J., Kashyap S.K., 1993. Characterization and problems of indoor pollution due to cooking stove smoke. Atmospheric Environment 27A, 1643-1655.

Ramachandran G., Johnson E.W., Vincent J.H., 1996. Inversion techniques for personal cascade impactor data. Journal of Aerosol Science 27, 1083-1097.

Ramachandran G., Paulsen D., Watts W., Kittelson D., 2005. Mass, surface area and number metrics in diesel occupational exposure assessment. Journal of Environmental Monitoring 7, 728-735.

Ramachandran G., Vincent J.H., 1997. Evaluation of Two Inversion Techniques for Retrieving Health-Related Aerosol Fractions from Personal Cascade Impactor Measurements. American Industrial Hygiene Association Journal 58, 15 – 22.

Renwick, L.C., Donaldson K. Clouter A., 2001. Impairment of alveolar macrophage phagocytosis by ultrafine particles. Toxicology and Applied Pharmacology 172, 119-127.

Roco M.C., 2005. Environmentally responsible development of nanotechnology. Environmental Science and Technology 39, 106A-112A.

Royal Society, 2004. Nanosicence and nanotechnology; opportunities and uncertainties. Available from URL http://www.nanotec.org.uk/report/Nano%20report%202004%20fin.pdf. Accessed July 2009.

Schwartz J., Dockery D.W., Neas L.M., 1996. Is daily mortality associated specifically with fine particles. Journal of Air Waste Management Association 46, 927-939.

Schwartz J., Marcus A., 1990. Mortality and air pollution in London: A time series analysis. American Journal of Epidemiology 131, 185-194.

Serita F., Kyono H., Seki Y., 1999. Pulmonary clearance and lesions in rats after a single inhalation of ultrafine metallic nickel at dose levels comparable to the threshold limit value. Industrial Health 37, 353-363.

Shin W.G., Pui D.Y.H., Fissan H., Neumann S., Trampe A., 2007. Calibration and numerical simulation of Nanoparticle Surface Area Monitor (TSI Model 3550 NSAM). Journal of Nanoparticle Research 9, 61-69.

Siegman K., Scherrer L., Siegman H.C., 1998. Physical and Chemical Properties of Airborne Nanoscale Particles and how to Measure the Impact on Human Health. Journal of Molecular Structure: THEOCHEM 458, 191-201.

Sreenath A. (TSI Inc.): personal communication.

Stoeger, T., Reinhard C., Takenaka S., Schroeppel A., Karg E., Ritter B., 2006. Instillation of Six Different Ultrafine Carbon Particles Indicates a Surface Area Threshold Dose for Acute Lung Inflammation in Mice. Environ Health Perspective 114, 328-333.

Stone, V., Shaw J., Brown D.M., MacNee W., Faux S.P., Donaldson K., 1998. The role of oxidative stress in the prolonged inhibitory effect of ultrafine carbon black on epithelial cell function. Toxicology *in Vitro* **12,** 649-59.

Sun, Q, Wang A., Natanzon A., Duquaine D., Brook R.D., 2005. Long-term air pollution exposure and acceleration of atherosclerosis and vascular inflammation in an animal model. Journal of American Medical Association 294, 3003-3010.

Takenaka, S., Karg E., Roth C., Schulz H., Ziesenis A., Heinzmann U., Schramel P.

Heyder J., 2001. Pulmonary and systemic distribution of inhaled ultrafine silver particles in rats. Environmental Health Perspectives **109,** 547-551.

Thornburg J., Leith D., 2000. Mist Generation During Metal Machining. Journal of Tribology 122, 544-549.

Tran C. L., Buchanan D., Cullen R.T., Searl A., Jones A.D., Donaldson K., 2000. Inhalation of poorly soluble particles. II. Influence of particle surface area on inflammation and clearance. Inhalation Toxicology 12, 1113-1126.

Welland M., and A. Porter (2005). Why Nanoparticles Are Different? Available from URL http://www.royalsoc.ac.uk/downloaddoc.asp?id=2372. Accessed July 2009.

Wichmann H.E., Spix C., Tuch T., Wolke G., Peters A., Heinrich J., Kreyling W.G., Heyder G., 2000. Daily mortality and fine and ultrafine particles in Erfurt, Germany. Part I: Role of particle number and particle mass. Research Report 98, Health Effects Institute, Cambridge, MA. (http://www.healtheffects.org/Pubs/st98.htm)

Wilson M.R., Lightbody J.H., Donaldson K., Sales J., Stone V., 2002. Interactions Between Ultrafine Particles and Transition Metals *in vivo* and *in vitro*. Toxicology Applied Pharmacology 184,172-179.

Woo K., Chen D., Pui D.Y.H., Wilson W.E., 2001. Use of Continuous Measurements of Integral Aerosol Parameters to Estimate Particle Surface Area. Aerosol Science and Technology 34, 57-65.

Zhiqiang Q., Siegmann K., Keller A., Matter U., Scherrer L., Siegmann H.C., 2000. Nanoparticle air pollution in major cities and its origin. Atmospheric Environment 34, 443-451.

Zimmer A.T., Maynard A.D., 2002. Investigation of the aerosols produced by a high-speed, hand-held grinder using various substrates. Annals of Occupational Hygiene 46, 663–672.